

KNEE JOINT BIOMECHANICS AFTER ANTERIOR CRUCIATE LIGAMENT  
RECONSTRUCTION

by

Hongsheng Wang

A dissertation submitted to the faculty of  
The University of North Carolina at Charlotte  
in partial fulfillment of the requirements  
for the degree of Doctor of Philosophy in  
Mechanical Engineering

Charlotte

2012

Approved by:

---

Dr. Nigel Zheng

---

Dr. Ronald E. Smelser

---

Dr. Edward P. Morse

---

Dr. Aidong Lu

---

Dr. Jianping Fan

©2012  
Hongsheng Wang  
ALL RIGHTS RESERVED

## ABSTRACT

HONGSHENG WANG. Knee joint biomechanics after anterior cruciate ligament reconstruction (Under the direction of Dr. NAIQUAN NIGEL ZHENG)

Anterior cruciate ligament (ACL) is an important stabilizer of the knee joint. After ACL rupture, the knee joint has difficulty maintaining its stability; thus the patient often has to receive an ACL-reconstructive surgery to regain the knee joint functions. Unfortunately, traditional transtibial surgical techniques could not fully restore the normal knee joint kinematics during daily activities. Moreover, a higher rate of osteoarthritis was found from the ACL-reconstructed knees compared to the knees without a history of ACL-injuries. The reason for the increased risk of knee osteoarthritis is still unclear, and the pathologies due to abnormal knee joint kinematics remain controversial. The dissertation was to delineate the knee joint motion and loading after ACL-reconstruction. Thirty patients who received ACL-reconstructive surgeries using the traditional transtibial technique and 14 using the recently developed anteromedial portal technique were recruited from the same center (OrthoCarolina). Twenty healthy subjects without history of knee injuries were recruited as the control group. Human motion data and ground reaction force data were collected during level walking and downstairs pivoting using an optical motion capture system. Three-dimensional (3D) knee joint motions were determined from redundant markers using an optimization approach. The 3D knee joint moments and forces were calculated from motion data, ground reaction data by using an inverse dynamics model of the lower extremity. A finite element model was created, and the distributions of stress/strain within articular cartilage

under physiological loading were estimated. The results from two groups of patients using different reconstruction techniques were compared.

In the transtibial group, excessive internal tibial rotation ( $2^\circ$  on average during stance phase), varus rotation and anterior femur translation (swing phase) were observed in the ACL-reconstructed knees when compared to the control group during level walking. The 3D knee joint motion following ACL-reconstruction was found to be influenced by the leg dominance. The motion and load in the uninjured contralateral knee were also affected. During downstairs pivoting, the normal varus rotation and adduction moment were not fully restored by the transtibial technique. Overall, the anteromedial portal technique improved the postsurgical knee joint kinematics by reducing the offsets in the internal tibial rotation, varus rotation and anterior femur translation during level walking. It also improved the adduction moment during downstairs pivoting. At the same time, the anteromedial portal technique may cause a flexion/extension deficit during the stance phase of walking. Results of finite element analysis demonstrated higher pressures within the medial femoral cartilage during the stance phase of walking; it also demonstrated that there is an increased knee joint laxity after ACL-reconstruction. The anteromedial portal technique was overall better than the traditional transtibial technique in respect to postsurgical knee joint compressive loading and contact pressure. The study provides evidence of the possibility by using anatomical single-bundle ACL-reconstruction technique to fight the knee joint osteoarthritis after ligament injury.

## ACKNOWLEDGEMENT

I thank Dr. Nigel Zheng for his direct mentoring on my program study and research work, for the encouragement to my whole Ph.D study and the impact on my life post-graduation. I thank Dr. Aidong Lu, Dr. Edward Morse and Dr. Ronald Smelser for serving on my dissertation committee and providing constructive suggestion to my research. Especially, I thank Dr. Ronald Smelser for his numerous help on my individual study topic: Finite Elasticity for Biological Materials. I thank Dr. James Fleischli for sending us the ACL patients and helping on manuscript preparation. I thank Anne Denny, Susan Odum and Brittany Denton for their assistance in subject recruitment and thank all the research subjects who participated in my study. I thank my colleagues, Bing Xiao, Hernando Pacheco, Xiaoqin Li and Jeffery Thousand for their help on data collection and reduction. I also thank my parents whose love and support sustained me throughout the journey and motivated me to where I am today.

Finally I would like to thank the financial supports: the UNC Charlotte Faculty Research Grant I & II, Major League Baseball, OrthoCarolina Research Institute, Travel Grant from the Center of Biomedical Engineering and Science of UNC Charlotte, as well as UNC Charlotte Graduate Assistant Support Plan (GASP) awards.

## DEDICATION

To my parents, Wang Xingbang, Wang Shuixiu and sister, Wang Qingfang.

## TABLE OF CONTENTS

LIST OF TABLES	x
LIST OF FIGURES	xii
LIST OF ABBREVIATIONS	xvi
CHAPTER 1: INTRODUCTION	1
1.1. Anatomy of the Knee	1
1.2. ACL Injury and Long-term Impact on the Joint Function	5
1.3. ACL Reconstructive Surgery	8
1.4. Relevant Literature Review of Experimental Studies	13
1.5. Relevant Literature Review of Computational Biomechanics	17
1.6. Objectives and Framework	20
CHAPTER 2: DATA COLLECTION AND MOTION ANALYSIS ALGORITHM	22
2.1. Techniques for Bone Motion Measurement	22
2.2. Investigation of Soft Tissue Movement on Lower Extremities	28
2.2.1. Introduction	28
2.2.2. Material and methods	30
2.2.3. Results	34
2.2.4. Discussion	36
2.2.5. Conclusion	42
2.3. An Algorithm Using the Characteristics of Soft Tissue Movement	43
2.3.1. Introduction	43
2.3.2. Material and methods	45
2.3.3. Results	51
2.3.4. Discussion	55

	viii
2.3.5. Conclusion	58
2.4. Summary	58
CHAPTER 3: DOES THE TRANSTIBIAL TECHNIQUE RESTORE KNEE KINEMATICS AND KINETICS?	60
3.1. Knee Joint Stability Following ACL-reconstruction Using the Transtibial Technique during Level Walking	60
3.1.1. Introduction	60
3.1.2. Material and methods	62
3.1.3. Results	66
3.1.4. Discussion	71
3.1.5. Conclusion	75
3.2. Knee Joint Stability Following ACL-reconstruction Using Transtibial Technique during Downstairs Pivoting	75
3.2.1. Introduction	76
3.2.2. Material and methods	78
3.2.3. Results	83
3.2.4. Discussion	85
3.2.5. Conclusion	90
3.3. Summary	91
CHAPTER 4: DOES THE ANTEROMEDIAL PORTAL TECHNIQUE IMPROVE POSTSURGICAL KNEE PERFORMANCE?	92
4.1. Knee Joint Stability Following ACL-reconstruction Using Anteromedial Portal Technique during Level Walking	92
4.1.1. Introduction	92
4.1.2. Material and methods	95
4.1.3. Results	97
4.1.4. Discussion	106

	ix
4.1.5. Conclusion	109
4.2. Knee Joint Stability Following ACL-reconstruction Using Anteromedial Portal Technique during Downstairs Pivoting	110
4.2.1. Introduction	110
4.2.2. Material and methods	110
4.2.3. Results	111
4.2.4. Discussion	112
4.2.5. Conclusion	113
4.3. Summary	113
CHAPTER 5:FINITE ELEMENT MODELING TO THE KNEE JOINT	114
5.1. Introduction	114
5.2. Material and Methods	115
5.2.1. Geometry reconstruction and mesh generation	115
5.2.2. Material properties	120
5.2.3. Boundary condition and loading	126
5.2.4. Finite element solution	131
5.3. Results	132
5.4. Discussion	138
CHAPTER 6: SUMMARY AND CONCLUSIONS	143
6.1. Summary	143
6.1.1. The novelties and strengths	143
6.1.2. Key points learned from this study	144
6.2. Future Directions	146
REFERENCES	149

## LIST OF TABLES

TABLE 1.1 Summary of recent publications about knee joint kinematics after unilateral ACL-reconstruction.	16
TABLE 1.2 Summary of previous finite element studies of human knee joint.	19
TABLE 2.1 the root mean square (RMS) errors (mean $\pm$ standard deviation) ( $^{\circ}$ ; mm) of skin marker based knee motion measurement. (Gao et al., 2007)	27
TABLE 2.2 Subject information (BMI-body mass index, HS-hamstring tendon, PT-patellar tendon).	30
TABLE 2.3 <i>S</i> values (involved, contralateral) of inter-subject similarity for skin rotations on the shank and thigh. AP-around anterior/posterior axis, ML-around medial/lateral axis, SI-around superior/inferior axis	34
TABLE 2.4 The range of skin stretches (mean $\pm$ std, unit: mm) at different locations on the thigh relative to the reference triad T7 during a complete gait cycle and their correlation with the nominal radius of thigh for the ACL reconstructed legs.	39
TABLE 2.5 The range of skin stretches (mean $\pm$ std, unit: mm) at different locations on the shank relative to the reference triad S3 during a complete gait cycle and their correlation with the nominal radius of shank for the ACL reconstructed legs.	41
TABLE 2.6 Pearson coefficients ( <i>r</i> ) of correlation between the range of skin stretches and segmental nominal radius. AP-anterior/posterior, ML-medial/lateral, SI-superior/inferior	42
TABLE 2.7 Root mean square error (RMS-E) and peak error (Peak-E) (unit mm for AP, ML, SI translations; unit ( $^{\circ}$ ) for FE, IE, VV rotations) for three motion analysis algorithms (LMS, BLC and PCT) in predicting knee joint kinematics. Mean (standard deviation).	52
TABLE 3.1 Demographics (mean (SD)) of patients with ACL reconstruction on the dominant side (Group-d) and patients with ACL reconstruction on the non-dominant side (Group-n) and the healthy controls; BMI: body mass index.	63
TABLE 3.2 Demographics (mean (SD)) of patients with ACL reconstruction on the dominant side (Group-d) and patients with ACL reconstruction on the non-dominant side (Group-n) and the healthy controls; BMI: body mass index.	80

TABLE 4.1 Demographics (mean (SD)) of patients with ACL reconstruction on the dominant side (Group-d) and patients with ACL reconstruction on the non-dominant side (Group-n) and the healthy controls; BMI: body mass index	96
TABLE 4.2 Spatial parameters of gait for different groups. Mean (standard deviation).	102
TABLE 4.3 Peak values of knee joints loading for different groups. Mean (standard deviation).	105
TABLE 5.1 Properties of solid elements of each part.	119
TABLE 5.2 Material properties used for cartilage, meniscus and bone. <sup>1</sup> fCart – femoral cartilage, <sup>2</sup> tCart – tibial cartilage	121
TABLE 5.3 Material properties used for the ligaments.	123
TABLE 5.4 Moment arm and line of action of muscles at different knee flexion adapted from (Yang et al., 2010).	126
TABLE 5.5 Interaction and constraint.	128
TABLE 5.6 ACL/graft tension at different key frames. (unit: N)	141

## LIST OF FIGURES

FIGURE 1.1 Anatomy of human knee joint (left) ( <a href="http://www.fencing.net/548/acl-injuries-rehabilitation/">http://www.fencing.net/548/acl-injuries-rehabilitation/</a> ), 3D knee joint model (middle and right).	2
FIGURE 1.2 (1) Double-bundle structure of natural ACL, (2) Computer model of the bones after anatomic double-bundle ACL reconstruction (Fu, 2011).	3
FIGURE 1.3 Important structural features of a typical diarthrodial joint at different hierarchical scales (Mow et al., 2005).	5
FIGURE 1.4 ACL reconstruction procedure, the surgery is being performed arthroscopically using an autograft cut from patella tendon. ( <a href="http://www.beantownphysio.com/pt-tip/archive/acl-tears.html">http://www.beantownphysio.com/pt-tip/archive/acl-tears.html</a> )	9
FIGURE 1.5 Femoral tunnel drilling in transtibial and anteromedial portal femoral drilling techniques.	12
FIGURE 1.6 Diagrams of commonly used fixation techniques for ACL graft. A – BTB, B and C – hamstring tendon.	12
FIGURE 2.1 Protocol of marker placement in optical video motion analysis.	23
FIGURE 2.2 Procedure of reproducing in vivo knee kinematics with use of the combined dual fluoroscopic and magnetic resonance imaging technique (Defrate et al., 2006).	24
FIGURE 2.3 Position vectors of thigh skin markers in GCS and LCS at the reference posture (left) and at a dynamic instant- $t$ (right).	26
FIGURE 2.4 The flowchart of retrieving the knee joint rotation and translation from skin markers.	27
FIGURE 2.5 Cadaver setup with skin markers and bone-pin markers.	28
FIGURE 2.6 Lower limb's nominal radius were measured from subject's 3D body scan.	32
FIGURE 2.7 Inter-marker translations on the thigh during walking.	35
FIGURE 2.8 Inter-marker translations on the shank during walking.	36
FIGURE 2.9 Linear regression between the range of skin stretches and nominal radius of thigh cross section at 3 different rows in three orthogonal directions during walking.	37

- FIGURE 2.10 Linear regression between the range of skin stretches and nominal radius of shank cross section at 3 different rows in three orthogonal directions during walking. 40
- FIGURE 2.11 The moving spaces of skin markers at medial-lateral epicondyles (T10/T11), medial-lateral tibia plateau edges (S1/S2), and tibia tuberosity (S11). At T10, T11, S1, and S2 locations, only medial-lateral direction displacements are constrained. At location S11, the displacement constraints are exerted on all three anatomical directions. 47
- FIGURE 2.12 Definitions of knee joint rotations angle by a projection method. 50
- FIGURE 2.13 The results of knee joint 6 degrees of freedom (3 rotations and 3 translations) using three different optimization algorithms. Baseline – the true bone motion from bone pins, LMS – traditional least-mean-square based algorithm, PCT – point cluster technique, BLC – improved algorithm considered bony landmark constraints. 54
- FIGURE 2.14 The accuracy of BLC algorithm in predicting secondary tibiofemoral rotation and medial-lateral translation under different moving limits. 55
- FIGURE 3.1 Subplot A-C: knee joint rotation for dACLr, nUnInv, nACLr and dUnInv knees during a gait cycle; subplot D-F: knee joint translation during a gait cycle. Knee flexion, varus and internal tibia rotation were illustrated as positive values; anterior, medial and superior translations (femur relative to tibia) were illustrated as positive values. 68
- FIGURE 3.2 Knee joint rotation angles for different groups at several key events. Int. rot @ flex peak of stance: the internal tibial rotation angle at the peak flexion instant of stance phase; Flexion valley: minimal flexion during middle stance phase; t-pose: neutral standing as the reference frame. Error bars represent the standard derivation. (\* $p < 0.05$  student's  $t$  test) 70
- FIGURE 3.3 Knee adduction moment (exerted by shank) for dACLr, nUnInv, nACLr and dUnInv knees during a gait cycle. \* denotes significant difference between dACLr and nUnInv ( $p < 0.05$ ). 71
- FIGURE 3.4 Root mean square of bilateral differences of knee joint VV rotation over a gait cycle. The shade area denotes the 95% confidence interval of the mean. The dACLr knees showed a statistically significant valgus offset of  $-2.4 \pm 2.3$  ( $p < 0.01$ ) relative to nUnInv knees, whereas no systematic difference existed between nACLr and dUnInv. 72
- FIGURE 3.5 Front and lateral radiographs of a typical patient taken 3 months after ACL-reconstruction surgery using transtibial single-bundle technique. 79
- FIGURE 3.6 Subject turns to the same of the supporting leg (left turn shown). IC – initial contact, TO – toe off. 81

FIGURE 3.7 Knee rotation and moment on the transverse plane from the initial contact (IC) to the toe off (TO) during downstairs turning. Dominant and non-dominant knees were plotted separately. Error bar denotes $\pm 1$ standard deviation of the control group. * $p < 0.05$ .	83
FIGURE 3.8 Knee rotation and moment on the frontal plane from the initial contact (IC) to the toe off (TO) during downstairs turning. Dominant and non-dominant knees were plotted separately. Error bar denotes $\pm 1$ standard deviation of the control group. * $p < 0.05$ .	85
FIGURE 3.9 Boxplot of the bilateral difference (ACLR minus ACLI) of the first peak varus rotation and the first peak external knee adduction moment with whisker length in 1.5 units of interquartile range (IQR). + Outliers.	87
FIGURE 4.1 Knee rotations and translations during a gait cycle. HS-heel strike, FP1-flexion peak during stance phase, FV-flexion valley, TO-toe off, FP2-flexion peak during swing phase. Translations represented the displacement of femoral origin in tibial ACS.	99
FIGURE 4.2 Timings of key events in the gait cycle for transtibial, AMP and healthy groups. The gait cycle was normalized from one heel strike (0%) to the next heel strike (100%).	100
FIGURE 4.3 Knee joint rotation at static posture. TT-transtibial ACL-reconstruction, AMP-anteromedial portal ACL-reconstruction.	101
FIGURE 4.4 Normalized external knee joint forces and moments during a gait cycle. HS-heel strike, FP1-flexion peak during stance phase, FV-flexion valley, TO-toe off, FP2-flexion peak during swing phase. The forces and torques are expressed in tibial ACS.	104
FIGURE 4.5 Diagram of graft orientation in 3d knee joint model (reconstructed from a typical patient's MR images) for different ACL-reconstruction techniques	109
FIGURE 4.6 Knee rotation and external knee axial moment on the transverse plane from the initial contact (IC) to the toe off (TO) during downstairs turning. Dominant and non-dominant knees were plotted separately. Error bar denotes $\pm 1$ standard deviation of the control group.	111
FIGURE 4.7 Knee rotation and external adduction moment on the frontal plane from the initial contact (IC) to the toe off (TO) during downstairs turning. Dominant and non-dominant knees were plotted separately. Error bar denotes $\pm 1$ standard deviation of the control group. * $p < 0.05$	112
FIGURE 5.1 Medical image segmentation for a typical subject in Mimics.	116

FIGURE 5.2 Process of surface extraction for the femur in Geomagic™. A – auto detect contour, B – create contour lines, C – construct patches, D – fit surfaces.	117
FIGURE 5.3 Assembly of FE knee model in ABAQUS.	119
FIGURE 5.4 Medical image segmentation, smoothing and NURB surface creation and mesh generation.	120
FIGURE 5.5 ACL-reconstruction using single bundle STG graft. The figure of insertion sites were adapted from Kopf et al. (Kopf et al., 2010)	124
FIGURE 5.6 External flexion/extension moment and the activation muscles during stance phase of level walking. The insets show the knee joint posture and activated muscle respectively at HS, CTO, CHS and TO.	126
FIGURE 5.7 Boundary conditions and loading in ABAQUS. Ligaments and meniscus horn attachments were modeled as springs. aACL anteromedial bundle, pACL posterolateral bundle.	128
FIGURE 5.8 Calculation of knee joint loading.	129
FIGURE 5.9 Total knee force during stance phase for different knees. The compressive force was the axial force and the shear force was the posterior force exerted on the femur in the FE model.	130
FIGURE 5.10 The adduction moment at knee joint during stance phase.	131
FIGURE 5.11 The contour of pressure on femoral cartilage surface at different key frames during stance phase. The numbers on the contour denote the maximum values of pressure.	134
FIGURE 5.12 Stress contour within tibial cartilage at different key frames during stance phase. The numbers on the contour denote the maximum values of pressure.	135
FIGURE 5.13 The normal load carried by the medial and lateral tibial compartments in different knees.	136
FIGURE 5.14 Anterior/posterior tibial translation. The tibial translation was reported as the opposite value of the femoral translation.	137
FIGURE 5.15 Internal tibial rotation and varus knee rotation. The internal tibial rotation was reported as the external femoral rotation.	138

## LIST OF ABBREVIATIONS

ACL	Anterior cruciate ligament
ACLD	ACL-deficient
ACLR	ACL-reconstructed
ACLI	ACL-intact
AMP	Anterior medial portal
AP	Anteroposterior
BLC	Bony landmark constraint
BMI	Body mass index
CHS	Contralateral heel strike
CT	Computed tomography
CTO	Contralateral toe-off
DOF	Degree of freedom
FE	Finite element
FE valley	Minimum knee flexion during midstance
GCS	Global coordinate system
HS	Heel strike
IE	Internal/external
IRB	Institutional review board
LCS	Local coordinate system
LMS	Least mean square
ML	Mediolateral
MRI	Magnetic resonance imaging

PCT	Point cluster technique
ROM	Range of motion
RMS	Root mean square
SD	Standard derivation
SI	Superior/inferior
STA	Soft tissue artifact
TO	Toe off
UnInv	Uninvolved
VV	Varus/valgus
1 <sup>st</sup> FE peak	Maximum knee flexion during the stance phase
2 <sup>nd</sup> FE peak	Maximum knee flexion during the swing phase
3D	3-dimensional
2D	2-dimensional
$O(0)$	Initial position of bone local origin in GCS
$O(t)$	Position of bone local origin in GCS at frame $t$
$O_{femur}(0)$	Global position of femur origin at reference posture
$P_iG(t)$	Global position of the $i^{th}$ marker at frame $t$
$P_iL(0)$	Position vector of the $i^{th}$ marker in LCS at the reference posture
$P_iL(t)$	Position vector of the $i^{th}$ marker in LCS at the frame $t$
$P_{T10}G(0)$	Global Position of T10 marker at reference posture
$P_{T10}G(t)$	Global Position of T10 marker at the frame $t$
$[R(t)]$	Rotation matrix of a segment at $t$ frame
$\vec{V}(t)$	Translation vector of a segment at frame $t$

## CHAPTER 1: INTRODUCTION

This chapter provides a basic knowledge of the knee joint, including the anatomy, anterior cruciate ligament (ACL) injuries and their long term impact on the joint function, as well as a review of previous experimental studies on knee joint kinematics and computational studies on knee joint loading. The objectives of this study were to investigate the postsurgical outcomes of knee joints after ACL-injury and reconstruction, and to compare the effectiveness of the two most commonly used surgical techniques in stabilizing the knee joint.

### 1.1. Anatomy of the Knee

The knee consists of four main parts: bone (femur, tibia and patella), ligament, cartilage and meniscus (FIGURE 1.1). The femur has two condyles (the medial and the lateral condyles) which individually have an articulation with the tibial plateau (proximal tibial surface). The third articulation is the femoropatellar articulation, which consists of the patella and the patellar groove on the front side of the femur bone through which it slides. The patella acts as a pulley which transmits the quadriceps muscle force to the tibia through the quadriceps tendon and the patellar tendon. The meniscus is a wedge shape fibrocartilage structure and is located between the tibial and femoral cartilage on the medial side and lateral side respectively. The horns of meniscus are attached to the tibial plateau.

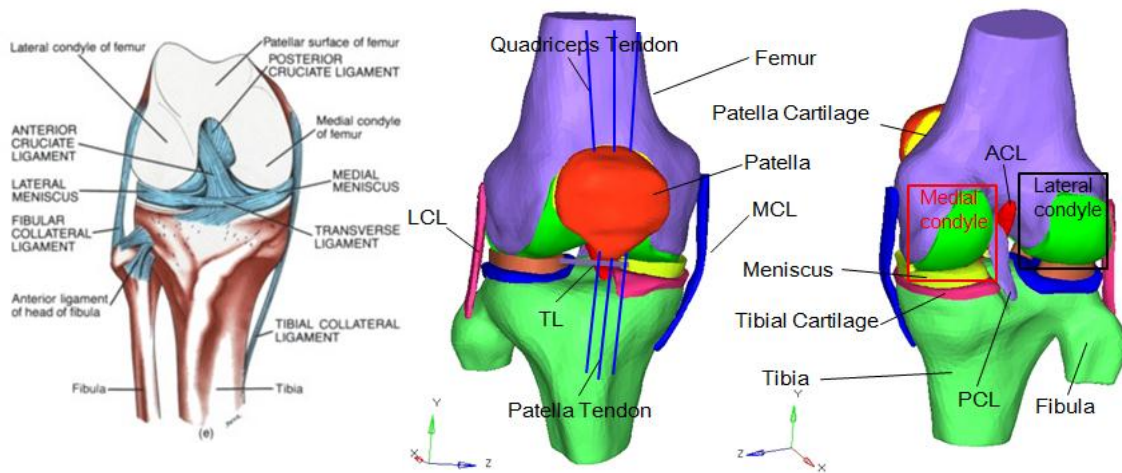


FIGURE 1.1 Anatomy of human knee joint (left) (<http://www.fencing.net/548/acl-injuries-rehabilitation/>), 3D knee joint model (middle and right).

The smart “design” of human joints avoids direct bone-to-bone contact; instead, there are articular cartilages (tibial cartilage, femoral cartilage and patellar cartilage) and menisci that lie between the bones which act as the lubricant and stabilizer. Additionally, the knee joint motion is constrained by four primary stabilizing ligaments: anterior cruciate ligament (ACL), posterior cruciate ligament (PCL), medial collateral ligament (MCL) and lateral collateral ligament (LCL). The ACL and PCL are intra-articular ligaments (inside joint capsule) which go in opposite directions between the femur and the tibia (FIGURE 1.1). The MCL and LCL are extra-articular ligaments that connect the femur to the tibia/fibula on the medial and lateral sides of the joint respectively. The transverse ligament (TL) connects the anterior horns of the medial and lateral meniscus.

Natural ACL consists of two bundles – the anteromedial (AM) bundle and the posterolateral (PL) bundle, named according to where the bundles insert into the tibial

plateau. The bundles attach to the deep notch of the distal femur (FIGURE 1.2), and come out along the medial wall of the lateral femoral condyle. The ACL attaches in front of the intercondyloid eminence of the tibia, being blended with the anterior horn of the medial meniscus. These attachments allow it to resist anterior translation and internal tibial rotation, in relation to the femur.

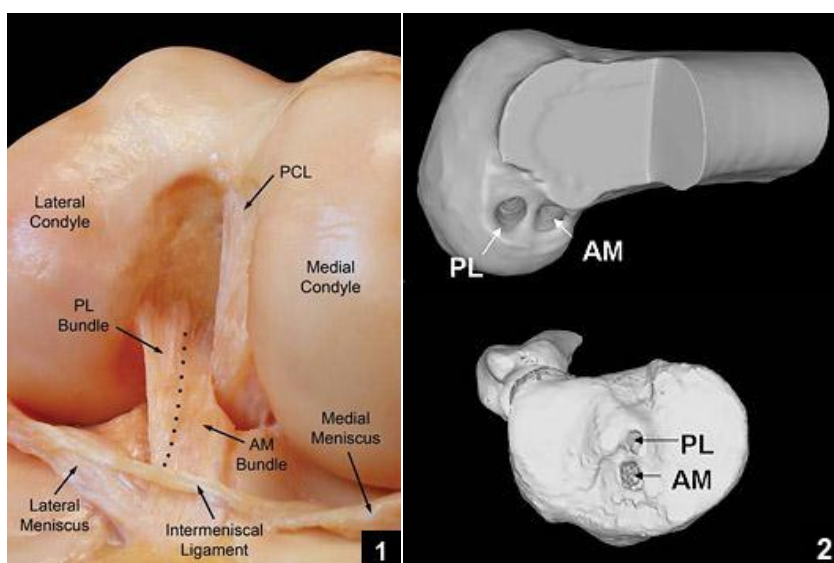


FIGURE 1.2 (1) Double-bundle structure of natural ACL, (2) Computer model of the bones after anatomic double-bundle ACL reconstruction (Fu, 2011).

Cartilage mainly consists of water which accounts for 60 to 80 percent and cartilage matrix which is made up of collagen, proteoglycans, and chondrocytes. Collagen is a family of fibrous proteins ensuring the elasticity and the ability to absorb shock in the cartilage. It is also referred to as the “glue” that holds the cartilage matrix together (Mow et al., 2005). Proteoglycans are big molecules made up of protein and sugars which interweave with collagen fibers to form a dense mesh-like tissue (FIGURE 1.3). This structure makes cartilage so resilient that it can stretch out when loaded and

bounce back when released. Chondrocytes are the only cells found within the cartilage matrix; they keep producing new collagen and proteoglycan molecules to help the cartilage stay healthy when the cartilage grows. Chondrocytes also produces enzymes that get rid of the aging collagen and proteins. In the healthy knee, the cartilage matrix and water work together to ensure smooth, pain-free knee motion. Normally, when the knee joint is at rest, cartilage soaks up liquid (synovial fluid); when the joint is under loading and in motion, the liquid is squeezed out. This continual in and out "squishing" happens hundreds of times during the course of a day. If the balance is broken, either by acute trauma or degenerative joint diseases (like osteoarthritis or rheumatoid arthritis), the protective barriers are disturbed, and cartilage erosion may be initiated. The cartilage degeneration usually begins in the cartilage matrix.

During daily walking, the knee joint bears as much as two times the body weight impact (Kutzner et al., 2011a, Kutzner et al., 2011b); it is also subject to constant twisting and grinding. Thus, abnormal or excessive repetitive loading at the joint surface could accelerate the wear of the knee cartilage matrix. In severe cases, orthopedic surgeons have to replace the patients' joints with artificial joints to restore their mobility. Nowadays, total knee replacement surgery has become a commonly performed orthopedic surgery among people over 60.

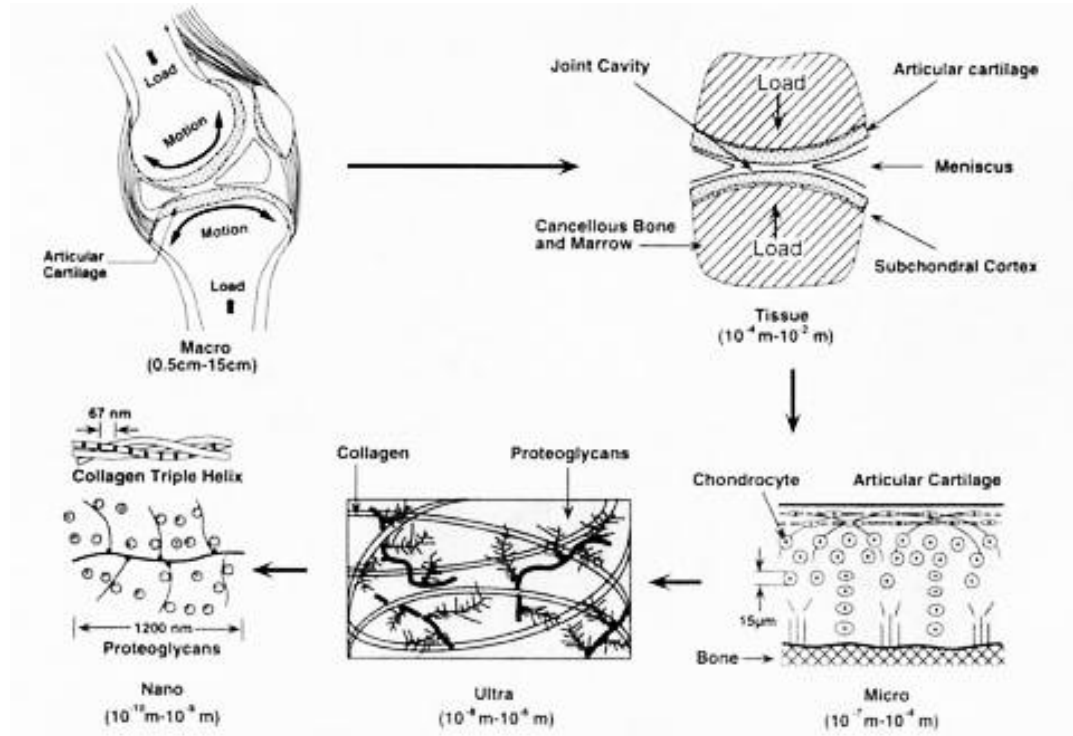


FIGURE 1.3 Important structural features of a typical diarthrodial joint at different hierarchical scales (Mow et al., 2005).

## 1.2. ACL Injury and Long-term Impact on the Joint Function

As a primary stabilizer of the knee, the ACL mainly prevents the tibia bone from excessively moving forward as well as restrains the internal tibial twisting during turning or side-stepping activities (Markolf et al., 1995). ACL injuries usually happen when the knee joint is hyperextended, twisted, or bent side to side; the risk is even higher when more than one of those movements occurs at the same time. Thus, ACL rupture is very common in sports activities, such as playing soccer, golf, skiing, and basketball, etc. Non-contact ACL tears (accounts for 80% in total) are the most frequent ligament injury in sports, especially among elite female athletes (Alentorn-Geli et al., 2009, Brophy et al., 2010, McLean et al., 2005, Negrete et al., 2007). A popping sensation can often be felt at the time of injury.

There are about 250,000 new ACL injuries each year in the US according to the data from the Centers for Disease Control and Prevention. After ACL rupture, patients often have a symptom of the knee “giving-out”, and their knee joint stability and load-bearing patterns between joint surfaces are often altered, resulting in abnormal loadings within the articular cartilage during daily activities (Chaudhari et al., 2008, Li et al., 2006). Without the ACL, excessive anterior tibial translation, medial tibial translation and internal tibial rotation were found in the knee joint during a quasi-static lunge (Defrate et al., 2006); abnormal knee joint kinematics has also been reported during level walking (Gao and Zheng, 2010a, Georgoulis et al., 2003, Andriacchi and Dyrby, 2005), stairs climbing (Gao et al., 2012) and pivoting (Ristanis et al., 2005) after ACL-rupture. The abnormal joint motion and loading has been associated with meniscal injuries, progressive cartilage degeneration and early onset of knee osteoarthritis (OA) (Andriacchi and Mundermann, 2006, Stergiou et al., 2007). Osteoarthritis has been found in 41% of the untreated ACL-deficient knees 11 years after the ACL-rupture (Noyes et al., 1983). Nebelung and Wuschech reported that 79% of the ACL-deficient knees had to receive meniscectomy surgery after 10 years, and 53% of the knees ended up with total knee replacements due to severe chondral lesion and cartilage damage (Nebelung and Wuschech, 2005).

Although nonsurgical treatments (i.e. knee bracing, physical therapy and rehabilitation) sometimes can restore the knee to a condition close to its pre-injury state (Buss et al., 1995), reconstructive surgeries are typically recommended, especially for those who want to keep active in sports (Woo et al., 2005). There are about 70,000 to 100,000 ACL reconstruction surgeries performed annually in the US (Gammons, 2011,

Fu and Cohen, 2008). The medical bill for ACL reconstruction ranges from \$20,000 to \$50,000 in the US (data from healthy.costhelper.com). Although the ACL-reconstructive surgeries can successfully restore the knee function, it may not fully reproduce the inherent joint kinematics and kinetics during dynamic activities (Gao and Zheng, 2010a, Georgoulis et al., 2007, Ristanis et al., 2003, Ristanis et al., 2005, Scanlan et al., 2010, Wang et al., 2012, Webster and Feller, 2011, Webster et al., 2012, Tashman et al., 2007). Previous investigations reported that the traditional ACL-reconstructive surgery cannot successfully prevent the cartilage degeneration and premature OA in the long term (Lohmander et al., 2004, Seon et al., 2006, Daniel et al., 1994, Holm et al., 2010), which might be caused to by the residual alteration in knee joint motion and loading after ACL reconstructive surgeries.

Osteoarthritis is the most common type of arthritis, and the percentage of people who have the disease is higher among old people. In the US, there are approximate 27 million people age 25 or older have osteoarthritis (Lawrence et al., 2008). The average out-of-pocket expense cost of OA is \$2,600 per year for a patient (Gabriel et al., 1997). The cartilage degeneration and bone scratch would cause knee pain and lead to joint replacements in the end. The financial burden was approximately \$7.9 billion in 1997 for all knee and hip replacements in the US (Lethbridge-Cejku et al., 2003). The cost of labor loss due to disability caused by OA was even greater. Moreover, since the joint replacement implants only last for 15 to 20 years, for those who received total joint replacement at relative young age (<60), revision of the failing artificial knee/hip joints is needed. (Meier, December 27, 2011).

Since ACL injuries occur commonly in individuals aged 14-29 years (Souryal, 2012), there will be a series of severe consequences if the ACL-reconstruction surgery is not performed well. For instance, a collegiate soccer player tore his ACL at 18 years old and returned to the field after he received ACL reconstruction surgery. Somehow, after the surgery, his knee still had abnormal joint motion; this would accelerate the cartilage degeneration. It is most likely that his knee joint surface will wear down, and it will be painful to do daily activities in 15-20 years (when he is about 40 years old). However, there is a great risk for him to receive total knee joint replacement in his 40s, because the total joint implants usually only last for 10-15 years ([www.zimmer.com](http://www.zimmer.com)). In this case, he has to receive an implant revision at 55, which usually only lasts about another 5 years. After that, he will end up staying in wheelchair when he is 60 years old. Therefore, if we can stop the vicious circle at the very beginning by improving the ACL-reconstruction technique, it will significantly reduce the suffering of the patient and cut down the financial burden on society.

### 1.3. ACL Reconstructive Surgery

The basic procedure of ACL reconstruction surgery is shown in the following diagram (FIGURE 1.4): 1) remove the damaged ACL and clean up the debris using arthroscopic technique, 2) cut an incision from the patella to the proximal tibia in front of the knee, 3) drill femoral and tibial tunnels for graft fixation, 4) harvest auto graft from patellar tendon or hamstring tendon, or prepare allograft, and 5) insert the graft into the tunnels and fix it.

A number of factors could potentially affect the outcome of the surgery. Among them are the graft type (i.e. hamstring tendon vs. patella tendon, allograft vs. autograft, single bundle vs. double bundle), tunnel position, graft orientation, and initial graft

tension are of great interest to the orthopedic researchers, although previous studies have found that the type of graft had no or minor effect on the postsurgical knee performance (Moraiti et al., 2009, Spindler et al., 2004). There were no studies found comparing the in vivo knee joint motion and loading after ACL reconstruction with different graft orientations and tunnel positions.

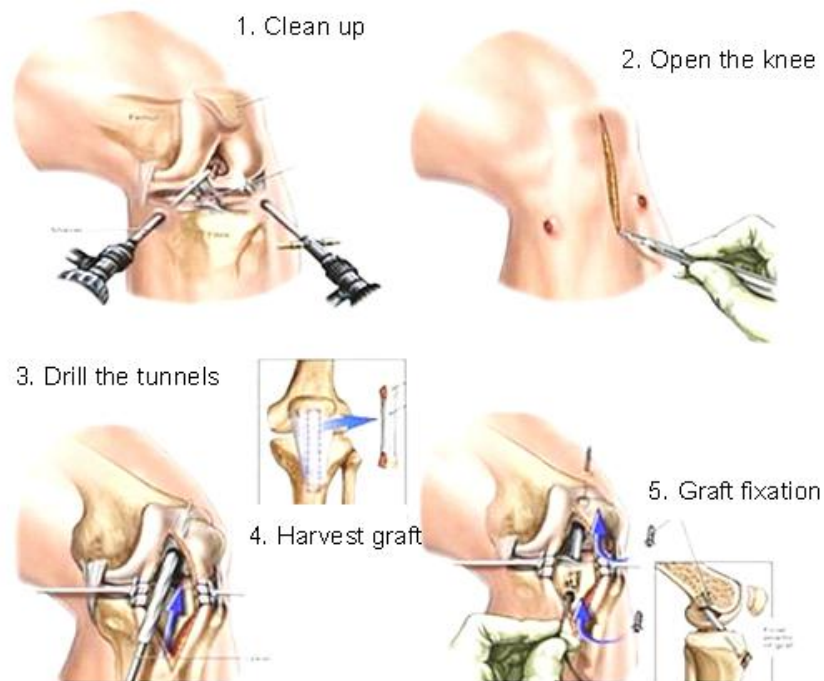


FIGURE 1.4 ACL reconstruction procedure, the surgery is being performed arthroscopically using an autograft cut from patella tendon. (<http://www.beantownphysio.com/pt-tip/archive/acl-tears.html>)

There are heated debates about the necessity and risk of performing double bundle ACL reconstruction. Since double-bundle grafts are closer to the anatomy of natural ACL, they have better ability to restore the knee joint rotational stability; however it requires four tunnels drilled instead of two into the bones which increases the operational complexity and causes more bone damage. Paul Trikha, who was a consultant orthopedic

surgeon specializing exclusively in knee surgery, did an on-site survey concerning the selection of double-bundle ACL-reconstruction. In his article entitled “Double bundle, traditional single bundle or 'more anatomic' single bundle ACL reconstruction?” wrote (<http://www.kneeguru.co.uk/KNEEnotes/node/2447>):

“In the UK, I think the number of double bundle procedures being performed is going down. In 2010, I was at a major knee meeting in Warwick and it seemed then that all the talk was about double bundle! This year (2012) they did a quick hands-up survey - accepting that a few of the leading knee surgeons in the country weren't there - but most were - when asked how many surgeons were routinely doing double bundle ACL reconstructions **not one** hand went up.

I think surgeons are gradually coming round to the important concept of anatomic single bundle reconstruction with the graft placed in a mid-bundle position on the femur through an independent femoral tunnel drilled through an appropriate medial portal. This allows both the femoral and tibial tunnels to be placed accurately and independently. This technique is straightforward, predictable and reproducible although it presents technical challenges for the traditional transtibial technique advocates.”

The more anatomic single bundle ACL reconstruction has received more and more attention among orthopedic surgeons, which is thought of as a practicable alternative to the complicated double-bundle ACL reconstruction for a more stable and functional knee. In the traditional transtibial tunnel drilling technique, the femoral tunnel is drilled through the tibial tunnel (FIGURE 1.5), in which the position of the femoral tunnel depends on the initial tibial tunnel location, and the femoral insertion of the ACL graft is often anteriorly and superiorly shifted compared to the natural ACL insertion site

(Piasecki et al., 2011) The graft is often too vertical using the transtibial technique. In the anteromedial portal (AMP) tunnel drilling technique, the femoral tunnel is drilled through the anteromedial arthroscopic portal (FIGURE 1.5). This allows the surgeon to have more control at the drilling location, thus it yields a more anatomic tunnel position and optimizes the orientation of the reconstructed ligament (Kopf et al., 2010). There are, however, some limitations when performing AMP ACL-reconstructive surgery: the knee needs to be hyper-flexed ( $>100^\circ$ ), and it demands extra effort to stabilize the knee. Therefore, for obese patients who cannot bend their knees that much, the surgeon has to make a compromise in continuing use of the transtibial technique.

The graft fixation also varies case by case. For most Bone-Patella Tendon-Bone (BPTB) graft cases, interference screws are used at the tibial fixation site and femoral fixation site (FIGURE 1.6 A). There has been a surge of interest in the use of hamstring tendon grafts due in part to improvements in the graft fixation technique (FIGURE 1.6 B-C). Concerns have been raised about the increased length of the graft when it was not fixed right at the insertion site which could cause a loss of graft stiffness and therefore create a 'bungee cord' effect.

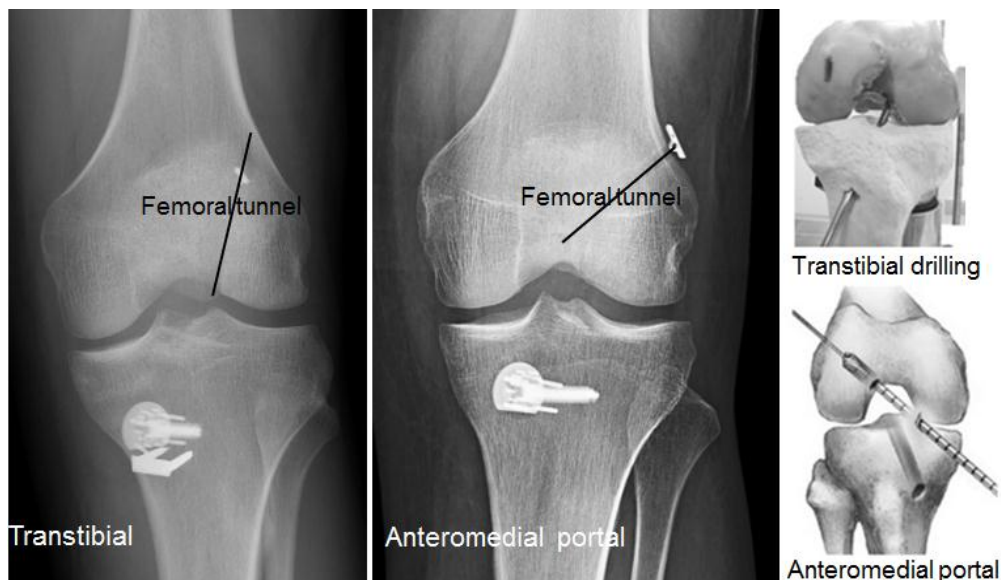


FIGURE 1.5 Femoral tunnel drilling in transtibial and anteromedial portal femoral drilling techniques.

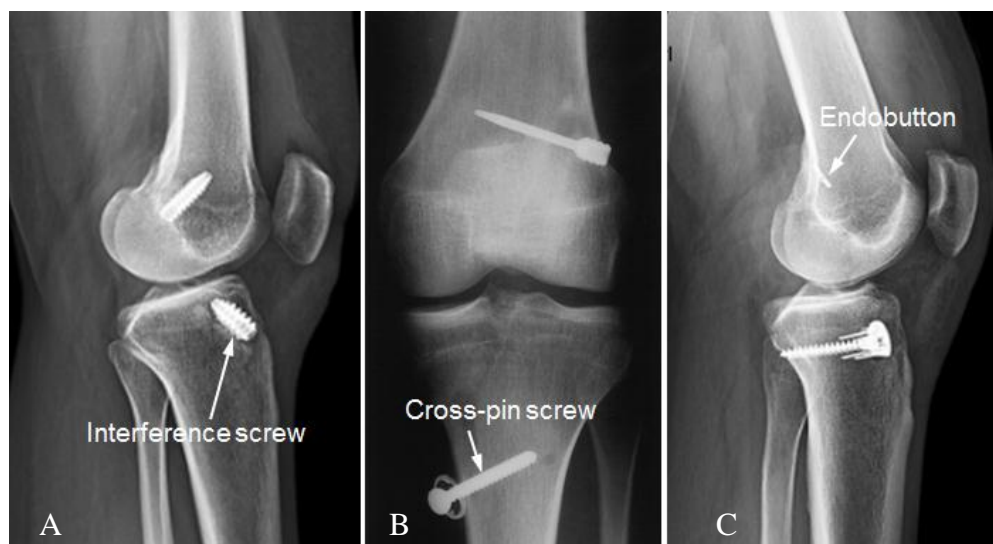


FIGURE 1.6 Diagrams of commonly used fixation techniques for ACL graft. A – BTB, B and C – hamstring tendon.

In this study, we aimed to evaluate and compare the postsurgical knee joint biomechanics after ACL-reconstruction by using non-anatomical (traditional transtibial) and more anatomical (anteromedial portal) tunnel drilling techniques.

#### 1.4. Relevant Literature Review of Experimental Studies

##### 1) Knee kinematics during quasi-static lunge

By using dual-fluoroscopic imaging and 3D modeling technique, Defrate et al. investigated the knee joint kinematics of ACL-deficient knees (Defrate et al., 2006). According to their findings, the ACL-deficient knees had significantly greater anterior tibial translation and internal tibial rotation at low flexion angles and had a medial tibial translation between 15 ° to 90 ° of knee flexion. By using the same technique, Li et al. investigated the contacting pattern of articular cartilage in the ACL-deficient knees (Li et al., 2006). The results showed that on the medial compartment the contacting center shifted towards the posterior and medial tibial spine, a region where degeneration was observed in patients with chronic ACL injuries. In another study from the same research group, Kozanek et al. proved that the kinematics of the uninjured contralateral knees was not affected by the ipsilateral ligament injury in the short term (Kozanek et al., 2008). Papannagari et al. investigated the in vivo knee kinematics during single-legged weight-bearing lunge after ACL-reconstruction (Papannagari et al., 2006); the results suggested that the restored knee laxity during a passive test (KT-1000 test) did not guarantee a fully restored normal knee kinematics during physiological loading conditions.

Unfortunately, so far the imaging technique has been limited to study the quasi-static situations due to the confined measurement volume. Therefore, the findings may not truly reflect the large range of motion during daily activities, i.e. straight walking and turning, etc. Moreover, the high radiation dose also excludes researchers from studying the knee joint kinematics using a large sample size.

## 2) Knee kinematics during level walking

Georgoulis et al. conducted a case control study comparing the knee joint kinematics between ACLR, ACLD subjects to the healthy controls (Georgoulis et al., 2003). According to that study, the normal patterns of knee rotations were maintained by all subjects. The rotational instability during early swing phase in ACLD subjects was basically restored by ACL-reconstruction. Whereas, Gao and Zheng found that the secondary kinematic alterations were not eliminated by ACL-reconstruction and a greater internal tibial rotation and varus rotation still existed in the ACLR knee (Gao and Zheng, 2010a). Scanlan et al. reported a significant offset towards external tibial rotation (reduced internal tibial rotation) in the ACLR knees compared to their contralateral knees throughout the whole stance phase (Scanlan et al., 2010). Webster and Feller also found a reduced internal rotation as well as a reduction in varus rotation in the ACLR knees compared to the healthy controls (Webster and Feller, 2011).

The large inconsistencies across studies may be caused by the differences in the methodologies. In Georgoulis's and Webster's studies, a simplified marker set was used which has limited accuracy in measuring the knee motion, especially the secondary rotation, due to the soft tissue artifact (Leardini et al., 2005). In Gao's study, the patients were recruited from more than one surgeon, and both patellar tendon graft and hamstring graft were used, which may contribute to the high variances. In Scanlan's study, no healthy controls were recruited, and the contralateral limbs may not be powerful enough to uncover the abnormalities in the involved limbs, since the motion of the contralateral limbs may also be affected by ACL injury.

### 3) Knee kinematics during high demand activities

Ristanis and the coauthors investigated rotational knee stability during landing and subsequent 90 ° pivoting (Ristanis et al., 2005). They found significant differences in knee joint kinematic between the ACLR knees and the healthy controls, which suggested that ACL reconstruction may not fully restore the tibial rotation to its pre-injury state. Whereas, Webster and Feller found that the ACLR knees had a reduced internal rotation compared to the healthy controls during pivoting (Webster and Feller, 2011), which indicated that the ACL reconstruction may have over corrected the knee stability. Lam et al. studied the jump-landing and pivoting task among ACL patients pre- and post- surgery (Lam et al., 2011). According to the results, the increased tibial rotation in the ACL-deficient knees was reduced and the significant bilateral differences were gone after ACL-reconstruction. Tsarouhas et al. found reduced knee rotational moments in both of the ACLD and ACLR knees compared to the healthy controls during pivoting, while no significant differences were found in the range of internal/external tibial rotation (Tsarouhas et al., 2010). Tashman et al. investigated the patients' running after ACL-reconstruction (Tashman et al., 2007), and found an increased external and varus rotation in the reconstructed knees during stance phase compared to the contralateral knees. A recent study by Gao and coauthors suggested that the ACL-reconstruction “under-corrected” instead of “over-corrected” the knee kinematics during ascending and descending stairs (Gao et al., 2012).

In those previous studies, only a few kinematic variables were reported, which cannot provide a whole picture of the knee joint motion. Furthermore, the joint moments and forces, which are very important in distributing the joint contact forces across medial

and lateral compartments (Erhart et al., 2010, Crenshaw et al., 2000), were not reported in most studies. The mark inconsistencies from study to study may be contributed by the large variances in surgical procedures and motion analysis protocols. The methodologies of several recent studies are organized in TABLE 1.1.

TABLE 1.1 Summary of recent publications about knee joint kinematics after unilateral ACL-reconstruction.

Reference	Included healthy controls, $\geq$ 10 subjects in each group?	Surgery done by the same surgeon?	The same type of graft used in each group?	Considered LLD as a factor? <sup>1</sup>	More than 6 markers on each segment?	Presented and discussed 6 DOFs?
Webster et al., <i>Clin Biomech</i> 2011	Yes, yes	Yes	Yes	No	No	No
Webster et al., <i>Clin Biomech</i> 2012	Yes, yes	Yes	Yes	No	No	No
Gao et al., <i>Clin Biomech</i> 2010	Yes, yes	No	No	No	Yes	Yes
Scanlan et al., <i>J. Biomech</i> 2010	No, yes	No	No	No	Yes	No
Lam et al., <i>AJSM</i> 2011	No, yes	No	Yes	No	No	No
Ristanis et al., <i>Arthroscopy</i> 2005	Yes, yes	Yes	Yes	No	No	No
Georgoulis et al., <i>AJSM</i> 2003	Yes, yes	N/A	Yes	No	No	No
Tashman et al., <i>CORR</i> 2007	No, yes	No	No	No	N/A <sup>3</sup>	No
Tsarouhas et al., <i>Arthroscopy</i> 2010	Yes, yes	Yes	Yes	No	No	No
Moraiti et al., <i>Arthroscopy</i> 2009	Yes, no	Yes	No	No	No	No
Gao et al., <i>Hum Mov Sci</i> 2012	Yes, yes	No	No	No	Yes	Yes
Wang et al., <i>Clin Biomech</i> 2012	Yes, yes	No <sup>2</sup>	No	Yes	Yes	Yes

<sup>1</sup>LLD – lower limb dominance; <sup>2</sup>30 patients were from OrthoCarolina (all using STG tendon graft), the rest 11 patients were from Shands Hospital (patellar tendon); <sup>3</sup>stereoradiographic system was used for motion measurement.

## 1.5. Relevant Literature Review of Computational Biomechanics

### 1) Dynamic knee joint model

The joint reaction forces and moments calculated by inverse dynamics are contributed to by multiple components (muscle, ligament and articular contact). However, the individual component (i.e. articular contact forces) is still unknown. Moeinzadeh and Engin incorporated articular surface profiles and nonlinear spring ligaments into a 2-dimensional (2D) dynamic knee model and estimated the ligament and articular contact forces during the simulated joint movement (Moeinzadeh and Engin, 1983). Kim and Pandy developed a 2D dynamic knee model including muscles, ligaments, and articular contact; they used the model to determine the force in each component during the human body standing up from a squatting position (Kim and Pandy, 1993). Zheng et al. developed an analytical knee model in the sagittal plane which was able to calculate the ligament and articular contact forces based on the motion analysis results and electromyographic (EMG) data during exercises (Zheng et al., 1998). Pandy et al. presented a 3D elastic knee model which included the articular cartilage, ligaments, and muscles; the model was used to study the ligament function during different functional tests and exercises (Pandy and Sasaki, 1998, Pandy et al., 1998).

The dynamic models were based on a series of assumptions and simplifications, such as the elastic modulus of ligaments, the relationship between EMG and muscle force, shapes of articular surfaces, the insertion site and path of muscles. However, the dynamic models cannot estimate the distribution of stress/strain within a component (i.e. within femoral cartilage).

## 2) Finite element knee joint model

Compared to the dynamic model, more literature was found on finite element (FE) modeling to the human knee joint. By using the state-of-the-art FE method and medical imaging technique, the stress/strain distribution within articular cartilage and meniscus, which is essential for understanding the development of knee joint degenerative diseases, is able to be estimated. Weiss et al. presented a 3-dimensional incompressible, transversely isotropic hyper-elasticity model for biological tissues and its FE implementation (Weiss et al., 1996). The constitutive model has been used in simulating the behavior of ligaments in a previous study (Pena et al., 2006b). In that study, FE analysis results showed an increased meniscal stress after ACL-reconstruction, and a lower ACL graft tension was obtained at a 60 °tunnel angle on the frontal plane. By using the FE knee model, the author also studied the effect of meniscal tears and meniscectomies; it was found that the maximal contact stress in the articular cartilage after meniscectomy was about twice that in a healthy joint (Pena et al., 2005). Donahue et al. proved the validity of taking the bones as rigid body in studying the response of soft tissues (results changed less than 2% when considering the bones as deformable bodies) (Donahue et al., 2002). Li et al. evaluated the influence of the geometrical error and material properties on the result of FE knee model (Li et al., 2001); according to their findings the geometrical error may cause 10% variations in peak contact stress, and the peak *von Mises* stress was dramatically reduced with the increase of Poisson's ratio. A partial FE knee model was developed to simulate the meniscus translation and deformation under anterior loads in the ACL-deficient knee (Yao et al., 2006). A similar approach has been used to predict the changes in meniscal strains associated with the

kinematic and kinetic changes among patients with partial medial meniscectomy (Netravali et al., 2011).

TABLE 1.2 Summary of previous finite element studies of human knee joint.

Reference	Included anatomic ligament models?	Hyper-elastic material for the ligament?	Included transverse ligament?	Simulated daily activities?	Used Implicit FE solver?	Hex elements for soft tissues?
Pena et al., <i>Clin Biomech</i> 2006	Yes	Yes	No	No	Yes	Yes
Pena et al., <i>Clin Biomech</i> 2012	Yes	Yes	No	Yes	N/A	Yes
Donahue et al., <i>J Biomech Eng</i> 2010	No	No	Yes	No	Yes	Yes
Li et al., <i>J Biomech Eng</i> 2001	No	No	No	No	Yes	Yes
Papaioannou et al., <i>J Biomech</i> 2008	No	No	No	No	Yes	Yes
Penrose et al., <i>CMBBE</i> 2002	No	No	No	Yes	No	Yes
Gardiner et al., <i>JOR</i> 2003	Yes	Yes	No	No	Yes	Yes
Netravali et al., <i>J Biomech Eng</i> 2011	No	No	Yes	No	Yes	Yes
Song et al., <i>J Biomech</i> 2004	Yes	Yes	No	No	Yes	No
Yang et al., <i>CMBBE</i> 2009	No	No	Yes	Yes	N/A	No
Yao et al., <i>J Biomech Eng</i> 2012	No	No	No	No	Yes	Yes

In those studies, only quasi-static loading scenarios (i.e. under an isolated axial compressive load, anterior drawing, or at a key frame of gait) were studied. An axial compressive load approximating the subject's body weight was usually used in previous studies. However, the actual knee joint contact force during the stance phase of walking

was much greater than the body weight. TABLE 1.2 lists some recent studies using the FE method to study the knee joint mechanics.

### 1.6. Objectives and Framework

In this dissertation, a series of motion measurements were conducted to investigate the knee joint motion and loading of ACL patients during daily activities. The effectiveness of different surgical techniques in stabilizing the knee joint was evaluated. In addition, a finite element knee model was developed to predict the changes in stress/strain within articular cartilage associated with the kinematic changes in the ACLR knee under physiological load during level walking. Findings in this dissertation will provide surgeons with valuable information on two commonly used surgical techniques. This study will also provide insightful information to the knee joint biomechanics after ACL reconstruction which will be helpful to understand the etiology of knee joint OA.

In chapter 2, the details of the motion analysis algorithm are presented. Since the accuracy of skin marker based motion analysis was limited by the soft tissue artifact, its characteristics on the lower limbs were investigated for the ACL patients. Based on the characteristics, an improved motion analysis algorithm was developed.

In chapter 3, the knee joint motion and loading of patients who received unilateral ACL-reconstruction using transtibial technique was evaluated during level walking and downstairs pivoting. The lower limb dominance was considered as an independent variable in the statistical analysis to evaluate the dominance effect on the postsurgical outcome of the knee joints.

In chapter 4, the knee joint kinematics and kinetics of patients who received unilateral ACL-reconstruction using anteromedial portal technique were quantified

during level walking and downstairs pivoting. Comparisons were made between two surgical techniques (transtibial vs. anteromedial portal).

In chapter 5, we aimed to investigate the differences in the stress/strain within articular cartilage and meniscus during stance phase of level walking between patients using transtibial technique and patients using anteromedial portal technique. The stress/strain was computed by using the state-of-the-art finite element method.

In chapter 6, major findings were summarized and clinical relevance was discussed.

## CHAPTER 2: DATA COLLECTION AND MOTION ANALYSIS ALGORITHM

This chapter covers three parts: 1) introduction to a motion analysis algorithm; 2) investigation of the characteristics of soft tissue artifact on the lower limbs; 3) design of an improved motion analysis algorithm.

### 2.1. Techniques for Bone Motion Measurement

Gait analysis has been widely used in diagnosis of locomotion pathology and limb disorder. Accurate measurement of bone motion is critical for understanding the normal function as well as clinical problems of the musculoskeletal system. Currently, different techniques have been used to measure the in vivo bone motion: 1) optical video motion capture using skin markers (Gao and Zheng, 2010a, Scanlan et al., 2010, Wang and Zheng, 2010a, Georgoulis et al., 2003) (FIGURE 2.1), 2) invasive technique, in which intra-cortical bone pins are directly inserted into bones (Ishii et al., 1997, Lafortune et al., 1992, Reinschmidt et al., 1997a, Houck et al., 2004), and 3) radiographic technique, including video fluoroscopy (Baltzopoulos, 1995, Tashman and Anderst, 2003), roentgen-stereo-analysis (Lundberg, 1989), biplanar image-matching (FIGURE 2.2) (Li et al., 2008, Van de Velde et al., 2009, Defrate et al., 2006) and cine-phase contrast magnetic resonance imaging (Barrance et al., 2005, Barrance et al., 2006, Sheehan and Drace, 1999, Sheehan et al., 1999).

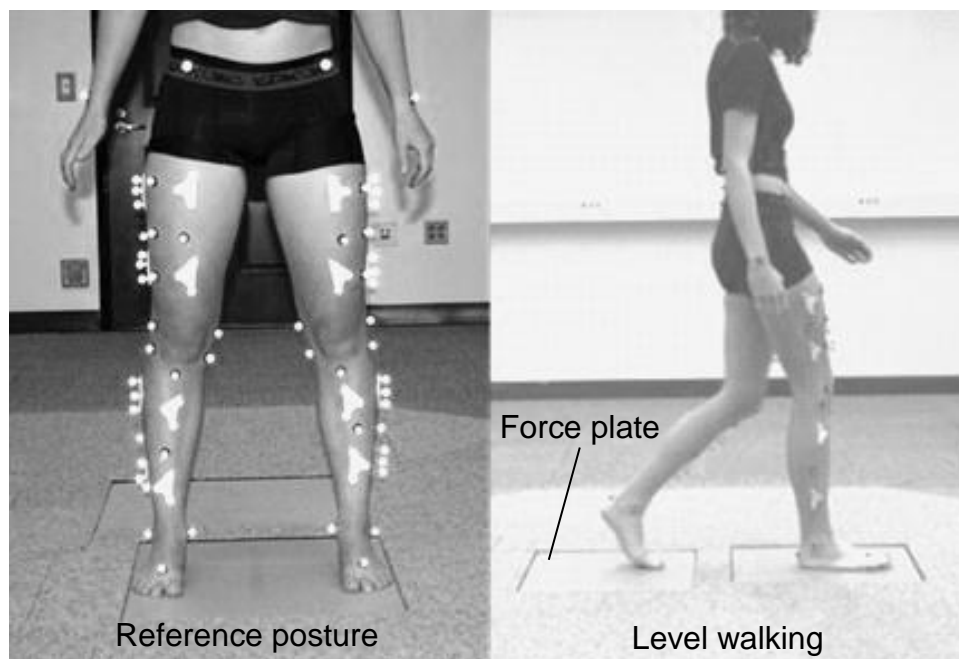


FIGURE 2.1 Protocol of marker placement in optical video motion analysis.

Compared to a video optical technique, bone motion can be measured with a relatively higher accuracy by using the radiographic or invasive bone-pin techniques. However, the application of the invasive technique is largely limited by its invasive nature to the subject. For the radiographic technique, although non-invasive, the high radiation dose and the confined measurement volume exclude it from studying a large sample or investigating the knee joint during daily activities which need a large capture volume. With the merits of being non-invasive and radiation-free, skin marker-based motion analysis is the most popular approach for in vivo measurement of skeletal movement. Unfortunately, 3D joint kinematics is largely limited by the soft tissue artifact (STA, referred to as the skin marker movement relative to the underlying bone) (Fuller et al., 1997, Holden, 2008, Leardini et al., 2005), especially in the frontal and transverse planes (usually referred as the secondary rotation) (Cappozzo et al., 1996). Therefore,

developing a reliable measurement of knee joint secondary motion (internal/external, varus/valgus) is important for better understanding the joint abnormalities.

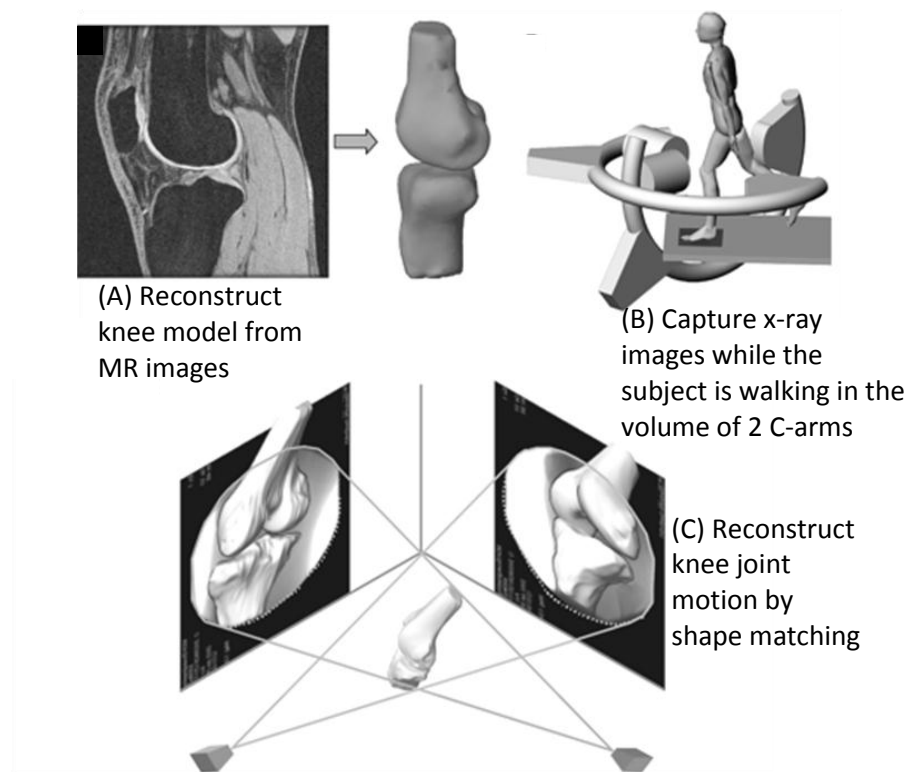


FIGURE 2.2 Procedure of reproducing in vivo knee kinematics with use of the combined dual fluoroscopic and magnetic resonance imaging technique (Defrate et al., 2006).

To retrieve the underlying bone motion from skin markers, the effects of non-rigidity in body segments need to be taken care of. So far, several optimization algorithms have been developed (Andriacchi et al., 1998, Lu and O'Connor, 1999, Spoor and Veldpaus, 1980, Holden, 2008). Among them, the algorithm proposed by Spoor and Veldpaus is the most widely used approach to isolate the rigid body bone motion from redundant skin markers ( $n > 3$ ) (Spoor and Veldpaus, 1980). In this study, we were mainly interested in the knee joint motion, so redundant markers ( $n = 19$ ) were placed on shank

and thigh in order to cancel out the effect of STA; the positions of skin markers at neutral standing posture (t-pose) and during dynamic trials were collected. By using Spoor's approach, the procedure to determine the bone motion at an instant  $t$  is described as follows (using the thigh segment in this text, the shank motion could be determined in the same way). First, define the local coordinate system (LCS) of the thigh (for details, refer to the next section). Second, calculate the position vectors of all markers in segmental LCS at t-pose (FIGURE 2.3). Third, plug in the coordinates of each marker in the global coordinate system (GCS) in to Eq. 2.1, and solve the optimization algorithm to get the rotation matrix and translation vector (Spoor and Veldpaus, 1980).

$$\text{Min: } \sum_{i=1}^n \{P_i G(t) - ([R(t)] \cdot P_i L(0) + \vec{V}(t) + O(0))\}^2 \quad (2.1)$$

$$P_i L(t) = [R(t)] \cdot P_i L(0) \quad (2.2)$$

$$\vec{V}(t) = O(t) - O(0) \quad (2.3)$$

where, the  $P_i L(0)$  and  $P_i L(t)$  denote the position vector of marker- $i$  in LCS at t-pose and at instant  $t$  respectively,  $P_i G(t)$  denotes the coordinates in GCS which are directly measured by the motion capture system,  $O(t)$  and  $O(0)$  are the coordinates of the LCS origin in GCS,  $[R(t)]$  and  $\vec{V}(t)$  denote the couple of rotation matrix and translation vector which uniquely determine the motion of the segment.

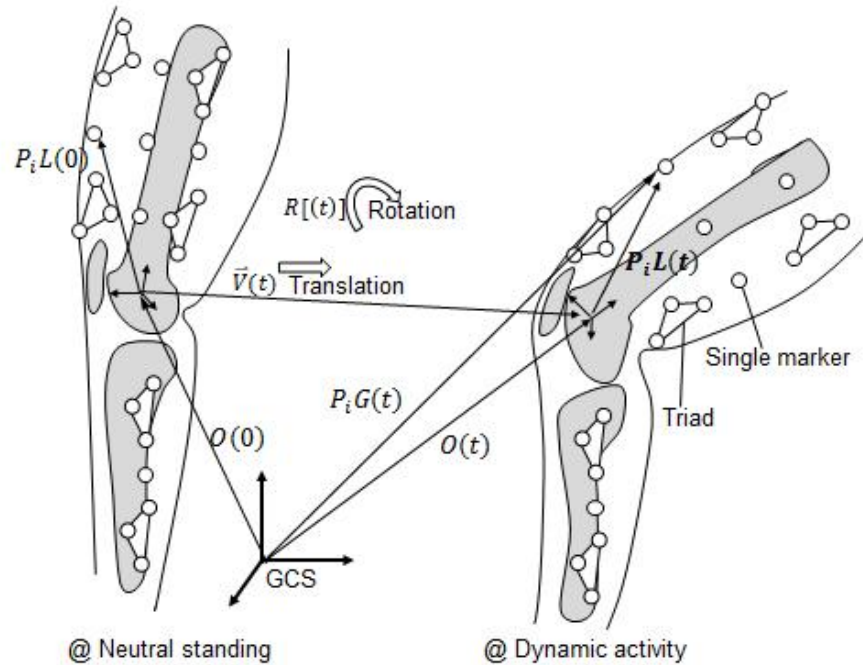


FIGURE 2.3 Position vectors of thigh skin markers in GCS and LCS at the reference posture (left) and at a dynamic instant- $t$  (right).

Therefore, the “continuous” femur motion can be solved by repeating the above procedures frame by frame. Following this same method, the tibia motion can also be determined. The knee joint translation and rotation were then determined by relating the motion of these two bones (FIGURE 2.4). The translation vector was then decomposed into 3 anatomical directions (anteroposterior-AP, mediolateral-ML and superoinferior-SI). Three rotation angles (flexion/extension-FE, internal/external-IE and varus/valgus-VV) were determined from the rotation matrix by using projection approach.

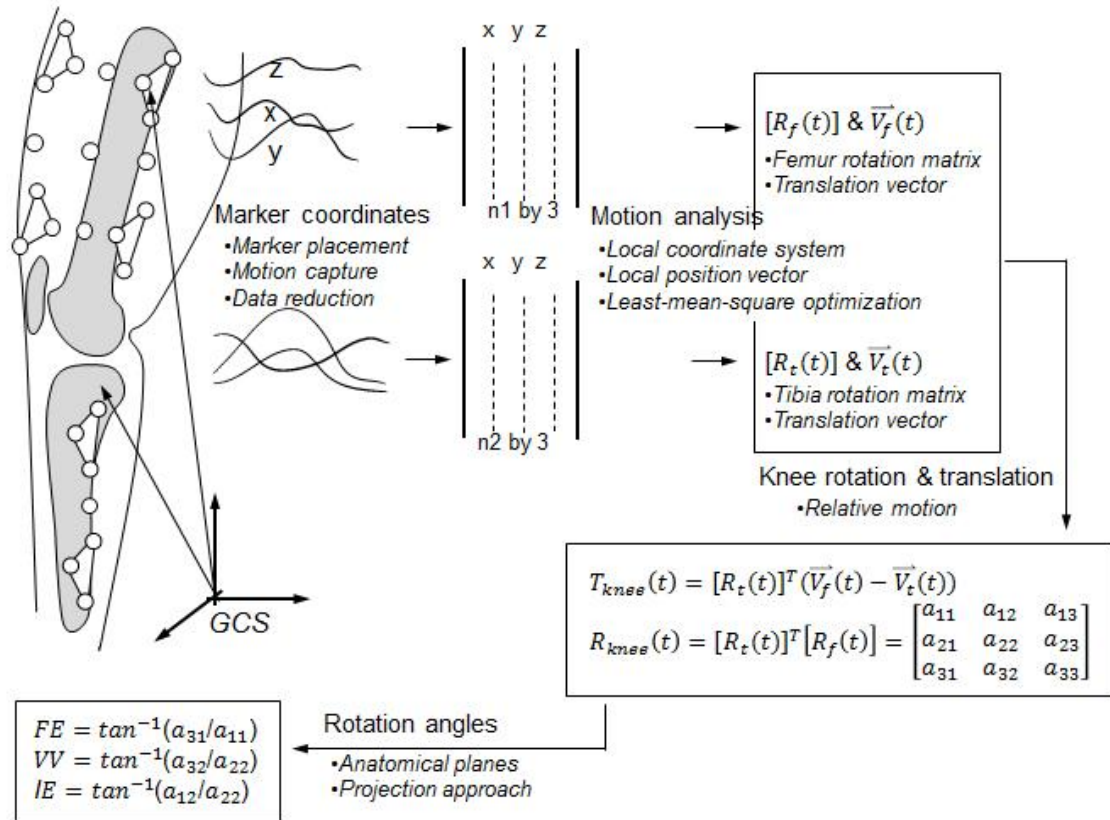


FIGURE 2.4 The flowchart of retrieving the knee joint rotation and translation from skin markers.

The accuracy of bone motion measurement by using our marker set has been quantified by using six fresh cadaver legs with bone-pin markers which were firmly fixed to the bones and skin markers at the same time. By comparing the results from bone-pin markers (baseline) and skin markers, the accuracy of motion analysis using our marker set was quantified (TABLE 2.1).

TABLE 2.1 the root mean square (RMS) errors (mean  $\pm$  standard deviation) ( $^{\circ}$ ; mm) of skin marker based knee motion measurement. (Gao et al., 2007)

Variable	AP	ML	SI	FE	IE	VV
Error	3.46 $\pm$ 2.15	0.80 $\pm$ 0.46	0.72 $\pm$ 0.07	0.71 $\pm$ 0.43	1.17 $\pm$ 0.23	0.34 $\pm$ 0.17

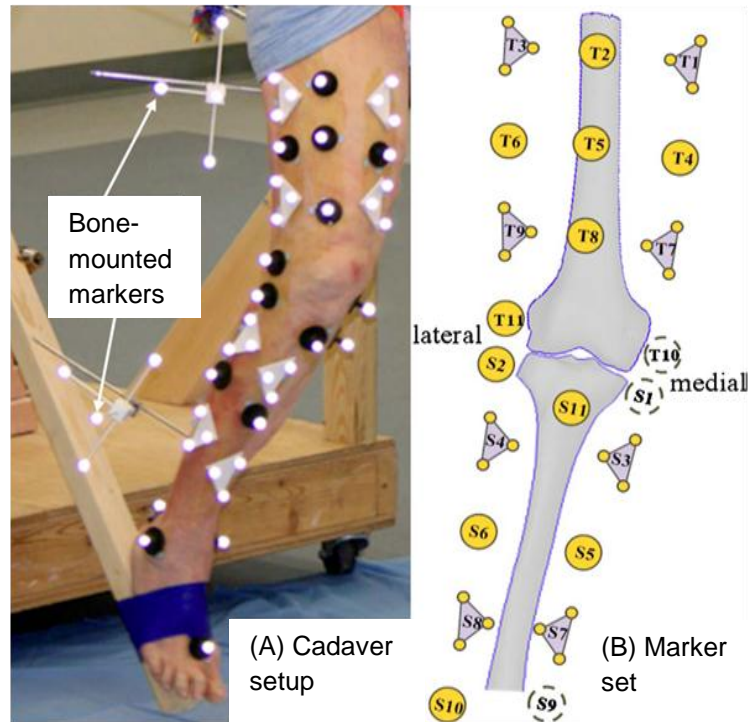


FIGURE 2.5 Cadaver setup with skin markers and bone-pin markers.

## 2.2. Investigation of Soft Tissue Movement on Lower Extremities

This work on characterizing the patterns of skin movements following ACL-reconstruction is submitted to *Clinical Biomechanics* for consideration of publication.

### 2.2.1. Introduction

Skin marker-based motion analysis has been widely used for understanding in vivo kinematics and pathological disorders of human musculoskeletal system during high range of motion activities (Andriacchi and Alexander, 2000). In clinic, assessment to knee joint motion during level walking is an important approach to exam the physical condition of the joint after anterior cruciate ligament (ACL) injury and treatment. By using skin marker-based motion analysis, kinematics alteration in knee joint motion was

identified among ACL-deficient knees (Andriacchi and Dyrby, 2005, Georgoulis et al., 2003) and ACL reconstructed knees (Gao and Zheng, 2010b, Scanlan et al., 2010) during level walking.

However, the accuracy of knee joint kinematics was largely limited by the non-rigidity nature of human segments (Leardini et al., 2005, Stagni et al., 2005, Akbarshahi et al., 2010a, Peters et al., 2010). Various error reduction or compensation algorithms had been developed which largely reduced the negative effects of soft tissue movement on bone motion estimation (Cereatti et al., 2006, Cheze et al., 1995, Begon et al., 2007, Klous and Klous, 2010, Andriacchi et al., 1998, Lu and O'Connor, 1999). With the increased understanding of soft tissue movements, it was believed that the characteristics of skin movement could provide additional information for improving the motion analysis algorithms (Gao and Zheng, 2008, Gao, 2009, Lucchetti et al., 1998, Dumas and Cheze, 2009).

The strength and morphology of knee joint muscles as well as the neuromuscular system have been affected by ACL injury and surgical intervention (Lorentzon et al., 1989, Konishi et al., 2007, Pereira et al., 2009, Johansson et al., 1990, Valeriani et al., 1999), which could result in changes of skin movement. According to the 2005-2006 National Health and Nutrition Examination Survey (NHANES), an estimated 32.7 percent of U.S. adults 20 years and older are overweight (body mass index,  $25.0 < \text{BMI} < 30.0$ ), 34.3 percent are obese ( $\text{BMI} \geq 30$ ) and 5.9 percent are extremely obese ( $\text{BMI} \geq 40$ ). The greater body weight may permit more skin movements during walking. Thus, the previous finding of strong skin movement patterns among healthy and healthy weight

(BMI  $22.0 \pm 2.8$ ) population may not apply to the group with ACL reconstruction and relatively larger BMI (Gao and Zheng, 2008).

In this study, we aimed to answer two questions: 1) whether the skin movement patterns still exist among ACL-reconstructed patients after discharge from their rehabilitation program, and 2) whether the range of skin stretches are greater among overweight population. If the skin stretches do have prominent patterns and significant correlation with limb size, then in the future, the measure of limb size may provide additional information for STA removal in skin marker-based motion analysis.

### 2.2.2. Material and methods

#### 1) Participants

Forty-one patients with unilateral ACL injury and reconstruction were recruited in this study (TABLE 2.2). The subjects had no injuries on their contralateral limbs. At the time of testing, they were at least four months after surgery (14 months in average) and discharged from their rehabilitation program. The study was conducted following an IRB approved protocol and informed consent was obtained from each subject before testing.

TABLE 2.2 Subject information (BMI-body mass index, HS-hamstring tendon, PT-patellar tendon).

Gender	Number	Age (years)	Height (cm)	Weight (kg)	BMI	HS	PT
Male	24	31.3 $\pm$ 9.4	182.5 $\pm$ 7.0	86.9 $\pm$ 15.7	25.4 $\pm$ 4.6	21	3
Female	17	33.2 $\pm$ 7.5	167.8 $\pm$ 5.6	73.9 $\pm$ 16.4	27.3 $\pm$ 5.3	14	3
Total	41	32.1 $\pm$ 9.9	176.5 $\pm$ 9.7	81.6 $\pm$ 17.1	26.2 $\pm$ 5.4	35	6

## 2) Experimental protocol

To track the skin movements on lower limbs, a cluster of retro-reflective markers (10 mm in diameter) and triads (a rigid triangle of  $30 \times 30 \times 42$  mm with three markers on vertices) were sparsely placed on the anterolateral regions of thigh and shank following the protocol of our previous study (Gao and Zheng, 2008). A 10-camera motion capture system (MX-F40, VICON, Oxford, UK) which has an accuracy of better than 1.0 mm after calibration was used to record the marker trajectories. A static trial (t-pose) and ten walking trials were recorded from each subject after adequate practice and the average of three good trials were used to represent each subject. Good trials were selected using the following criteria: 1) no marker drops or marker missing for more than 4 consecutive frames, 2) trial was long enough to include two complete heel strikes for both legs.

After the motion test, a 3D body scan (Cyberware Inc., Monterey, CA, USA) of lower limbs was taken with layer space of 1 mm at straight standing (FIGURE 2.6); the total scanning time was about 20 seconds. Since body scan measurement was introduced in the middle of the study, some of the patients (13 out of 41) tested earlier did not have body scan data. Thigh length was measured as the distance from the great trochanter to lateral femoral epicondyle and tibia length was measured as the distance from lateral edge of tibial plateau to lateral malleolus.

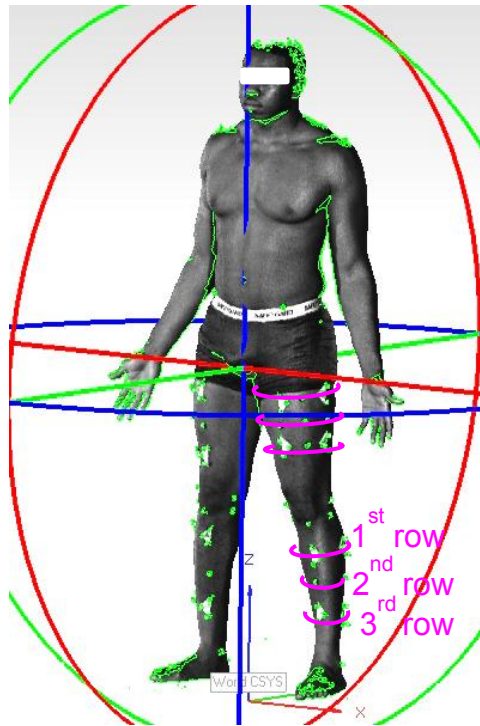


FIGURE 2.6 Lower limb's nominal radius were measured from subject's 3D body scan.

### 3) Data analysis

A 4th order Butterworth low-pass filter (cut-off frequency 6 Hz) was used for smoothing the raw motion data. One triad was selected as the reference on each segment (T7 on the thigh FIGURE 2.7, S3 on the shank FIGURE 2.8). At each marker location, skin movements were quantified by skin stretch and skin rotation relative to the reference triad by following a published approach (Gao and Zheng, 2008).

The first heel strike (HS) and toe off (TO) were detected by the force plates with a threshold of 5% body weight; the second heel strike was determined by a gait event detecting algorithm (Hreljac and Marshall, 2000). All variables were normalized to a gait cycle from heel strike (0%) to the next heel strike (100%) by using linear interpolation (Helwig et al., 2011). A ratio  $S$  was used to assess the prominence of inter-subject

similarity (Gao and Zheng, 2008). For variables with strong inter-subject similarity, the formula would yield a large  $S$  value.

$$S = \frac{\max_1^{100}(f_{avg}(t)) - \min_1^{100}(f_{avg}(t))}{\sqrt{\sum_{i=1}^{100} f_{std}^2(t)/100}} \quad (2.4)$$

where  $f_{avg}(i)$  and  $f_{std}(i)$  denote the mean value and standard derivation (SD) of the variable at  $i$  % of gait cycle across subjects. For  $S$  value greater than 2, it was taken as an indication of strong inter-subject similarity (Gao and Zheng, 2008).

The 3D body scan models (.ply format) of 28 subjects were input to reverse modeling software (Geomagic Studio, Research Triangle Park, NC, USA) to generate the cross sections at different heights (FIGURE 2.6). A MATLAB (MathWorks, Natick, MA, USA) program was developed to calculate the cross section area enclosed by 2D points based on Green's theorem (Kreyszig, 2005).

The range of skin stretch was defined as the difference between the maximum and minimum values in each direction during a whole gait cycle (FIGURE 2.7). The nominal radius ( $r_{nominal}$ ) of thigh and shank was calculated from the cross section area ( $Area$ ), eq. (2-5).

$$r_{nominal} = \sqrt{Area/\pi} \quad (2.5)$$

#### 4) Statistical analysis

Paired student's  $t$ -test (SPSS v16, SPSS Inc, IL, USA) was performed to test the bilateral difference of the range of skin movements. Correlation and regression analyses were performed to study the relationship between the range of skin stretches and the limb size (nominal radius and segmental length) across different subjects by using Matlab Statistic and Curve Fitting tool boxes. Significance level ( $p$ ) of 0.05 was used to indicate

the significant correlation, and strong correlation was defined as the Pearson coefficient ( $r$ ) greater than 0.65.

### 2.2.3. Results

No significant bilateral differences were found from the range of skin stretch at all marker locations on both thigh and shank ( $p > 0.1$ ). The skin movements over a gait cycle were illustrated as mean values and standard deviations of all subjects' reconstructed legs (FIGURE 2.7 and FIGURE 2.8), and the data presented in this study were from the involved legs without further specification.

TABLE 2.3  $S$  values (involved, contralateral) of inter-subject similarity for skin rotations on the shank and thigh. AP-around anterior/posterior axis, ML-around medial/lateral axis, SI-around superior/inferior axis

Shank Location	Shank			Thigh Location	Thigh		
	AP	ML	SI		AP	ML	SI
S4	1.4, 1.3	1.7, 1.8	2.3, 1.8	T1	2.4, 2.0	2.2, 2.3	3.8, 3.7
S7	1.3, 1.1	1.1, 1.2	1.0, 1.0	T3	1.9, 1.5	4.3, 3.5	2.1, 1.7
S8	0.7, 0.9	0.6, 1.1	1.1, 1.0	T9	1.3, 1.0	4.7, 2.4	2.6, 2.3

Strong inter-subject similarities ( $S > 2$ ) of skin stretches were found from most locations on the thigh and from more than half locations on the shank (FIGURE 2.7 and FIGURE 2.8). Some strong patterns ( $S > 2$ ) were also observed from the skin rotations on the thigh (TABLE 2.3). The range of skin stretches was much greater on the thigh (anterior/posterior (AP) 12.9 mm, medial/lateral (ML) 10.5 mm, superior/inferior (SI) 11.0 mm, average of all locations) than those on the shank (AP 4.4 mm, ML 3.2 mm, SI 4.5 mm) (TABLE 2.3 and TABLE 2.4).

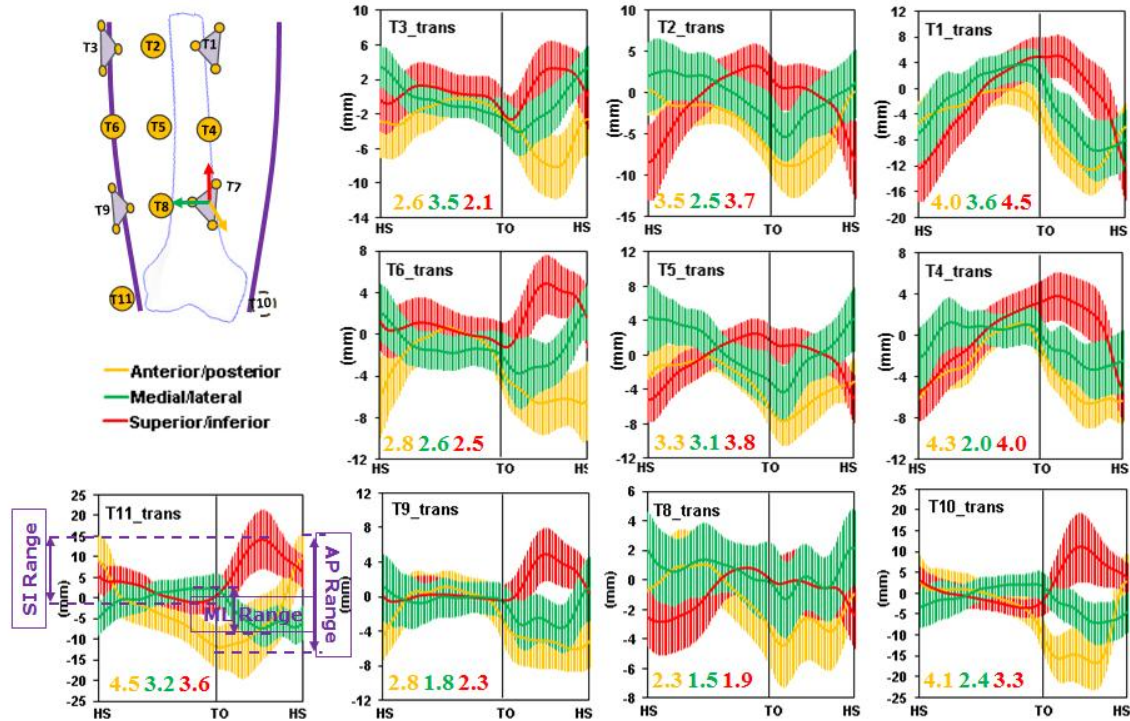


FIGURE 2.7 Inter-marker translations on the thigh during walking.

Significant correlations ( $p < 0.05$ ) between the range of skin stretches and nominal radius of segment were observed from the thigh and shank during walking (FIGURE 2.9 and FIGURE 2.10). Most of the correlations were positive ( $r > 0$ ), except for the skin stretch in the AP direction at T2 ( $r = -0.2$ ). The correlations between skin stretches and nominal radius were much weaker on the shank than those on the thigh. In the SI direction, the skin stretches at most locations on the 1<sup>st</sup> and 2<sup>nd</sup> rows (T1-T5) had significant ( $p < 0.01$ ) and strong ( $r > 0.65$ ) correlation with nominal radius of the thigh. Although some significant correlations ( $p < 0.05$ ) between skin stretches and nominal radius were found on the shank, all the correlations were not strong ( $r < 0.65$ ) (S4-S8, TABLE 2.5). The segment's length had no significant ( $p > 0.1$ ) or strong correlation ( $r < 0.5$ ) (TABLE 2.6) with the range of skin stretches for both thigh and shank.

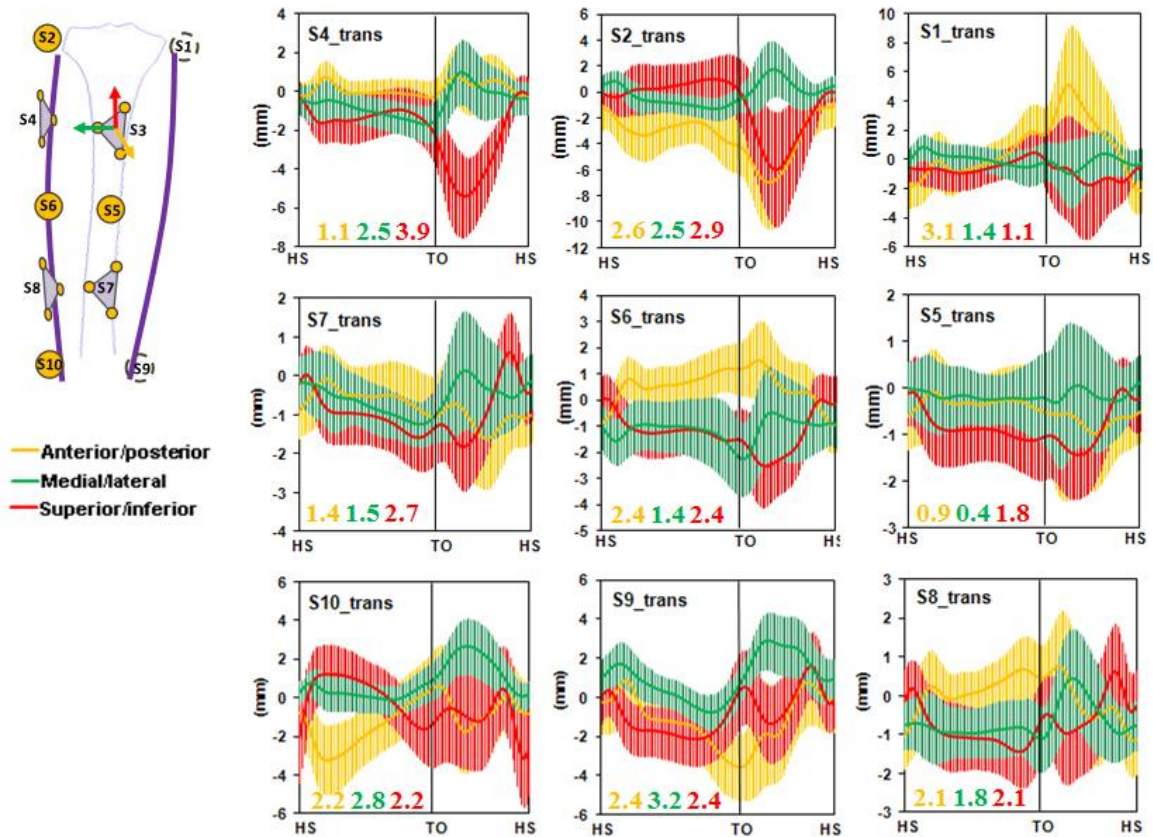


FIGURE 2.8 Inter-marker translations on the shank during walking.

#### 2.2.4. Discussion

By using a previously described proxy technique (Gao and Zheng, 2008), the soft tissue deformation on lower limb was illustrated as a 4D picture (3D space and time) of inter-marker translations and rotations during a gait cycle. According to our finding, most of the skin movement variables on the thigh and about half of variables on the shank still exhibited strong patterns among ACL-reconstructed patients. The limb with larger nominal radius was more likely to have greater skin stretches in all three directions, although the strength of the response was different across directions. For instance, the skin stretches in the SI direction had much stronger ( $r > 0.65$ ) correlation with the nominal radius of thigh than in the other directions ( $r < 0.65$ ) at the 1<sup>st</sup> and 2<sup>nd</sup> rows.

These features could be explained by the anatomical structures of quadriceps muscles which contract concentrically and eccentrically mainly along the SI direction during activities. In algorithm design, the inter-direction variability could be considered by assigning a weighting vector  $\vec{W} = \begin{bmatrix} W_{AP} \\ W_{ML} \\ W_{SI} \end{bmatrix}$ , instead of a weighting scalar as in most conventional algorithms (Andriacchi et al., 1998, Arun et al., 1987, Cheze et al., 1995, Lu and O'Connor, 1999), to each marker (Gao, 2009).

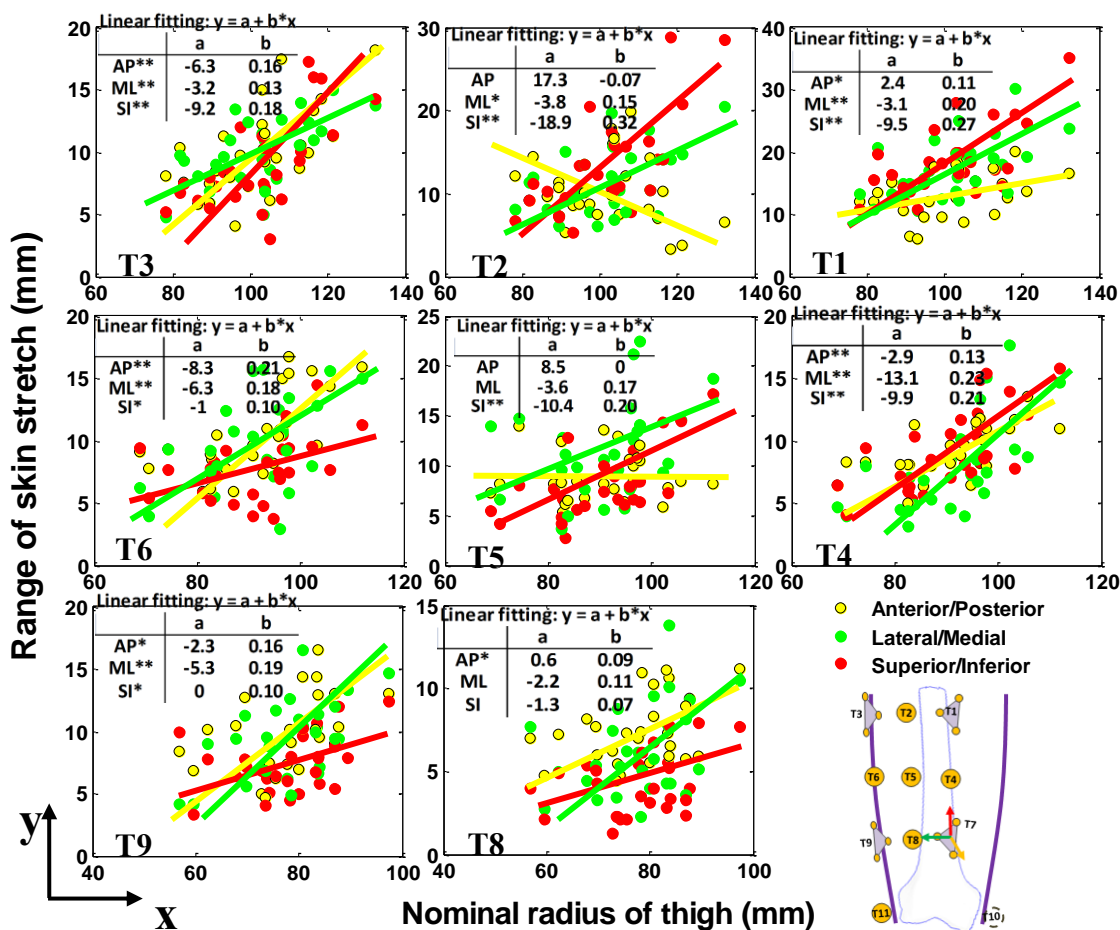


FIGURE 2.9 Linear regression between the range of skin stretches and nominal radius of thigh cross section at 3 different rows in three orthogonal directions during walking.

In this study, the range of skin stretches was much smaller on the shank than those on the thigh, which was consistent with previous studies (Stagni et al., 2005, Akbarshahi et al., 2010a). The profiles of skin movement curves in this study were very similar to those of the healthy population in our former study. The inter-subject similarities of skin stretches slightly decreased across ACL patients compared with those across healthy subjects in a former study (Gao and Zheng, 2008), except at some locations (T2, T5, T10 and T11) where the similarities in SI direction became even stronger. Neuromuscular system might have been altered after ACL injuries and reconstruction which could result in abnormal muscle activities (Valeriani et al., 1999, Johansson et al., 1990). Following ACL injury and surgical intervention, the strength and morphology of knee joint muscles also had been changed according to previous studies (Lorentzon et al., 1989, Konishi et al., 2007, Pereira et al., 2009). Those neuromuscular abnormalities might have decreased the inter-subject similarities in skin movements. After ACL reconstruction, patients exhibited significantly greater gait variability than the healthy controls, even though clinical outcomes indicated complete restoration (Moraiti et al., 2010, Dingwell and Cusumano, 2000). The enlarged variability could also contribute to the weakened inter-subject similarities of skin stretches.

TABLE 2.4 The range of skin stretches (mean  $\pm$  std, unit: mm) at different locations on the thigh relative to the reference triad T7 during a complete gait cycle and their correlation with the nominal radius of thigh for the ACL reconstructed legs.

Location	Nominal radius	Range of skin stretch		
		AP	ML	SI
T1	102.0 $\pm$ 51.2	13.7 $\pm$ 3.7*	17.2 $\pm$ 4.7†**	18.6 $\pm$ 5.5‡**
T2	102.0 $\pm$ 51.2	10.6 $\pm$ 4.2 <sup>-</sup>	11.5 $\pm$ 4.0*	13.3 $\pm$ 5.8‡**
T3	102.0 $\pm$ 51.2	10.1 $\pm$ 3.4†**	10.0 $\pm$ 2.7†**	9.0 $\pm$ 3.5‡**
T4	90.8 $\pm$ 42.6	9.1 $\pm$ 2.1†**	7.7 $\pm$ 3.7†**	9.2 $\pm$ 3.2‡**
T5	90.8 $\pm$ 42.6	9.0 $\pm$ 2.4	11.3 $\pm$ 4.6	8.1 $\pm$ 3.3‡**
T6	90.8 $\pm$ 42.6	10.3 $\pm$ 3.1‡**	9.7 $\pm$ 3.5†**	7.8 $\pm$ 2.5*
T8	78.2 $\pm$ 37.0	7.4 $\pm$ 2.0*	6.3 $\pm$ 2.7	4.3 $\pm$ 1.9
T9	78.2 $\pm$ 37.0	10.0 $\pm$ 3.0*	9.4 $\pm$ 3.1†**	7.4 $\pm$ 2.3*
T10	N/A	22.9 $\pm$ 6.5	10.4 $\pm$ 4.3	15.8 $\pm$ 7.1
T11	N/A	24.8 $\pm$ 7.1	11.2 $\pm$ 3.6	16.9 $\pm$ 5.8

The symbol †  $r$  value $>$ 0.5 indicates moderate and ‡  $r$  value  $>$ 0.65 indicates strong correlation between the nominal radius and range of skin stretch; \*  $p$  $<$ 0.05 and \*\*  $p$  $<$ 0.01 indicate the significance of correlation; <sup>-</sup>  $r$  value $<$ 0.

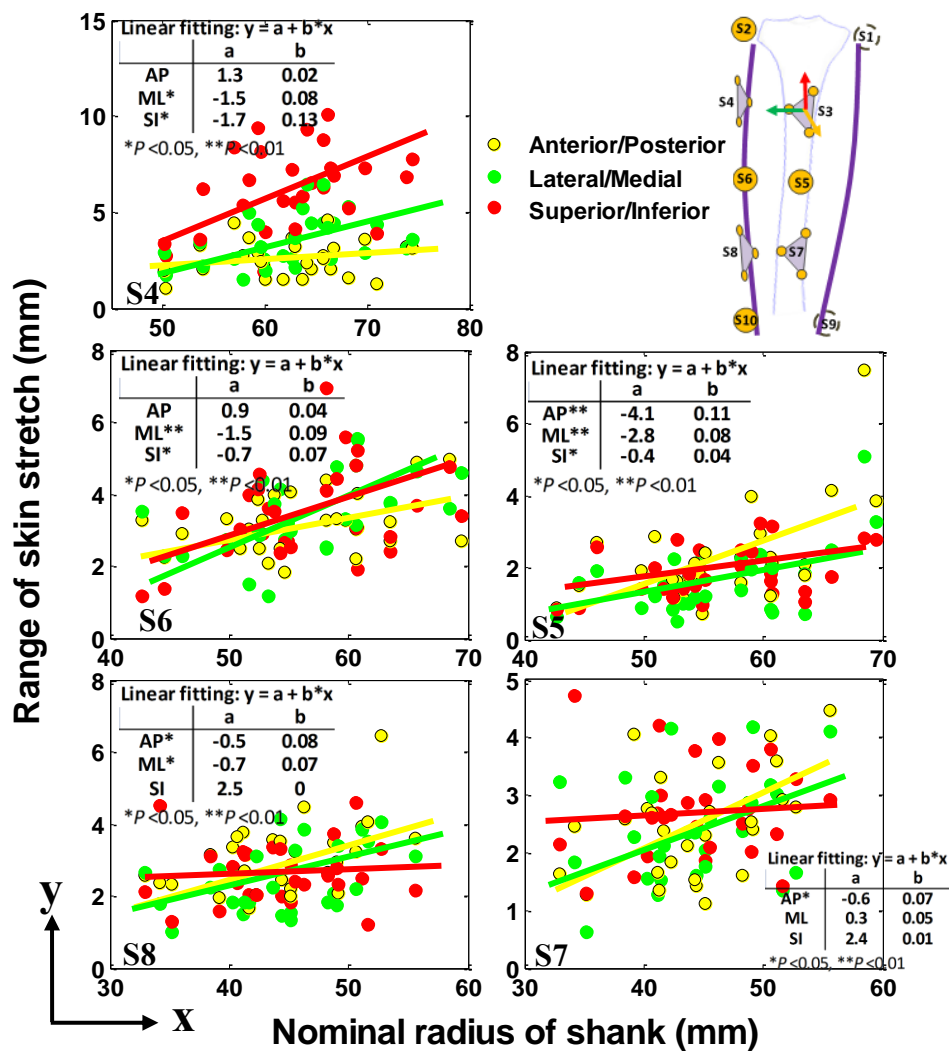


FIGURE 2.10 Linear regression between the range of skin stretches and nominal radius of shank cross section at 3 different rows in three orthogonal directions during walking.

The ranges of skin stretch were increased by about 40% on the thigh and about 20% on the shank compared with the healthy population in our previous study. The increased skin stretches may be contributed by the relatively greater (BMI 26.2 vs. 22.0 in previous study) body weight of the subjects in this study. Higher BMI means more fatness or greater muscle mass which may permit more soft tissue movements. It indicated that the major factor that may influence skin stretch could be BMI, thus the measure of skin

movement could be used as a proxy measure of fatness or muscle mass. Unfortunately, we had no data from fatness measurement instruments such as DEXA scans. Given the strong associations identified between the limb's nominal radius and the magnitude of skin stretches, in the future we would include the fatness measure in our study design and check the correlation between skin stretches and fatness during level walking.

TABLE 2.5 The range of skin stretches (mean  $\pm$  std, unit: mm) at different locations on the shank relative to the reference triad S3 during a complete gait cycle and their correlation with the nominal radius of shank for the ACL reconstructed legs.

Location	Nominal radius	Range of skin stretch		
		AP	ML	SI
S1	N/A	8.9 $\pm$ 3.7	3.9 $\pm$ 1.5	5.2 $\pm$ 2.2
S2	N/A	7.1 $\pm$ 2.5	4.1 $\pm$ 1.5	8.3 $\pm$ 3.2
S4	62.5 $\pm$ 6.1	2.7 $\pm$ 0.9	3.6 $\pm$ 1.3*	6.2 $\pm$ 2.1*
S5	56.3 $\pm$ 6.6	2.2 $\pm$ 1.3 $\dagger$ **	1.6 $\pm$ 0.9 $\dagger$ **	1.9 $\pm$ 0.7*
S6	56.3 $\pm$ 6.6	3.2 $\pm$ 0.8	3.4 $\pm$ 1.1 $\dagger$ **	3.5 $\pm$ 1.3*
S7	44.3 $\pm$ 5.6	2.5 $\pm$ 0.9*	2.4 $\pm$ 0.9	2.7 $\pm$ 0.8
S8	44.3 $\pm$ 5.6	3.1 $\pm$ 1.0*	2.5 $\pm$ 0.9*	2.7 $\pm$ 0.8
S9	N/A	5.7 $\pm$ 1.6	4.1 $\pm$ 1.3	4.6 $\pm$ 1.1
S10	N/A	4.5 $\pm$ 1.3	3.6 $\pm$ 1.3	5.0 $\pm$ 1.0

The symbol  $\dagger$   $r$  value $>$ 0.5 indicates moderate correlation between the nominal radius and range of skin stretch; \*  $p$  $<$ 0.05 indicates the significance of correlation.

Several limitations should be kept in mind when interpreting the results. Firstly, the study indirectly inspected the soft tissue movement by quantifying the skin stretches and skin rotations during level walking using a published proxy technique; however, the absolute skin motion relative to the bone is still unknown. With the advance of radiostereometric technique (Barrance et al., 2005, Defrate et al., 2006), in the future it

will be possible to capture dynamic medical imaging and skin marker trajectories at the same time during a large range of activities, then the skin-bone relative movement could be accurately determined. Secondly, we did not have the body scan data from our first 13 subjects. With a larger sample size, the correlation between skin stretch and limb size may be slightly different, but should be similar to what we reported here. Thirdly, the body type of the subjects in the current study were not matched with the subjects in our previous study; like the other studies the uninjured contralateral legs were used as the control group (Scanlan et al., 2010, Defrate et al., 2006).

TABLE 2.6 Pearson coefficients ( $r$ ) of correlation between the range of skin stretches and segmental nominal radius. AP-anterior/posterior, ML-medial/lateral, SI-superior/inferior

Thigh Location	Thigh			Shank Location	Shank		
	AP	ML	SI		AP	ML	SI
T1	0.39	0.55	0.65	S4	0.15	0.38	0.38
T2	-0.20	0.48	0.70	S5	0.56	0.55	0.38
T3	0.61	0.62	0.65	S6	0.35	0.53	0.38
T4	0.64	0.64	0.68	S7	0.44	0.30	0.05
T5	0.02	0.37	0.65	S8	0.46	0.45	0.02
T6	0.67	0.51	0.40	T9	0.48	0.57	0.39
T8	0.41	0.37	0.36				

### 2.2.5. Conclusion

This is a follow up study to our previous publication (Gao and Zheng, 2008). We investigated the skin movements on the lower limbs among a larger number of ACL patients during level walking. The results showed that similar patterns of skin movements were retained among ACL patients. Subjects with thicker limbs tend to have greater skin stretches in all three directions, and the skin stretches in superior/inferior direction have

the strongest response to the limb thickness. Measurement of limb nominal radius may provide additional information for compensating skin movements in motion analysis algorithms. Also it may be more practical to assign a weighting vector to each marker, and treat the 3 coordinates separately during the optimization process.

### 2.3. An Algorithm Using the Characteristics of Soft Tissue Movement

It has been proved in the previous section that the soft tissue movement had strong patterns, i.e. the displacements of skin markers on the tibial plateau edges (S1 and S2 on FIGURE 2.8) along mediolateral direction were very small. Therefore, in motion analysis algorithms those patterns may be helpful to search for the optimal solution of the bone motion. A new algorithm has been developed which was published in the *Journal of Biomechanical Engineering*, 2010 Dec; 132(12): 124502

#### 2.3.1. Introduction

Gait or motion analysis has been widely used in diagnosis of locomotor pathology or limb disorder. Accurate bone motion is critical for understanding the normal function as well as clinical problems of the musculoskeletal system. With the merits of being non-invasive and radiation-free, skin marker-based motion analysis is the most popular means for in vivo skeletal kinematics measurement. Unfortunately, in skin marker-based motion analysis, soft tissue artifact (STA) has been reported as the main error source of 3-dimensional (3D) joint kinematics (Holden, 2008, Leardini et al., 2005, Fuller et al., 1997), especially in the frontal and transverse planes, where the ranges of motion are much smaller than that in the sagittal plane (Cappozzo et al., 1996). Injuries may change joint kinematics and loading, even a minor rotation offset may place the joint loads onto a non-weight bearing cartilage area, which may trigger cartilage degeneration (Appleyard et al., 1999, Quinn et al., 2005, Thambyah et al., 2006). Therefore, more precise

measurement of secondary joint motion of the knee is critical for us to better understand the relationships between the abnormalities in knee joint kinematics and the pathological changes of articulating surface.

To retrieve underlying bone motion from skin markers, several optimization algorithms have been developed to minimize the effects of STA (Andriacchi et al., 1998, Lu and O'Connor, 1999, Spoor and Veldpaus, 1980). In all those algorithms, the skin markers were taken as the same entities or were assigned with the same initial weighting factors, regardless of their anatomical locations. Those techniques have insufficient certainty to assess the secondary rotations and translations (Leardini et al., 2005, Stagni et al., 2005, Reinschmidt et al., 1997b).

In the past decade, several techniques were developed using cine-MRI (Barrance et al., 2005), fluoroscopy (Defrate et al., 2006, Papannagari et al., 2006, Dennis et al., 2005) which successfully obtained more accurate tibiofemoral joint motion. Based on the shape matching technique and accurate 3-D bone model built from CT, the knee joint kinematics were obtained from 2D fluoroscopic imaging sequence, which claimed to have reduced the error to  $<0.1\text{mm}$  in translation and  $<1^\circ$  in rotation (Li et al., 2008). However, those techniques are not suitable in studying daily activities like level walking because of their small capture volume and low frequency of data capture. Therefore, a compromise must be made between the acceptance of the larger error associated with skin markers and its applicability of measuring a large range of motion during daily activities (Andriacchi and Mundermann, 2006).

Recently, several studies have found that the STA had location- and direction-specific characteristics (Gao and Zheng, 2008, Garling et al., 2007, Akbarshahi et al.,

2010b). Although a number of studies were carried out to quantify the soft tissue movements. To our knowledge, little has been done concerning how to use that information in developing a better algorithm for determining the underlying bone motion from skin markers.

Motivated by progressive understanding of STA, we incorporated the STA characteristics into the optimization problem of kinematic analysis. The objective of this study is to develop a new algorithm that uses the STA constraints at special landmarks and test its efficiency in removing STA errors in quantifying secondary knee joint motions.

### 2.3.2. Material and methods

#### 1) Algorithm by using bony landmark constraints

Basing on the rigid body assumption of the human segment, Spoor and Veldpas presented an analytical technique to calculate the bone rotation matrix and translation vector from redundant skin markers (Spoor and Veldpaus, 1980). That analytical algorithm was to find the optimal combination of rotation matrix and translation vector which minimized the objective function  $f(\vec{V}(t), R(t))$  (Eq. 3-4) without any constraints (the algorithm would be referred to as a least mean square (LMS) algorithm later). Anatomically, the skin markers at medial and lateral femur epicondyles could not move much in the medial-lateral direction, which had also been proved in a previous study (Gao and Zheng, 2008) (FIGURE 2.11); the same situation was applicable for the skin markers at medial and lateral edges of the tibial plateau. Moreover, the marker at the tibia tuberosity had a very small range of motion relative to the underlying bone in all three anatomical directions.

$$f(\vec{V}(t), R(t)) = \frac{1}{n} \sum_{i=1}^n \{R(t)^{-1}(P_i G(t) - O(t)) - P_i L(0)\}^2 \quad (2.6)$$

$$O(t) = O(0) + \vec{V}(t), R(t)^{-1}(P_i G(t) - O(t)) = P_i L(t) \quad (2.7)$$

where,  $P_i G(t)$  ( $i = 1, 2, 3 \dots, n$ ) denotes the position vector of the  $i^{th}$  marker in the global coordinate system (GCS) at frame  $t$ ;  $P_i L(0)$  denotes the marker position vector in LCS at the reference posture;  $O(0)$  denotes the origin of the bone local coordinate system (LCS) in GCS at the reference posture;  $O(t)$  denotes the origin of LCS at frame  $t$ ;  $\vec{V}(t)$  and  $R(t)$  denote the translation vector and rotation matrix which transport the bone from initial posture to the posture at frame  $t$ ; and  $n$  denotes the number of skin marker.

In our new algorithm, the characteristic of soft tissue movement at special bony landmark locations was considered and incorporated into the constraint functions of the optimization problem, Eq. 2.8-2.9. The constraint functions limited the STA of certain markers in certain direction and refined the optimization results (the new algorithm would be referred to as bony landmark constraint (BLC) algorithm henceforth).

For the femur segment, the optimization problem was organized as:

$$Min : f(\vec{V}(t), R(t)) = \frac{1}{n} \sum_{i=1}^n \{R(t)^{-1}(P_i G(t) - O_{femur}(t)) - P_i L(0)\}^2 \quad (2.8)$$

$$s.t. \begin{cases} |(R(t)^{-1}(P_{T10} G(t) - O_{femur}(0)) - \vec{V}(t)) - (P_{T10} G(0) - O_{femur}(0))|_y < \Delta l_1 \\ |(R(t)^{-1}(P_{T11} G(t) - O_{femur}(0)) - \vec{V}(t)) - (P_{T11} G(0) - O_{femur}(0))|_y < \Delta l_2 \end{cases} \quad (2.9)$$

where,  $P_i G(t)$ ,  $O_{femur}(0)$ ,  $P_i L(0)$  are known from motion data after defining the LCS at reference posture (t-pose);  $\Delta l_1$ ,  $\Delta l_2$  denote the soft tissue moving limits at T10 and T11 respectively (FIGURE 2.11).

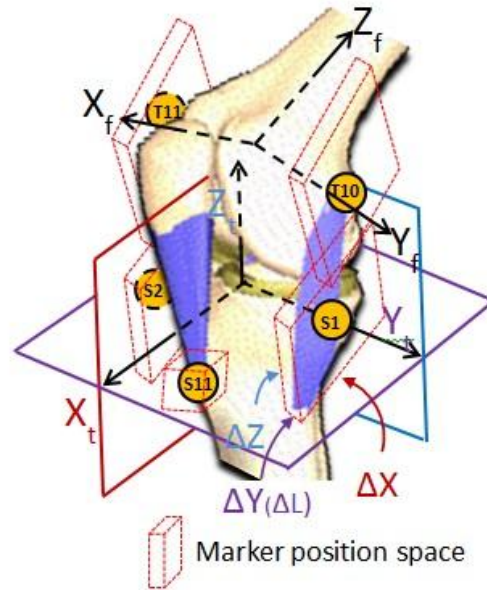


FIGURE 2.11 The moving spaces of skin markers at medial-lateral epicondyles (T10/T11), medial-lateral tibia plateau edges (S1/S2), and tibia tuberosity (S11). At T10, T11, S1, and S2 locations, only medial-lateral direction displacements are constrained. At location S11, the displacement constraints are exerted on all three anatomical directions.

The problem yields to searching for the optimal combination of  $\vec{V}(t)$  and  $R(t)$  which minimizes the objective function  $f(\vec{V}(t), R(t))$  subjected to constraint functions. The 3-dimensional spatial rotation can be uniquely determined by the rotation axis  $(ai + bj + ck)$  and rotation angle  $\alpha (\leq 180^\circ)$ . Then it can be expressed by a norm-1 quaternion which was defined as (Kuipers, 2002, Schmidt and Niemann, 2001, Hamilton, 1866):

$$\begin{aligned}
 q &= w + x \cdot i + y \cdot j + z \cdot k \\
 w &= \cos(\alpha/2) \\
 x &= a \cdot \sin(\alpha/2) \\
 y &= b \cdot \sin(\alpha/2) \\
 z &= c \cdot \sin(\alpha/2)
 \end{aligned} \tag{2.10}$$

The rotation matrix can be represented as:

$$R^j = \begin{bmatrix} w^2 + x^2 - y^2 - z^2 & 2xy - 2wz & 2xz + 2wy \\ 2xy + 2wz & w^2 - x^2 + y^2 - z^2 & 2yz - 2wx \\ 2xz - 2wy & 2yz + 2wx & w^2 - x^2 - y^2 + z^2 \end{bmatrix} \quad (2.11)$$

Therefore, there are seven designing variables to be determined ( $\alpha$ ,  $a$ ,  $b$  and  $c$  for  $R(t)$ , and  $v_1$ ,  $v_2$  and  $v_3$  for  $\vec{V}(t)$ ) and the constraint function was increased by one which guaranteed the norm-1 property of the quaternion, Eq. 3-10.

$$w^2 + x^2 + y^2 + z^2 = 1 \quad (2.12)$$

The Eq. 3-10 could be restated as  $a^2 + b^2 + c^2 = 1$ , according to the definition of quaternion.

The tibia segment's mathematical statement was similar, except for the bony landmark constraint at the tibia tuberosity (S11, FIGURE 2.5). To solve the constrained optimization, the constraint functions were integrated into the objective function by introducing the Lagrangian multipliers ( $\lambda_i$ ). For example, for constraint function (6), the form  $\lambda_i(a^2 + b^2 + c^2 - 1)^2$  was added into the objective function. To minimize  $f(\vec{V}(t), R(t))$ , the LMS solution provided the initial guess to the optimizer.

The optimal solution  $(\vec{V}(t), R(t))$  was then searched by Fletcher's version of the Levenberg-Marquardt optimization technique (Fletcher, 1971, Levenberg, 1944, Marquardt, 1963). MatLab codes were developed for iteration and solution. To reduce the computation time, the Lagrangian multipliers  $\lambda_i$  were assigned with a constant penalty number. For simplification, all moving limits were assigned with equal values ( $\Delta l_i = \Delta l$ ). By assigning different constraint conditions ( $\Delta l = 1 \sim 15 \text{ mm}$ , FIGURE 2.14), the sensitivity of the BLC algorithm was also investigated. After the design variables were

determined at each frame, the knee joint rotation angles could then be expressed by projection method, which will be discussed in the next section.

## 2) Definition of local coordinate system and joint rotation angles

The segmental LCS is defined by the anatomical landmarks at the reference posture (Andriacchi et al., 1998). The origin of the femur LCS is the midpoint of the medial and lateral epicondyles. The femur superior-inferior (SI) axis (Z-axis) runs parallel with the long axis of the femur, passing through the origin of the femur LCS (FIGURE 2.12). The medial-lateral (ML) axis (Y-axis) passes through the femur medial and lateral epicondyles, and the anterior-posterior (AP) axis (X-axis) is the cross product of the Y-axis and Z-axis. The final position of the superior-inferior axis is made orthogonal to the X-axis and Y-axis. The origin of the tibial LCS is set at the midpoint of the medial and lateral edges of the tibial plateau. The SI axis (Z-axis) points along the long axis of the tibia. The ML axis (Y-axis) passes through the medial and lateral edges of the tibial plateau. The AP axis (X-axis) is the cross product of the Y-axis and Z-axis. The final SI axis is the cross product of the X-axis and Y-axis (FIGURE 2.12).

The projection method was used to represent the knee joint rotation in terms of 3 angles: 1) flexion/extension (FE) in the sagittal plane, 2) internal/external (IE) in the transverse plane and 3) varus/valgus (VV) angles in the frontal plane (FIGURE 2.12). By projecting the femur LCS X-axis ( $X_f$ ) onto the XZ-plane of the tibial ACS, the projection  $X_{f-xz}$  has an intersection angle with  $X_t$ , which is defined as the FE angle. By projecting the femur LCS Y-axis ( $Y_f$ ) onto the YZ-plane of the tibial ACS, the projection  $Y_{f-yz}$  has an intersection angle with  $Y_t$ , which is defined as the VV angle. By projecting the femur

LCS Y-axis ( $Y_f$ ) onto the XY-plane of the tibial ACS, the projection  $Y_{f-xy}$  has an intersection angle with  $Y_t$ , which is defined as the IE angle.

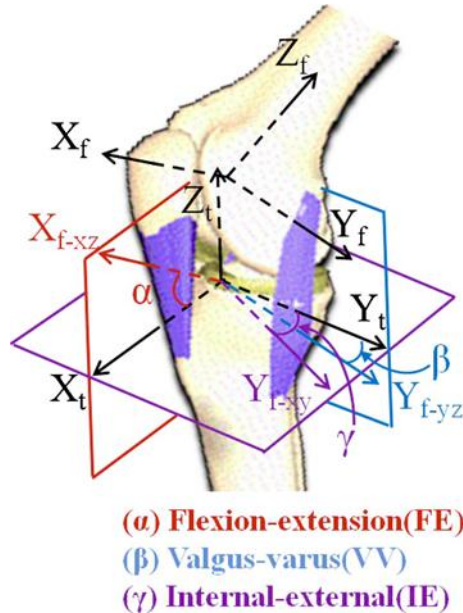


FIGURE 2.12 Definitions of knee joint rotations angle by a projection method.

Given the rotation matrix  $R_t$  for the tibia, and  $R_f$  for the femur in the GCS, the knee joint rotation in the tibia LCS could be calculated by multiplying the inverse tibia rotation matrix with the femur rotation matrix. The rotational angles are calculated in Eq. 3-11 as well.

$$R_{knee} = R_t^T \cdot R_f = \begin{bmatrix} a_{11} & a_{12} & a_{13} \\ a_{21} & a_{22} & a_{23} \\ a_{31} & a_{32} & a_{33} \end{bmatrix} \quad (2.13)$$

$$\alpha = a \tan(a_{31}/a_{11}), \beta = a \tan(a_{32}/a_{22}), \gamma = a \tan(a_{12}/a_{22}) \quad (2.14)$$

### 3) Validation and Comparison

Two fresh cadavers were used for validation. Passive knee flexion/extension that simulated the knee joint range of motion during walking was created during data

collection (FIGURE 2.5). Nineteen skin markers with 10 mm diameter (four triads with three markers on each vertex, and seven single markers) were sparsely placed on the anterolateral side skin of the shank and thigh according to the marker set in a previous publication (Gao and Zheng, 2008), and one extra marker (S11) was mounted at the tibial tuberosity (FIGURE 2.5). A bicortical bone pin with four markers was rigidly inserted in the tibia bone and femur bone from the posterior to track the 6-degree knee joint spatial movement. An 11-camera motion capture system (MAC, Santa Rosa, CA) was used to record motion data at 60 Hz; the instrument accuracy was less than 1 mm after calibration. A reference posture with the cadaver leg in natural extension was recorded to define the segmental local coordinate system; after capturing the reference trial, three good dynamical trials were collected from each cadaver during simulated walking.

After reconstructing the 3-D locations of the markers, the ground truth bone motion was generated from pin-mounted markers using a rigid-body transform function. Matlab codes were developed based on the LMS algorithm and point cluster technique (PCT) (Andriacchi et al., 1998). For each trial, three different methods (LMS, PCT and BLC) were run respectively to estimate the knee joint motion from skin-mounted markers. The root means square error (RMS-E) and peak error (Peak-E) were calculated from all three algorithms; and errors for all three algorithms were compared using one way ANOVA with significant factor  $p=0.05$ .

### 2.3.3. Results

Three knee joint rotation angles (FE, IE and VV) and three displacements (AP, ML and SI) were expressed in the tibia ACS. The rotations and translation of one typical

trial is plotted in FIGURE 2.13. The plotted results were solved at  $\Delta l = 4$  mm in the constraint functions of the BLC algorithm and constraint conditions (Eq. 3-7).

TABLE 2.7 Root mean square error (RMS-E) and peak error (Peak-E) (unit mm for AP, ML, SI translations; unit (°) for FE, IE, VV rotations) for three motion analysis algorithms (LMS, BLC and PCT) in predicting knee joint kinematics. Mean (standard deviation).

	LMS		BLC		PCT	
	RMS-E	Peak-E	RMS-E	Peak-E	RMS-E	Peak-E
FE	0.6(0.1)	1.1(0.1)	1.1(0.3)	2.0(0.2)	2.2(0.4)	3.5(0.2)
IE	1.7(0.4)	2.2(0.6)	0.7(0.1)	1.7(0.3)	2.4(0.6)	3.7(0.6)
VV	0.7(0.1)	1.6(0.1)	0.4(0.1)	0.9(0.1)	1.4(0.1)	2.1(0.1)
AP	5.9(0.8)	9.0(0.9)	7.7(0.8)	7.7(4.7)	10.2(1.1)	14.0(1.0)
ML	1.2(0.2)	2.0(0.3)	0.4(0.1)	1.4(0.3)	4.3(0.4)	6.6(0.7)
SI	2.1(0.4)	4.6(0.3)	5.5(1.1)	11.6(1.1)	3.0(0.6)	6.9(0.6)

The rotation angle in the sagittal plane was reproducible among all three algorithms (FIGURE 2.13). The maximum error came from PCT (peak error:  $3.5 \pm 0.2^\circ$ ) in the sagittal plane, TABLE 2.7. The most accurate FE angle was predicted by LMS (peak error:  $1.1 \pm 0.1^\circ$ ). The BLC algorithm had significantly higher accuracy in the IE and VV angles than the other two algorithms ( $p = 0.01$ ). For the IE angle, the RMS error of BLC reduced from  $1.7 \pm 0.4^\circ$  of LMS algorithm and  $2.4 \pm 0.6^\circ$  of PCT to  $0.7 \pm 0.1^\circ$ , and the peak error was significantly smaller than the other two algorithms (BLC  $2.0 \pm 0.3^\circ$ , LMS  $2.2 \pm 0.6^\circ$ , PCT  $3.7 \pm 0.6^\circ$ ) ( $p = 0.02$ ), TABLE 2.7. In the frontal plane, there were significant differences in the RMS error ( $p < 0.05$ , BLC  $0.4 \pm 0.1^\circ$ , LMS  $0.7 \pm 0.1^\circ$  and PCT  $1.4 \pm 0.1^\circ$ ) and in the peak error ( $p < 0.05$ , BLC  $0.9 \pm 0.1^\circ$ , LMS  $1.6 \pm 0.1^\circ$ , PCT  $2.1 \pm 0.1^\circ$ ) (TABLE 2.7).

The curves were shifted from each other in the translation results (FIGURE 2.13). One interesting finding was noted in the medial-lateral direction, where the BLC algorithm had significantly less RMS error ( $0.4 \pm 0.1$  mm) than LMS ( $1.2 \pm 0.2$  mm) and PCT ( $4.3 \pm 0.4$  mm). In the other two directions, although the BLC curves showed comparable patterns with the curves of the ground truth bone motion (from bone-mounted markers), the BLC's accuracy was very low (percentage RMS error =  $60.6 \pm 11.3\%$  ROM in AP, and  $37.6 \pm 7.9\%$  in SI). In the SI direction, the LMS (RMS error:  $2.1 \pm 0.4^\circ$ ) and PCT (RMS error:  $3.0 \pm 0.6^\circ$ ) were the better algorithms to estimate the femur translation in the tibia LCS compared with the BLC algorithm.

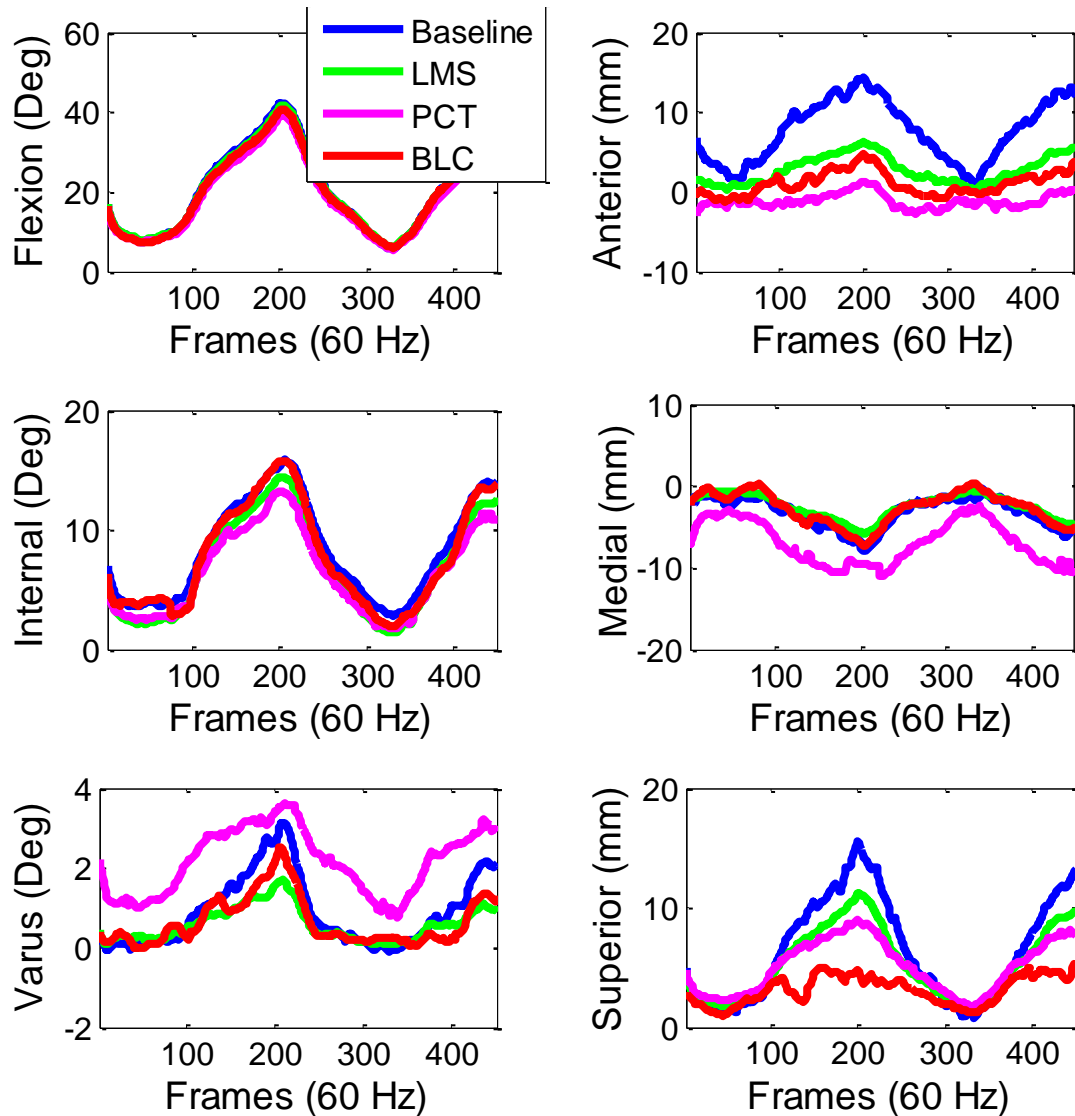


FIGURE 2.13 The results of knee joint 6 degrees of freedom (3 rotations and 3 translations) using three different optimization algorithms. Baseline – the true bone motion from bone pins, LMS – traditional least-mean-square based algorithm, PCT – point cluster technique, BLC – improved algorithm considered bony landmark constraints.

Eighteen simulations were respectively run under different constraints ( $\Delta l$  was changed from 1.0 mm to 15.0 mm) in the BLC algorithm, constrained conditions (3.2). The peak errors of the BLC algorithm changed as the constraints were changed between 1 mm and 8 mm (FIGURE 2.14). After that, the RMS errors converged to certain values (0.6° for IE rotation, 0.7° for VV rotation, and 1.3 mm for ML translation). The

converged RMS errors of VV rotation and ML translation were close to the LMS algorithm ( $0.7^\circ$  for VV rotation, 1.2 mm for ML translation on average), and the converged RMS error of IE rotation was smaller than that of the LMS algorithm ( $1.7^\circ$  on average).

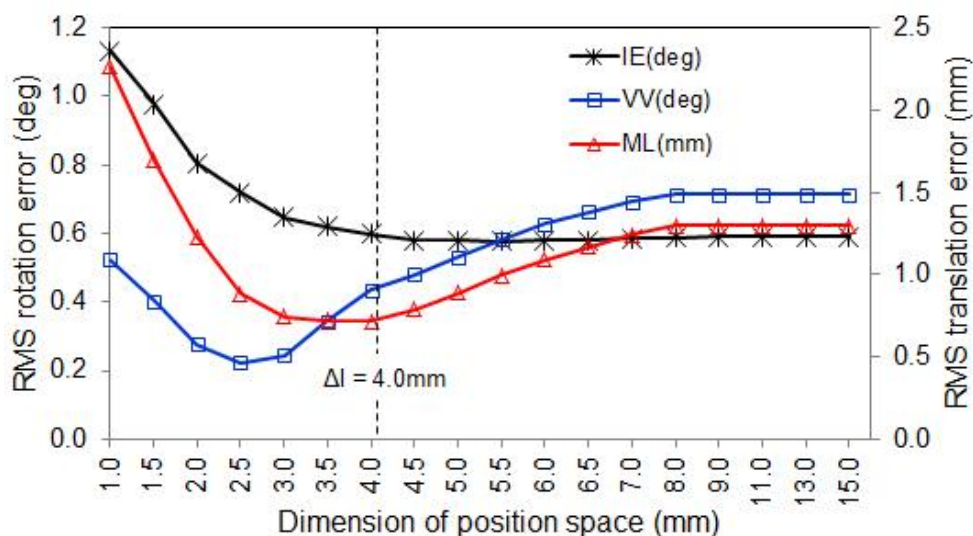


FIGURE 2.14 The accuracy of BLC algorithm in predicting secondary tibiofemoral rotation and medial-lateral translation under different moving limits.

#### 2.3.4. Discussion

The preliminary findings of our study suggested that the bony landmarks could provide useful constraints to refine the knee joint kinematics results in certain components. For more than two decades, the low accuracy of the secondary rotation has been one of the most notable limitations of skin marker-based motion analysis (Leardini et al., 2005). These small secondary rotations are of high interest in initialization and progression of knee osteoarthritis (Andriacchi and Dyrby, 2005). According to our findings, with additional constraint functions, the bony landmark constraint (BLC)

algorithm increased the accuracy of IE and VV angles by 45% from LMS and by 65% from PCT. Therefore, for secondary rotations of the knee, the BLC algorithm is more helpful for detecting abnormal knee kinematics with our marker set. The accuracy of the knee joint ML translation was also improved by using the BLC algorithm compared with LMS and PCT (FIGURE 2.13). The outcome was probably contributed by the ML directional constraints at five bony landmarks (T10, T11, S1, S2 and S11, FIGURE 2.5) in optimization. However, the accuracy was deteriorated in the AP and SI directions. It was probably because no additional constraints were exerted in AP or SI directions on the femur landmarks. During the optimization process, the bone position was fitted in the ML direction with priority, while more than likely sacrificing the accuracy in the other two directions. Another cause may come from the fixation of Lagrangian multipliers ( $\lambda_i$ ). Future study will work on designing a more functional marker set and employing more reasonable landmark constraints in the optimization.

The sensitivity analysis showed that the VV and ML curves had an obvious valley (neighboring  $\Delta l=3$  mm), while the accuracy of IE was relatively insensitive to the constraint value (FIGURE 2.14). That typical value ( $\Delta l \approx 3$  mm) was probably related to the maximum magnitude of soft tissue movement during flexion/extension movement. According to a previous fluoroscopic study of seven patients with total knee arthroplasty (TKA), the STA could be estimated by a multi-linear function of hip and knee flexion angles (Gao, 2009). According to the multi-linear functions, the knee joint flexion angle was around 45 °in the current study, and the ML component of STA was around 1.8 mm at the femur epicondyles, and smaller than 2.4 mm at the tibia plateau edges during a whole gait cycle; at the tibia tuberosity, the STA was smaller than 3.4 mm in all three

directions. For better functionality, the limits should be adjusted according to the body type and the involved activity of the individual subject.

The sensitivity study showed that the IE, VV and ML results did not change after  $\Delta l > 8$  mm (FIGURE 2.14), which probably indicated the magnitudes of STA were smaller than 8 mm in those specific directions and the bony landmarks constraints lost their function when they exceed the maximum STA. Another interesting finding was noted that the IE rotation result of BLC did not converge to the LMS algorithm. The inconsistency may be contributed to by different methods used in the algorithm. In the BLC algorithm, a numerical method (Fletcher's version of the Levenberg-Marquardt) was used to solve the constrained optimization problem, whereas, an analytical method was developed to minimize the objective function in the LMS algorithm.

Andriacchi et al. (Andriacchi et al., 1998) introduced the PCT with an optimal marker set covering the entire segmental surface. Unfortunately, the skin markers were only placed on anterolateral segmental sides, in order to be more visible by the cameras in the current study. The marker set limitation might have affected the accuracy of the PCT and caused the whole period offsets in predicting VV rotation and ML translation. Also in this study, the cadaver knee was passively driven by a rod under the foot. The secondary motion of the non-weight bearing cadaver knee may be different from that of weight-bearing condition during level walking (Dyrby and Andriacchi, 2004). Before implementing this algorithm in clinical application, future in vivo validation work should be undertaken during daily activities.

### 2.3.5. Conclusion

By considering the soft tissue movement at special bony landmarks, the proposed bony landmark constraint (BLC) algorithm has higher accuracy in predicting the secondary rotations (internal/external, varus/valgus) than the least mean square algorithm (LMS) and point cluster technique (PCT) during knee flexion/extension. Also the current BLC algorithm can predict more accurate medial-lateral translation. Therefore, the presented algorithm may be helpful in detecting abnormal secondary kinematics of the knee joint, which is important to early detection of the onset of joint pathologies. This pilot study is a start of using STA characteristics as constraints to tune the optimization results. More exquisite work should be done on the basis of this study to develop a better motion analysis algorithm.

## 2.4. Summary

In this chapter we reviewed the commonly used bone motion measurements including invasive, fluoroscopic and optical video techniques, etc. We discussed the advantages and limitations of dual-fluoroscopic and skin marker-based motion analysis, and decided to use skin marker-based motion analysis in this dissertation. This chapter also introduced the technical procedures of how to retrieve the rigid bone motion from redundant skin markers by using the LMS based algorithm.

The accuracy of knee joint motion measurement by using our redundant marker set has been quantified in this chapter. We also introduced a quaternion-based optimization algorithm which takes the bony landmark as external constraints to improve the accuracy of knee joint secondary rotations (referred to as BLC algorithm). Although the BLC algorithm has an improved accuracy on the internal/external and varus/valgus rotation, it has a relative low accuracy on knee translation measurement compared to the

Spoor's LMS based algorithm. Therefore, in this study we continued to use the Spoor's LMS based motion analysis algorithm in retrieving the bone motion from our subjects.

## CHAPTER 3: DOES THE TRANSTIBIAL TECHNIQUE RESTORE KNEE KINEMATICS AND KINETICS?

In this chapter, we investigated: 1) knee joint kinematics and kinetics after ACL-reconstruction using the transtibial technique during low demand level walking and high demand downstairs pivoting; 2) the effect of lower dominance on the postsurgical knee performance.

### 3.1. Knee Joint Stability Following ACL-reconstruction Using the Transtibial Technique during Level Walking

Normal ambulatory kinematics of the knee joint is often not fully restored after ACL-reconstruction, which may increase the risk of cartilage degeneration and premature osteoarthritis in the involved knees. Lower limb dominance may have impacts on knee joint kinematics after ACL reconstruction. In this chapter, we presented a study on knee joint kinematics among patients with dominant side reconstruction and those with non-dominant side reconstruction using the traditional transtibial technique. This work was published in the *Clinical Biomechanics*, 2012 Feb; 27(2): 170-175 (Wang and Zheng, 2010b).

#### 3.1.1. Introduction

Altered knee joint motion has been observed after anterior cruciate ligament (ACL) injury (Andriacchi and Dyrby, 2005, Georgoulis et al., 2003, Defrate et al., 2006). The kinematic alteration has not been fully restored by ACL reconstruction surgeries and

the rehabilitation that follows (Gao and Zheng, 2010a, Scanlan et al., 2010, Tashman et al., 2007, Brandsson et al., 2002, Papannagari et al., 2006). This residual change in knee joint motion might contribute to a higher risk of articular cartilage degeneration and premature osteoarthritis (OA) in the involved knees according to previous investigations (Andriacchi and Mundermann, 2006, Daniel et al., 1994, Lohmander et al., 2004, Seon et al., 2006).

According to a previous survey of 1538 people (94.8% right dominant), the prevalence of knee joint OA was 19% higher on the right side than on the left side (Wang et al., 2007). In another study, healthy right dominant individuals displayed significant bilateral differences in the cartilage volume of the lateral compartment ( $-6.5\%$  (SD  $5.9\%$ ); left - right) and in the mean cartilage thickness of the medial compartment ( $-6.2\%$  (SD  $4.6\%$ ); left - right), while no systematic difference was found in the left dominant individuals (Eckstein et al., 2002). These asymmetries in knee joint anatomy may lead to the different knee joint kinematics after ACL injury and reconstruction. Thus, it is of great interest to consider the leg dominance as a factor in knee joint kinematic analysis to ACL-reconstructed (ACL-R) patients.

The cartilage degeneration and OA development after ACL injury are considered as a progressive process that develops during even the most frequent daily activities, such as level walking (Chaudhari et al., 2008). Routine tests of knee instability (KT-1000 testing and Lachman's test, etc.), which are based on knee joint passive response to static and non-weight bearing situations, do not necessarily reflect physiological loading conditions (Brandsson et al., 2002, Papannagari et al., 2006, Pollet et al., 2005, Borjesson

et al., 2005). Instead, level walking was studied as the more relevant ambulatory activity for understanding the etiology of OA (Miyazaki et al., 2002).

In this study, the knee joint motion of patients who had unilateral ACL reconstruction on the dominant and non-dominant side was compared to that of healthy controls. The purpose was to identify the kinematic alteration of dominant ACLR knees and non-dominant ACLR knees during level walking after rehabilitation. We specifically tested the hypothesis that individuals with unilateral ACL reconstruction on the dominant side developed significantly different motion patterns at the knee joint from those with ACL reconstruction on the non-dominant side.

### 3.1.2. Material and methods

#### 1) Participants

Forty-one patients with unilateral ACL reconstruction using the transtibial technique and no other history of serious lower limb injury were recruited (11 were from Shands Hospital, University of Florida, Gainesville, FL and 30 from OrthoCarolina, Charlotte, NC). Twenty healthy subjects with no history of lower extremity injuries or functional disorders were also recruited to test the pre-injury dominance effect on knee joint kinematics (TABLE 3.1). The study was conducted following an IRB approved protocol and informed consent was obtained from each subject before testing. Nineteen subjects underwent ACL reconstruction on their dominant side (Group-d) and twenty-two subjects underwent ACL reconstruction on their non-dominant side (Group-n). Patients with chondral lesions, posterior cruciate or collateral ligament tears were excluded from this study. Hamstring tendon grafts or patellar tendon grafts were used in both groups according to surgeon preference (TABLE 3.1). At the time of testing, patients were at least 4 months post-operative from surgery (~14 months in average) and had received

permission to perform all daily activities from their treating physician. The involved knees' KT-1000 measurements did not differ significantly ( $p = 0.67$ ) among groups. None of the subjects had diagnosed radiographic or symptomatic OA. No statistically significant differences in post-surgery time ( $p = 0.24$ ), body weight ( $p = 0.51$ ), height ( $p = 0.47$ ), and body mass index (BMI) ( $p = 0.53$ ) were found between these two groups (TABLE 3.1). The lower limb dominance was determined by ball kicking and confirmed with subjects afterwards (Porac and Coren, 1981).

TABLE 3.1 Demographics (mean (SD)) of patients with ACL reconstruction on the dominant side (Group-d) and patients with ACL reconstruction on the non-dominant side (Group-n) and the healthy controls; BMI: body mass index.

Variables	Group-d	Group-n	Controls
Gender (m:f)	12:7	12:10	13:7
Age (years)	32.4 (8.6)	31.1 (8.0)	23.4 (3.0)
Weight (kg)	83.9 (18.8)	81.4 (16.4)	70.8 (13.2)
Height (cm)	179 (10)	174 (7)	176 (10)
BMI ( $\text{kg}/\text{m}^2$ )	25.6 (5.0)	26.1 (6.7)	22.7 (2.6)
Hamstring tendon graft	16	19	N/A
Bone -patella tendon-bone graft	3	3	N/A
Post Surgery (months)	14.1 (4.4)	13.9 (5.5)	N/A

## 2) Experimental protocol

Redundant retro-reflective markers (10 mm in diameter) were placed on major joint landmarks and lower extremity segments (19 on the thigh and 19 on the shank) according to previously reported studies (Gao and Zheng, 2010a, Gao and Zheng, 2008, Wang and Zheng, 2010b) (FIGURE 2.1). Five markers were placed on the pelvis (the left

and right anterior superior iliac spines, the left and right posterior superior iliac spine and the sacrum), which were used to predict the hip joint center using a previously reported method (Bell et al., 1990). A 10-camera motion capture system (MX-F40, VICON, Oxford UK) was used to record the motion data at 60 Hz while the subject was walking through a calibrated volume at their self-selected speed. Two floor embedded force platforms (OR6-6, AMTI, MA) were used to synchronously record ground reaction force at 1200 Hz, which would be used to determine the key frames of a gait cycle (Gao and Zheng, 2010a). A static trial (t-pose) was recorded with feet shoulder width apart and toes facing forwards at a neutral standing position as the reference posture. After the subjects were familiarized with the testing procedure, ten walking trials were recorded from each subject at a self-selected walking speed.

### 3) Data analysis

The motion data were initially low-pass filtered with a cut-off frequency of 6 Hz in order to get rid of high-frequency noise. The movement of thigh and shank during walking was determined using a previously reported approach (Gao and Zheng, 2010a). A MATLAB (MathWorks Inc., MA, USA) program was developed to retrieve the knee joint kinematics from the spatial coordinates of skin markers by using a least-square-based algorithm (Spoor and Veldpaus, 1980, Veldpaus et al., 1988). The technique was validated by 6 fresh cadaveric lower extremities using intracortical bone pins, which had an accuracy of  $0.71^\circ$  (SD  $0.43^\circ$ ) for flexion/extension (FE),  $1.17^\circ$  (SD  $0.23^\circ$ ) for axial rotation (internal/external, IE), and  $0.34^\circ$  (SD  $0.17^\circ$ ) for varus/valgus (VV) (Gao et al., 2007). At t-pose,  $Z_f$  of femur local coordinate system (LCS) pointed from the femur origin  $O_f$ , which was at the midpoint of femoral epicondyles, to the hip joint center.  $Y_f$

was the cross product of  $Z_f$  and the vector from the heel to the second metatarsal;  $X_f$  was the cross product of  $Y_f$  and  $Z_f$ .  $Z_t$  of tibia LCS pointed from the ankle joint center (midpoint of medial and lateral malleoli) to tibia origin  $O_t$  which was at the midpoint of medial and lateral tibial plateau edges.  $Y_t$  was the cross product of  $Z_t$  and the vector from the heel to the second metatarsal;  $X_t$  was the cross product of  $Y_t$  and  $Z_t$  (Gao and Zheng, 2010a). By projecting the  $Y_f$  onto the YZ plane of tibia LCS, the VV angle ( $\phi$ ) was determined as the intersection angle between the projection vector ( $Y_{f-yz}$ ) and  $Y_t$ ; in the same way, the FE angle was the intersection between  $X_{f-xz}$  and  $X_t$ ; and IE angle was the intersection angle between  $Y_{f-xy}$  and  $Y_t$  (FIGURE 2.12)(Wang and Zheng, 2010b). The FE and VV angles were zero when the leg was completely straight ( $Z_f$  was collinear with  $Z_t$ ). Knee translations were expressed as the femur displacements relative to the tibia in tibial LCS. In order to group and compare knee joint motion at the same instant of a gait cycle, data was normalized from 0% at heel strike (HS1) to 100% at the next heel strike (HS2) of the same foot using linear interpolation (Helwig et al., 2011). The first heel strike (HS1) and toe off (TO) were detected by the force plates with a threshold of 5% body weight; the second heel strike (HS2) was determined by a gait event detecting algorithm (Hreljac and Marshall, 2000). Good trials were selected using the following criteria: 1) No marker drops or marker missing for more than 4 consecutive frames, 2) Foot completely stepped inside the force plate, and 3) Trial was long enough to include two complete heel strikes for both legs. Joint motions from three good trials were averaged to represent each subject.

Net external joint reaction moments were determined from an inverse dynamic model using previously reported anthropometry data (Winter, 1991). Knee adduction

moment was computed for each subject and expressed as the frontal plane component of the knee joint moment in the tibia local coordinate system and was normalized by the subject's body mass (Wang and Zheng, 2010a).

#### 4) Statistical analysis

All knees were categorized according to their dominance (dominant or non-dominant) and status (reconstructed or uninvolved): dACLR and nUnInv from Group-d, and nACLR and dUnInv from Group-n. A mixed-effect ANOVA with two factors (SPSS Inc., Chicago, IL, USA) was used to compare the knee joint kinematics between reconstructed and uninvolved contralateral sides. The two factors used were the knee status (between-knees factor: reconstructed vs. uninvolved) and the time point (within-knee factor: HS1, midstance, flexion valley, toe off, flexion peak and HS2). Measures of joint kinematic variables were compared bilaterally for group-d, group-n and healthy controls at neutral standing and at different time points along a gait cycle using one-way ANOVA. Root-mean-squares (RMS) of the bilateral differences over a gait cycle were also computed as a comprehensive evaluation of the kinematic asymmetry for each subject. Significance level of the statistical analysis was set at 0.05.

#### 3.1.3. Results

There were no significant differences in all 3 rotations ( $p = 0.78$  for FE, 0.45 for IE and 0.63 for VV) or 3 translations ( $p = 0.43$  for AP, 0.25 for ML and 0.31 for SI) or external knee adduction moments ( $p = 0.57$ ) between the dominant and contralateral knees for the control subjects during both static and dynamic trials.

Group-n: The reconstructed (nACLR) knees were less extended than the uninvolved (dUnInv) knees throughout the whole stance phase (FIGURE 3.1 A), and the lower extension was statistically significant during the midstance phase ( $p = 0.02$ ) and at

HS1 and HS2 ( $p = 0.01$ ) (FIGURE 3.1 A). The involved knees had significantly ( $p = 0.02$ ) less lateral translation than their contralateral knees at the HS1 and the HS2 (FIGURE 3.1 E). SI translation showed no significant bilateral difference, although there was a significant interaction between knee status and time point ( $p = 0.024$ ) (FIGURE 3.1 F). At neutral standing, the involved knees were in slight flexion ( $1.6$  (SD  $1.3$  °)) while the contralateral knees were in slight hyper-extension ( $-1.7$  (SD  $1.2$  °)), and the difference was statistically significant ( $p=0.015$ ) (FIGURE 3.2).

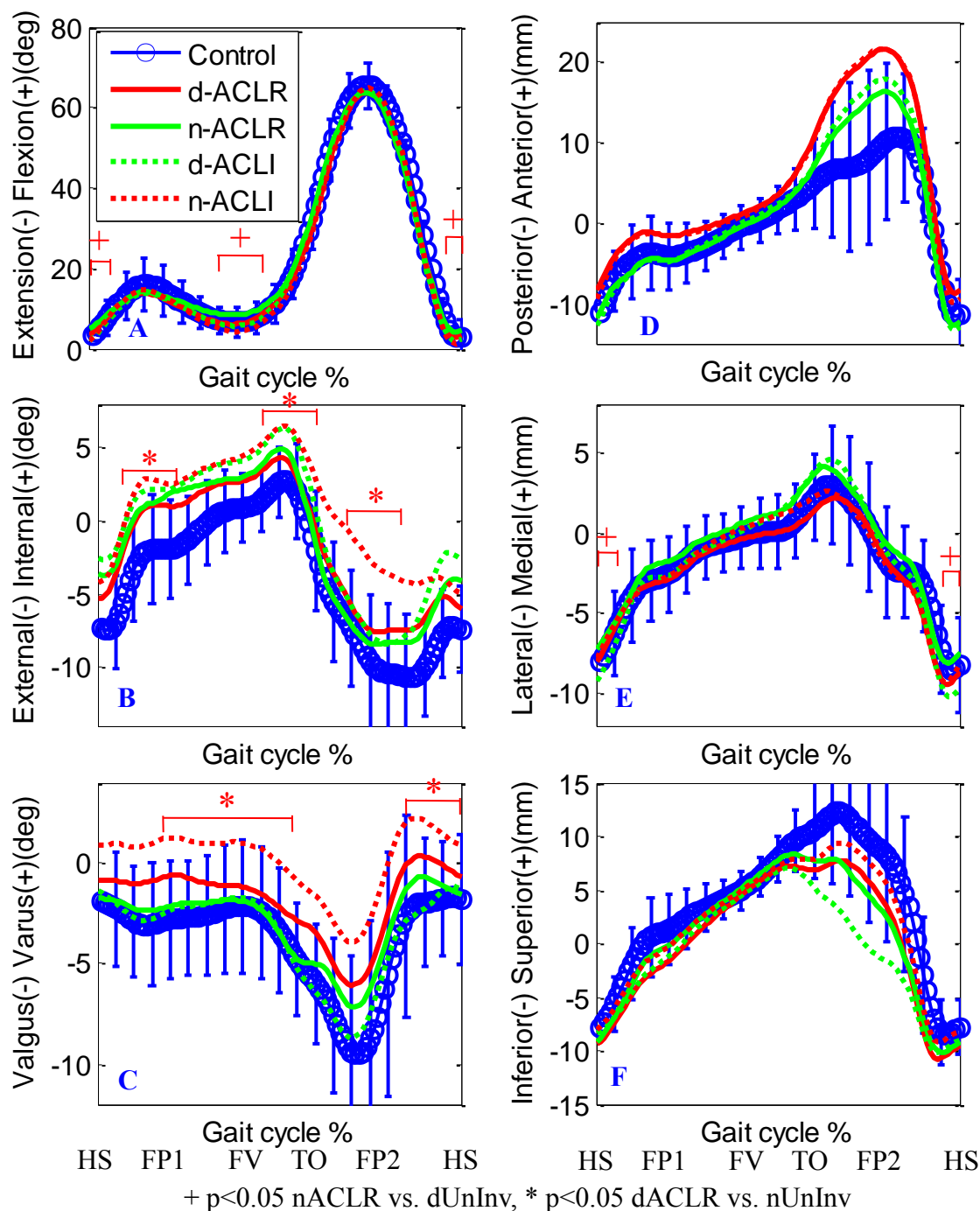


FIGURE 3.1 Subplot A-C: knee joint rotation for dACLR, nUnInv, nACLR and dUnInv knees during a gait cycle; subplot D-F: knee joint translation during a gait cycle. Knee flexion, varus and internal tibia rotation were illustrated as positive values; anterior, medial and superior translations (femur relative to tibia) were illustrated as positive values.

Group-d: The involved (dACLRL) knees had significantly greater ( $p=0.034$ ) external tibial rotation than the uninvolved contralateral (nUnInv) knees at the midstance and right before toe off during stance phase and during the midswing phase (FIGURE 3.1 B). The uninvolved knees exhibited varus offset ( $2.1^\circ$  on mean) throughout the whole gait cycle, and the offset was significant during the middle and late stance phase and late swing phase ( $p=0.027$ ) (FIGURE 3.1 C). Also the peak valgus rotations during stance phase were significantly greater ( $p=0.017$ ) for the involved knees than the contralateral knees. The involved knees had significantly ( $p=0.031$ ) lower external knee adduction moment (peak value:  $0.35$  (SD  $0.16$ ) Nm/kg) than their contralateral knees (peak value:  $0.46$  (SD  $0.15$ ) Nm/kg) during stance phase (FIGURE 3.3). At neutral standing, the involved knees exhibited significantly greater external tibial rotation and valgus (IE:  $-0.2^\circ$  (SD  $0.2^\circ$ ), VV:  $-1.7^\circ$  (SD  $0.7^\circ$ )) than the contralateral knees (IE:  $0.1^\circ$  (SD  $0.1^\circ$ ), VV:  $0.3^\circ$  (SD  $0.6^\circ$ )) (FIGURE 3.2). The mixed-effect ANOVA showed no significant interaction between knee status and time point in translations or rotations.

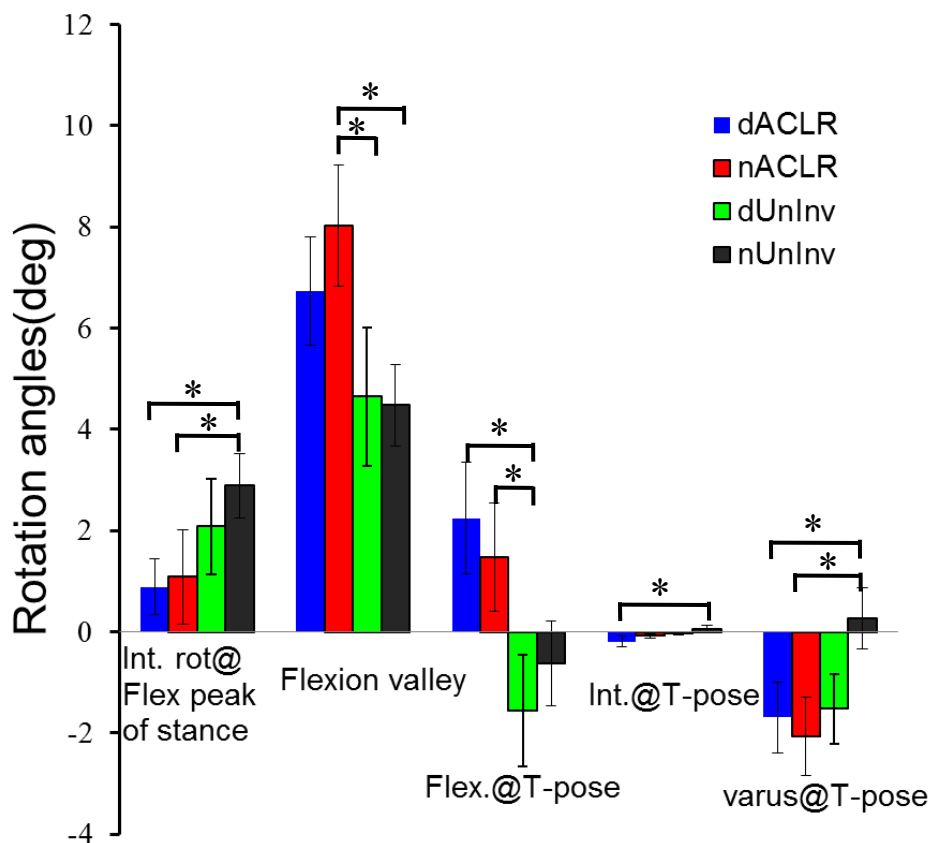


FIGURE 3.2 Knee joint rotation angles for different groups at several key events. Int. rot @ flex peak of stance: the internal tibial rotation angle at the peak flexion instant of stance phase; Flexion valley: minimal flexion during middle stance phase; t-pose: neutral standing as the reference frame. Error bars represent the standard deviation. (\* $p < 0.05$  student's  $t$  test)

For the varus and valgus of the knee, the RMS values of bilateral differences were significantly ( $p = 0.024$ ) different between the two ACLR groups (FIGURE 3.4). Sixteen (13 with hamstring tendon graft and 3 with patellar tendon graft) out of the 19 dominant involved subjects had reduced varus rotation in the reconstructed knees compared with their uninvolved contralateral knees ( $-2.1^\circ$  (SD  $2.2^\circ$ )), whereas no obvious trend was observed from non-dominant involved subjects ( $0.9^\circ$  (SD  $3.1^\circ$ )). Bilateral differences of VV in Group-d were significantly different from those in Group-n throughout the whole stance phase ( $p = 0.021$ ).

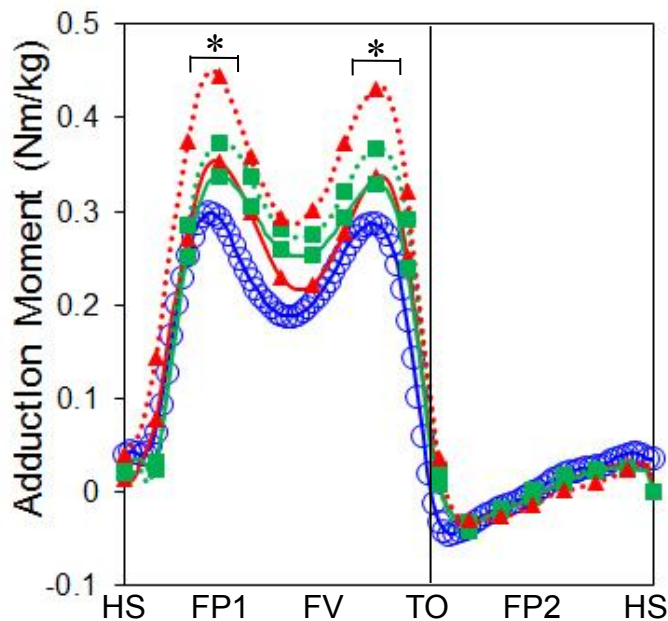


FIGURE 3.3 Knee adduction moment (exerted by shank) for dACLR, nUnInv, nACLR and dUnInv knees during a gait cycle. \* denotes significant difference between dACLR and nUnInv ( $p < 0.05$ ).

#### 3.1.4. Discussion

The results of this study supported the hypothesis that significantly different kinematics are developed between the subjects with dominant involved knees and subjects with non-dominant involved knees following ACL reconstruction and a rehabilitation program. The results of this study, therefore, demonstrate the effect of knee dominance on knee kinematic outcomes following ACL reconstruction.

For the healthy control group, the same side-to-side knee joint kinematics reflected the same pre-injury starting point between the dominant and non-dominant knees. The sagittal plane rotation of the dACLR knees were restored to the normal level of the contralateral knees at the time of testing. Whereas 18/22 nACLR knees exhibited less extension during the mid-stance than their contralateral knees, which might be explained by a stiffening strategy involving less knee motion and higher muscle

contraction to consistently stabilize their ligament in impaired knees (Hurd and Snyder-Mackler, 2007). The reduced extension of nACL R knees was also found at their neutral standing position, which may be explained by an adaptation strategy preventing the ACL graft from being overstressed. The finding of extension deficit on the reconstructed knees was in line with previous studies (Gao and Zheng, 2010a, Gokeler et al., 2003, Hurd and Snyder-Mackler, 2007).

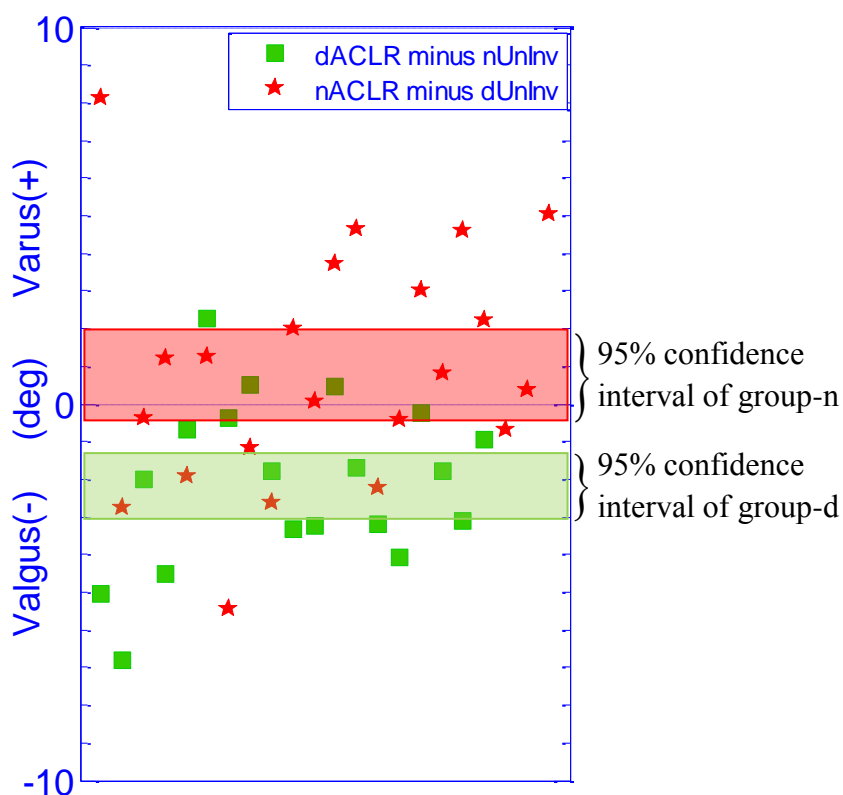


FIGURE 3.4 Root mean square of bilateral differences of knee joint VV rotation over a gait cycle. The shade area denotes the 95% confidence interval of the mean. The dACL R knees showed a statistically significant valgus offset of  $-2.4 \pm 2.3^\circ$  ( $p < 0.01$ ) relative to nUnInv knees, whereas no systematic difference existed between nACL R and dUnInv.

In the transverse plane, the dACL R knees exhibited external tibial rotation offsets relative to their contralateral knees which was consistent with previous studies (Scanlan

et al., 2010, Tashman et al., 2007). On the other hand, the axial tibial rotation of nACL knees was not significantly different from their contralateral knees. These differences suggest that different compensatory motion patterns were developed between Group-n and Group-d patients. According to a study by Brady and coworkers (Brady et al., 2007), an increase in initial graft tension might cause the tibia to rotate externally. However, in this study, all surgeries using hamstring tendon grafts and patellar tendon grafts were performed respectively by the same surgeon and patients went through similar aggressive rehabilitation programs; thus, the graft tension should not be significantly different between the two groups. Differences in axial rotation may correlate with progressive cartilage degeneration and the development of arthritis. Previous morphological studies have demonstrated the histological and morphological variation of knee joint articular cartilage at different locations (Quinn et al., 2005, Thambyah et al., 2006). Stergiou and coauthors suggested that the altered tibiofemoral rotation would change the load distribution and might place joint loadings onto non-weight bearing regions of the articular cartilage which could initiate cartilage breakdown (Stergiou et al., 2007). Therefore, the altered tibia rotation (relative to uninvolved contralateral knees) may cause degenerative changes in meniscus and articular cartilage in the long term (Andriacchi and Dyrby, 2005, Lohmander et al., 2004).

The increased varus rotation of the uninvolved knees for Group-d subjects was contradicted by a previous finding where the reconstructed knees were more varus than their contralateral knees during downhill running (Tashman et al., 2007). The discrepancy may be explained by the fact that level walking is much less intensive than downhill running, which may initiate different neuromuscular control patterns in the lower

extremities. The result was also inconsistent with another study where no difference was found in varus rotation compared with the contralateral knee for patients with hamstring tendon graft (Webster and Feller, 2011). This difference may be explained by the fact that all subjects (9/18 were dominant side involved) were grouped together in that study. Medial compartment osteoarthritis is a common knee joint disease that can result from undue force on the medial compartment. The valgus offset in dominant involved knees would be helpful in maintaining the joint space at the medial side by more evenly distributing the loading across the medial and lateral compartments (Adili et al., 2002). It may also be protective to shift the trunk's center of gravity closer to the uninvolved leg, which would reduce the weight bearing stress on the involved knee. Adduction moment is directly related to the loading of the medial knee compartment (Zhao et al., 2007), thus the smaller peak adduction moment in this study may help to relieve the medial compartment loading for dominant reconstructed knees. For Group-n subjects, the knees had no difference in varus between two sides during stance phase, which was consistent with a previous investigation (Scanlan et al., 2010). Previous studies reported no relevant bilateral differences in knee kinematics for healthy population (van der Harst et al., 2007, Petschnig et al., 1998), which was further confirmed by 20 healthy subjects during level walking in the current study. It may be concluded that the bilateral balance of knee joint kinematics was affected by ACL injury and reconstruction.

There were several limitations in the study. First, all the ACL patients had relatively short post-surgery intervals, so the findings may not be applicable to long-term post-surgery ACLR population. Second, when interpreting the findings of this study, it is important to note that two types of ACL grafts (hamstring tendon and patellar tendon,

half allograft) were used. In this study, the subject number of each graft type was matched (hamstring tendon 16 vs.19, patellar tendon 3 vs. 3) between the two groups and the factor of graft type was not considered. It was supported by previous studies that the graft type may not have an important effect on the knee performance after ACL reconstruction (Moraiti et al., 2009, Spindler et al., 2004). Also the consistent results of dACLR knees (13/16 of the subjects with hamstring tendon graft and all the subjects with patellar tendon graft showed valgus offset on the reconstructed knees) suggested that the effect of graft type was minimal. Third, the anthropometry (height, weight) of the control subjects were different from that of the ACL patients, and we assumed that the finding of no dominance effect on knee joint kinematics among the healthy subjects would predict the pre-injury situation for the ACL patients.

### 3.1.5. Conclusion

The study showed that the lower limb dominance has significant effects on knee joint kinematics following ACL reconstruction and rehabilitation, especially in varus and internal tibial rotation. These motion changes could alter the normal contacting and loading on articular cartilage, which may contribute to the development of knee osteoarthritis. Considering the lower limb dominance may help explain variability in ACL reconstruction outcomes and may lead to changes in ACL techniques and rehabilitation programs that may improve upon outcomes.

## 3.2. Knee Joint Stability Following ACL-reconstruction Using Transtibial Technique during Downstairs Pivoting

It has been shown in the previous section that tibial rotation has not been fully restored by traditional single-bundle ACL reconstruction during walking. Downstairs turning, a more demand frequently engaged activity, may provide insightful information

to evaluate the function of single bundle. This study was submitted to the International Journal of Sports Medicine for consideration of publication on May 23, 2012. The work on healthy controls is published in the International Journal of Sports Medicine, 2010 Oct; 31(10): 742-746 (Wang and Zheng, 2010a).

### 3.2.1. Introduction

The balance of knee joint mobility and stability has been broken after anterior cruciate ligament (ACL) rupture, which leads to abnormal joint movements during dynamic activities (Andriacchi and Dyrby, 2005, Gao and Zheng, 2010a, Georgoulis et al., 2003, Li et al., 2006). A reconstruction surgery, which aims to restore joint stability using a replacement graft, is regularly recommended by orthopedic surgeons (Woo et al., 2005). Although reconstruction surgery is an effective treatment to restore the knee function, it does not necessarily restore the normal knee moment after the surgery and rehabilitation. Abnormal kinematics were observed, especially for the rotation on nonsagittal planes, during daily and high demanding sports activities (climbing stairs, pivoting, cutting, jump and land, etc.) (Gao and Zheng, 2010a, Lam et al., 2011, Scanlan et al., 2010, Stergiou et al., 2007, Webster et al., 2012, Ristanis et al., 2003, Ristanis et al., 2006, Ristanis et al., 2005, Gao et al.). The abnormal knee rotation could alter the normal cartilage contacting and loading which may increase the risk of cartilage degenerative diseases in the long term.

Most ACL reconstruction techniques have focused on reproducing the anteromedial bundle of the native ACL. In those techniques, the single-bundle graft is too close to the central axis of the tibia and femur that makes it insufficient for resisting rotational loads (Woo et al., 2005). The in situ forces in single-bundle graft under

rotational knee loading were range from 45% to 61% of those of the intact knees (Woo et al., 2002), which indicated the insufficiency. Marked inconsistencies in the type of rotational changes were reported across studies. During walking some studies found an increase in internal tibial rotation (Gao and Zheng, 2010a, Georgoulis et al., 2003), while a decrease in internal tibial rotation was reported in other studies (Scanlan et al., 2010, Webster and Feller, 2011). In recent years, concerns have been raised about the success of single-bundle techniques in stabilizing axial tibial rotation during high demanding activities like downstairs pivoting and jump-to-landing (Chouliaras et al., 2007, Georgoulis et al., 2007, Misonoo et al., 2012, Ristanis et al., 2003, Ristanis et al., 2006, Ristanis et al., 2005, Tsarouhas et al., 2010, Webster et al., 2012).

Making a turn is a common daily activity which, on average, happens twice in every 10 steps during daily living (Sedgman, 1994). In daily living, the supporting foot is sliding on the floor when making a sharp ( $\geq 90^\circ$ ) direction change (Wang and Zheng, 2010a). However, in previous studies, which investigated the tibial rotation during pivoting, the supporting foot was planted on the ground that allowed no foot sliding during the task (Chouliaras et al., 2007, Georgoulis et al., 2007, Webster et al., 2012, Ristanis et al., 2003, Ristanis et al., 2006, Ristanis et al., 2005). Thus, the planted foot position in previous studies would trigger excessive tibial rotation which may not reflect the situation of daily turning activities.

Therefore, the purpose of this study was to evaluate the function of transtibial single bundle technique in stabilizing the knee joint during downstairs turning without any external constraint to the foot. A group of subjects who had undergone unilateral ACL-reconstruction were tested. It was hypothesized that on the nonsagittal planes the

knee rotation and moment have not been fully restored by using transtibial single-bundle ACL-reconstruction technique.

### 3.2.2. Material and methods

#### 1) Participants

We recruited thirty subjects (28 right dominant, 2 left dominant) who had undergone unilateral ACL reconstruction and had no other history of serious lower limb injury. All surgeries were performed arthroscopically by a single experienced surgeon using traditional transtibial single-bundle technique. Hamstring tendon (semitendinosus with gracilis enforcement, STG) grafts were used in all subjects. Tibial interference screw and femoral endobutton were used for graft fixation. Tunnel locations and graft fixation of a typical patient are shown on x-ray images in FIGURE 3.5. All subjects completed their rehabilitation program and were released for daily activities. Six of them were still not confident in completing a 90° downstairs pivot turning at the time of testing. Another four subjects (all of which were obese, body mass index > 33) tilted their torso to one side when descending stairs, and were excluded from data analysis. For the remaining 20 subjects, half of them had ACL reconstruction on their dominant side (TABLE 3.2). Ten healthy subjects (with similar body type as ACL patients) with no lower extremity injuries or functional disorders were selected as the control group (TABLE 3.2). The study was conducted following an IRB approved protocol and signed consent form was obtained from each subject before testing.

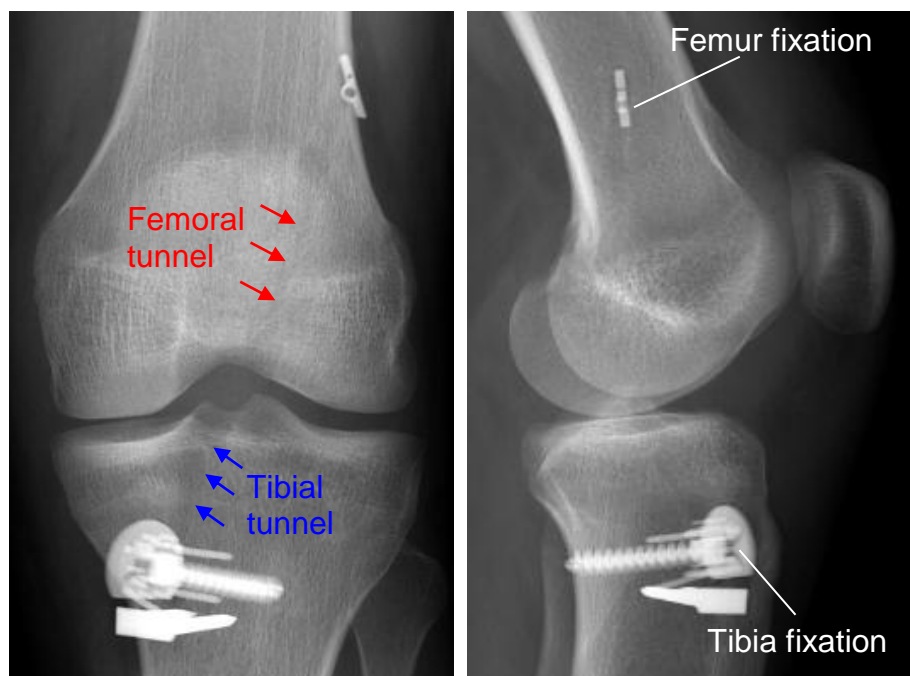


FIGURE 3.5 Front and lateral radiographs of a typical patient taken 3 months after ACL-reconstruction surgery using transtibial single-bundle technique.

In our foregoing study of healthy people, the side by side difference was found from knee rotation and loading during downstairs turning (Wang and Zheng, 2010a). It is possible that some important information could be overshadowed if we group all ACL-patients together. Therefore, subjects were divided into two groups (Group-d and Group-n) according to the dominance of the involved leg which was determined by ball kicking and confirmed with the subjects afterwards. The subjective IKDC scores were not significantly different ( $p = 0.67$ ) between groups at the time of testing (TABLE 3.2). Subjects with chondral lesions, posterior cruciate or collateral ligament tears were excluded from this study. None of the subjects had diagnosed radiographic or symptomatic OA. No statistically significant differences were found in post-surgery time, body weight, height, and body mass index (BMI) between these two groups (TABLE 3.2).

TABLE 3.2 Demographics (mean (SD)) of patients with ACL reconstruction on the dominant side (Group-d) and patients with ACL reconstruction on the non-dominant side (Group-n) and the healthy controls; BMI: body mass index.

Variables	Group-d	Group-n	Controls
Age (years)	31.4 (8.1)	33.9 (7.8)	22.8 (2.8)
Weight (kg)	77.6 (17.0)	81.6 (16.0)	73.8 (19.2)
Height (m)	1.75 (.11)	1.75 (.05)	1.76 (.13)
BMI (kg/m <sup>2</sup> )	24.8 (4.7)	26.7 (5.3)	23.5 (2.9)
Post Surgery (months)	12.4 (6.2)	15.8 (8.3)	N/A
IDKC subjective knee evaluation	72.4 (10.7)	72.9 (10.3)	N/A

## 2) Experimental protocol

Redundant retro-reflective markers (10 mm in diameter) were placed on the shank and thigh including major bony landmarks according to a marker set described in our previous studies (Gao and Zheng, 2010a, Wang et al., 2012, Wang and Zheng, 2010a, Wang and Zheng, 2010b, Gao et al., 2012). Briefly, nine markers were placed on the medial and lateral femoral epicondyles, the medial and lateral ridges of the tibial plateau, the medial and lateral malleoli, the tibial tuberosity, the second metatarsal head and the heel. Five markers were placed on the pelvis (the left and right anterior superior iliac spines, the left and right posterior superior iliac spine and the sacrum), which were used to predict the hip joint center using a previously reported method (Bell et al., 1990). A 10-camera motion capture system (MX-F40, VICON, Oxford UK) was used to record the motion data at 60 Hz while the subject was walking through a calibrated volume at their self-selected speed. The system was calibrated following manufacturer's standard procedure in NEXUS™ software (VICON, Oxford UK) prior to each motion capture session. A floor embedded with force platforms (OR6-6, AMTI, MA) was used to

synchronously record ground reaction force at 1200 Hz. A threshold of 5% body weight was used to determine the initial foot contact time (IC) and toe-off time (TO) of the turning process.

Subjects were allowed to acclimate to the lab environment and the test procedure. Practice was suggested before data collection. A neutral standing trial (t-pose) with feet shoulder width apart and toes facing forward was recorded to be used as a reference position. Then subjects were instructed to walk down a custom-made staircase and make a 90° turn around the ipsilateral leg immediately after the foot makes contact with the ground (FIGURE 3.6). The ipsilateral foot was free to move while the subject turns. The stairs was built following regular building stairs with tread and riser lengths of 0.3 m and 0.195 m, respectively. Five trials were recorded respectively from each side (land on the left foot and turn to left, and land on the right foot and turn to right) at their normal speed (FIGURE 3.6).

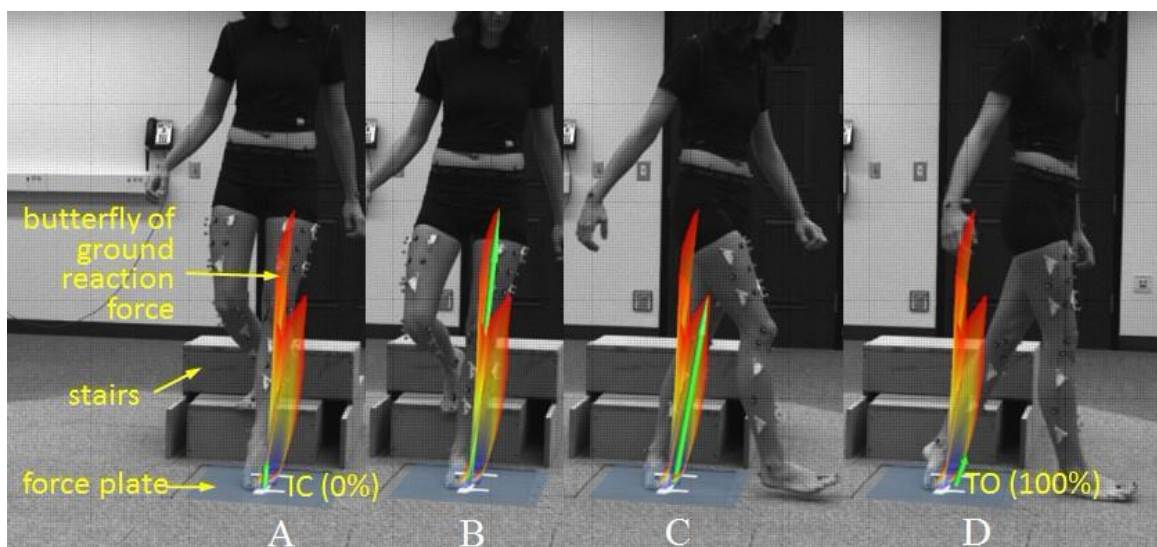


FIGURE 3.6 Subject turns to the same of the supporting leg (left turn shown). IC – initial contact, TO – toe off.

### 3) Data analysis

The motion data were low-pass filtered with a cut-off frequency of 6 Hz in order to get rid of high-frequency noise. The knee joint movement during walking was determined from skin markers following a previously reported procedure (Gao and Zheng, 2010a, Wang et al., 2012, Wang and Zheng, 2010a). The technique was validated by 6 fresh cadaveric lower extremities using intracortical bone pins, which had an accuracy of  $0.71^\circ$  (SD  $0.43^\circ$ ) for flexion/extension (FE),  $1.17^\circ$  (SD  $0.23^\circ$ ) for axial rotation (internal/external, IE), and  $0.34^\circ$  (SD  $0.17^\circ$ ) for varus/valgus (VV) (Gao et al., 2007). Inverse dynamics was used to calculate external joint moments (Andriacchi et al., 2005) using the previously reported anthropometry data (Winter, 1990). A custom-developed MATLAB (R2008a, MathWorks Inc., Natick, MA, USA) program was used to perform the kinematic and kinetic analysis.

The profile of axial tibial rotation, knee varus/valgus rotation, internal/external moment, and adduction-abduction moment were identified and normalized to 0-100% stance phase from IC to TO. Three good trials were blindly picked out and the ensemble average was used to represent each subject. Moments were normalized by each subject's height (m) multiplied by body mass (kg). One way ANOVA and Tukey's post hoc tests were used to test the difference of each variable between the dominant knees (dACL: dominant ACL-reconstructed vs. dACLI: dominant ACL-intact vs. dControl: dominant healthy controls) and between the non-dominant knees (nACL vs. nACLI vs. nControl) in SPSS™ (v16, Chicago, IL, USA). A student's *t*-test was performed to compare the bilateral difference (ACL minus ACLI) of the first peak varus rotation and adduction

moment to test the effect of leg dominance. Significance level of the statistical analysis was set at 0.05.

### 3.2.3. Results

Transverse plane: On the dominant side, after ACL reconstruction (dACLR) the mean internal tibial rotation was significantly smaller ( $p<0.03$ ) than that of dACLI knees at early and middle stance (FIGURE 3.7 A). On the non-dominant side, the internal tibial rotation was increased following ACL-reconstruction during the middle and later stance

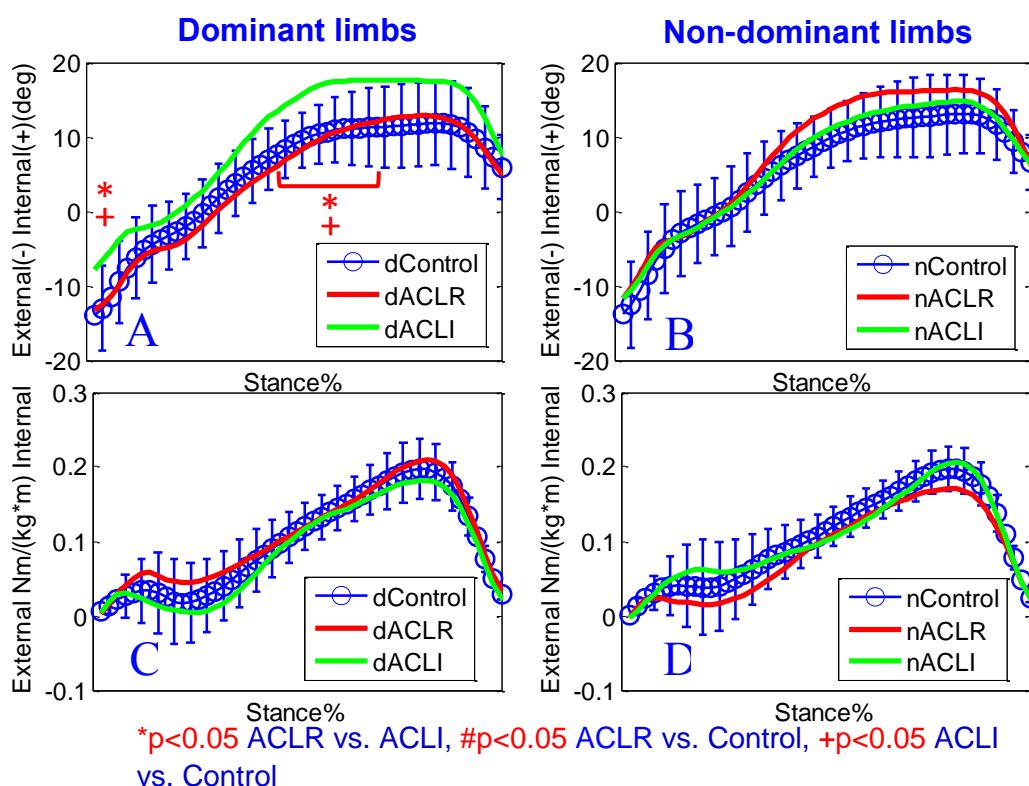


FIGURE 3.7 Knee rotation and moment on the transverse plane from the initial contact (IC) to the toe off (TO) during downstairs turning. Dominant and non-dominant knees were plotted separately. Error bar denotes  $\pm 1$  standard deviation of the control group. \* $p < 0.05$ .

(FIGURE 3.7 B), although it was not statistically significant. The moment curves of the ACLR and ACLI were ‘swapped’ to each other between the dominant and non-dominant limbs in relative to the control curves (FIGURE 3.7 C-D).

Frontal plane: On the dominant side, significantly greater ( $p<0.025$ ) varus rotation was observed from the dACLR knees compared to the dACLI knees at early stance (FIGURE 3.8 A). On the non-dominant side, both the nACLR and nControl knees had significantly less ( $p<0.02$ ) varus rotation than the nACLI knees around early and late stance phase (FIGURE 3.8 B). Significantly reduced ( $p<0.05$ ) external knee adduction moments were also found from the nACLR knees compared to that of nACLI knees around the 1<sup>st</sup> and 2<sup>nd</sup> peaks. The bilateral difference (ACLR minus ACLI) of 1<sup>st</sup> peak adduction moment was significantly greater for group-d subjects ( $-0.10 \pm 0.10$  Nm/(kg\*m)) than that of group-n subjects ( $0.01 \pm 0.09$  Nm/(kg\*m)) ( $p<0.01$ ), as shown in FIGURE 3.9; the bilateral difference of the peak varus rotation was also significantly greater for group-d ( $-1.5 \pm 2.2$  °) than that of group-n ( $0.3 \pm 1.9$  °) ( $p=0.02$ ).

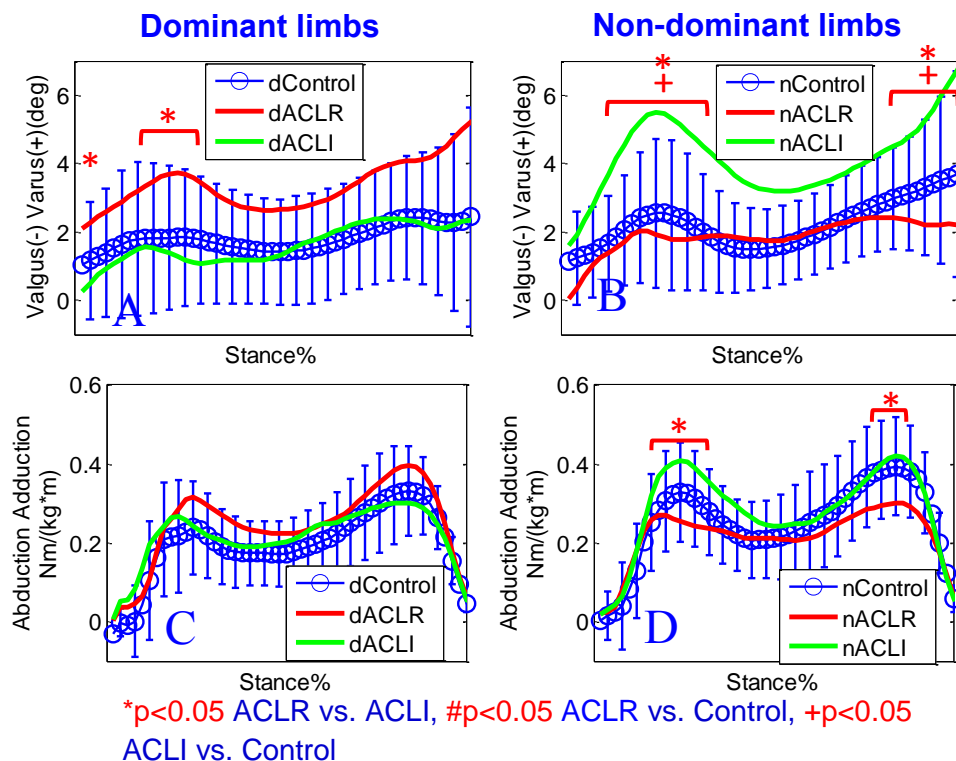


FIGURE 3.8 Knee rotation and moment on the frontal plane from the initial contact (IC) to the toe off (TO) during downstairs turning. Dominant and non-dominant knees were plotted separately. Error bar denotes  $\pm 1$  standard deviation of the control group. \* $p < 0.05$ .

### 3.2.4. Discussion

Although the axial tibial rotation of the ACL-reconstructed knees had been basically restored, significant malalignment in the frontal plane was found in group-d subjects during downstairs turning. The findings proved the hypothesis that the knee motion had not been fully restored by single-bundle ACL-reconstruction on the frontal plane. The findings also indicated that the dominant knees had developed different motion patterns from the non-dominant knees following ACL-reconstruction.

On the transverse plane, the increased internal tibial rotation in dominant ACL-intact knees and non-dominant ACL-reconstructed knees, which were from the same group of subjects (group-n), suggested that for the group the axial rotation of both the

ipsilateral and contralateral knees had been changed. The alteration in the contralateral knees was even greater than that in the involved knees, which may be due to a self-protective strategy. The finding of the increased internal tibial rotation was in agree with previous studies which found an excessive internal tibial rotation during pivoting following walking downstairs (Chouliaras et al., 2007, Georgoulis et al., 2007, Ristanis et al., 2003, Ristanis et al., 2006, Ristanis et al., 2005). In this study, the statistical insignificance of the internal rotation offset for nACL R knees indicated that the single bundle ACL graft may be capable of limiting the internal knee twisting during daily downstairs turning, in which the foot position was not constrained. On the other side, the axial tibial rotation had been mainly restored for group-d subjects. The dominant ACL-reconstructed knees actually exhibited a reduced mean internal tibial rotation compared to the controls during early and middle stance, which was in line with previous studies (Webster et al., 2012, Tsarouhas et al., 2010). The inconsistent results between these two groups suggested that the limb dominance needs to be considered in the future when selecting the tunnel location or setting-up rehabilitation programs.

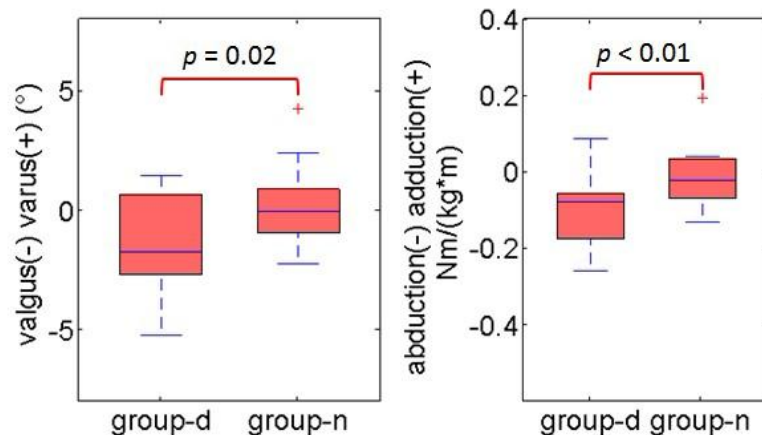


FIGURE 3.9 Boxplot of the bilateral difference (ACLR minus ACLI) of the first peak varus rotation and the first peak external knee adduction moment with whisker length in 1.5 units of interquartile range (IQR). + Outliers.

On the frontal plane, the dominant reconstructed knees had greater varus rotation and a little higher adduction moment compared to the controls. This indicated the existence of dynamic instability on the frontal plane after ACL-reconstruction on the dominant side. With a more varus position, the lateral compartment of the knee joint tends to be more separated while the medial compartment tends to be more compressed. This could cause much higher stresses on the medial compartment of cartilage and menisci. A previous study to a patient with an instrumented knee prosthesis found that the increase in knee adduction moment corresponded to an increase in medial contact force (Erhart et al., 2010); a similar results was also found in another study by using an analytical knee model (Crenshaw et al., 2000). Thus, the adduction shift of the moment curve on the dominant reconstructed knee could increase the contact force on the medial compartment. The increased contacting force provided a potential explanation why ACL patients are at a higher risk of premature osteoarthritis (OA) in the reconstructed knees (Andriacchi and Mundermann, 2006, Daniel et al., 1994, Lohmander et al., 2004, Seon et

al., 2006, Sharma et al., 1998). By watching the profiles of varus rotation and adduction moment, it was noticed that a decrease in varus rotation related with a reduction in external knee adduction moment.

An earlier study found that ACL was also a primary restraint to valgus laxity (Inoue et al., 1987), which was consistent with another study that the valgus rotation was significantly increased by 123% after the ACL was transected (Woo et al., 2005). Previous study found that the ACL was also important in resisting abduction torque when the knee was close to full extension (Fukuda et al., 2003). In this study however, varus offset was found in dominant ACL-reconstructed knees, which may indicate the ACL-graft in our dominant involved patients resulted in an over-correction to the valgus laxity. Shimokochi and Shultz found that the ACL loading was high when a valgus load was combined with internal rotation as compared with external rotation, and the excessive valgus knee moment during sports activities also increased the ACL loading (Shimokochi and Shultz, 2008). In this study, the abduction offset in non-dominant ACL-reconstructed knees therefore may increase the ACL loading. The different inter-group bilateral differences in knee varus rotation and adduction moment further proved the existence of the dominance effect on knee performance after surgery.

Most single-bundle ACL reconstruction techniques have focused on reproducing the anteromedial (AM) bundle, however, recent studies revealed that the in situ force in posterolateral (PL) bundle was also significant (>30% of the total ACL force) which is also important for rotational stability (Gabriel et al., 2004). Therefore, single-bundle has been recognized as the 'prime suspect' for the increased knee laxity. It was suggested that more anatomic reconstruction techniques may better stabilize the knee rotational stability.

Lam et al. found that the knees with double-bundle ACL-reconstruction exhibited a restored axial tibial rotation during pivoting task (Lam et al., 2011). However, other studies found that both single- and double- bundle resulted in a dynamic overcorrection to the axial tibial rotation, and it found that double-bundle ACL reconstruction did not reduce knee rotation further compared with the single-bundle reconstruction technique (Tsarouhas et al., 2010, Tsarouhas et al., 2011, Misonoo et al., 2012). According to the findings of this study, the contralateral knees exhibited even more alteration than the involved knees did. Given the fact that the contralateral knees were completely injury free, the changes in dynamic stability should mainly come from the adaptation of neuromuscular control system. Therefore, physicians should also give enough attention to maintain the motor function of the contralateral limbs in rehabilitation training. We should be more cautious when using the contralateral limbs instead of healthy subjects as the control group in ACL study.

The finding of valgus offset in dACLR knees compared to their contralateral knees was consistent with a foregoing study of level walking (Wang et al., 2012), in which the nACLI knees has significantly greater varus rotation than the other knees (dACLR, dACLI and nACLR) during the stance phase of walking. This suggested that the similar kinematic alteration had been maintained during walking and the relatively more demand downstairs turning activities. Unfortunately, no literature was found which investigated the knee stability on the frontal plane after ACL reconstruction during downstairs turning activity.

Several limitations need to be acknowledged in this study. First, the post-surgery time was relatively short for some patients (7 less than 12 months), thus the ACL graft-

tunnel healing might not have completed yet. The contralateral limb might have developed compensatory strategies to protect the involved limb or/and the contralateral limb may become weak without doing enough exercise during the rehabilitation, which potentially explain the marked alteration in knee motion and moment on the contralateral side. Second, our sample size (10 ACL patients for each group) was relatively small, which may not be large enough to undercover some significant differences. This may explain why some differences were on the border of statistically significant ( $p$ -values were between 0.05 and 0.07). Strengths of the present study include the use of a healthy control group, the same surgeon, the same surgical technique and the similar rehabilitation protocol for every patient.

#### 3.2.5. Conclusion

This study investigated the knee rotation and moment on the nonsagittal planes during downstairs turning. Normal axial tibial rotation had been mainly restored by using transtibial single-bundle ACL-reconstruction; however an increased varus rotation was found from the dominant ACL-reconstructed knees which may increase the stresses in articular cartilage on the medial compartment. There were even more alterations in knee joint motion and moment that had been identified from the contralateral knees. Although it is unclear whether the alteration in the contralateral knees will persist for a long term, the short term results still highlights the issues in the current rehabilitation protocol. By grouping the subjects according to the dominance of the involved limb, this study proved that the limb dominance plays as an important factor in knee postsurgical outcomes after ACL-reconstruction surgery.

### 3.3. Summary

In this this chapter, we investigated the knee joint kinematics and kinetics for transtibial ACL patients during the most engaged level walking. The results show that the knee joint kinematics has been bilaterally altered after ACL reconstruction during walking, especially for the secondary rotations. The findings demonstrated that lower limb dominance had a significant effect on postsurgical knee kinematics. This chapter also investigated the knee performances during downstairs pivoting which is the more challenging daily activity. The findings suggest that the normal kinematics on the frontal plane has not been fully restored by ACL-reconstruction, especially for those with dominant leg involved. The findings demonstrate that lower limb dominance effect does exist in postsurgical knee performance which should be considered during rehabilitative therapy.

The hypotheses that 1) knee joint kinematics has not been fully restored after ACL-reconstruction and 2) individuals with unilateral ACL reconstruction on dominant side developed significantly different motion pattern at the knee joint from those with ACL reconstruction on non-dominant side has been proved.

## CHAPTER 4: DOES THE ANTEROMEDIAL PORTAL TECHNIQUE IMPROVE POSTSURGICAL KNEE PERFORMANCE?

The following hypothesis was tested in this chapter: by using the anteromedial portal ACL-reconstruction technique, the knee joint kinematics and kinetics have been improved compared to those of the knee joint with ACL-reconstruction by using the traditional transtibial technique during low demand level walking and high demand downstairs pivoting.

### 4.1. Knee Joint Stability Following ACL-reconstruction Using Anteromedial Portal Technique during Level Walking

The more anatomic single bundle ACL reconstruction is thought of as a practicable alternative to the complicated double-bundle ACL reconstruction for a more stable and functional knee. However, few studies have presented convincing evidence showing that the outcomes of the knee joint during daily activities were exceling when using the anteromedial portal technique. In this chapter, the surgical technique was evaluated by comparing the spatial and temporal parameters of knee joint motion for ACL patients to those of the healthy controls.

#### 4.1.1. Introduction

Anterior cruciate ligament (ACL) reconstruction has become a commonly performed surgery in recent decades. Transtibial (TT) technique, in which the femoral tunnel is drilled through the pre-drilled tibial tunnel, has been widely used in endoscopic single bundle ACL reconstruction (Duquin et al., 2009). By using this technique, it is

possible to further reduce the operative time and surgical trauma in a single-incision arthroscopic surgery (Kopf et al., 2010). However, it has been postulated recently that the TT technique fails to place the bone tunnels within the insertion sites of the native ACL, especially on the femoral side (Arnold et al., 2001, Chhabra et al., 2006, Heming et al., 2007, Kopf et al., 2010). The non-anatomical tunnel position may lead to abnormal postsurgical knee kinematics (Gao and Zheng, 2010a, Scanlan et al., 2010, Loh et al., 2003, Scopp et al., 2004) and a high rate of post trauma osteoarthritis after ACL-reconstruction (Daniel et al., 1994, Lohmander et al., 2007, Lohmander et al., 2004).

Given that the non-anatomical tunnel position is a frequent cause of surgical failure (Tudisco and Bisicchia, 2012, Johnson et al., 1996, Kohn et al., 1998, Scopp et al., 2004), the double-bundle ACL reconstruction emerged which replicates the anatomy of the native ACL. Unfortunately, the advantages of the double-bundle technique are controversial. It was found that the double-bundle reconstruction resulted in better knee functions (Sadoghi et al., 2011) and anterior-posterior stability (Muneta et al., 1999). However, the results of another study suggested that the double-bundle reconstruction may not better control knee rotation in knee stability tests (Meredick et al., 2008). Tsarouhas et al. did not find the exceling rotational stability from patients with double-bundle reconstruction compared to those with single-bundle reconstruction during pivoting maneuver (Tsarouhas et al., 2010, Tsarouhas et al., 2011). There are intense debates over the necessity of performing double-bundle ACL reconstruction because it increases the operational complexity (Brophy et al., 2009, Meredick et al., 2008) without convincing evidences for better clinical outcome.

Anteromedial portal (AMP) femoral tunnel drilling technique yields a more anatomical placement of the femoral tunnel without increasing operative complexity compared to the TT technique (Gavriilidis et al., 2008, Kopf et al., 2010, Steiner, 2009, Dargel et al., 2009). Nowadays, more surgeons resort to the AMP technique for drilling the femoral tunnel in single bundle ACL-reconstruction (Tripathi, 2012). Previous studies also showed that the AMP technique improved the knee stability compared to the traditional TT technique (Alentorn-Geli et al., 2010a, Alentorn-Geli et al., 2010b, Tudisco and Bisicchia, 2012, Sadoghi et al., 2011). In those studies, the routine tests of knee stability (KT-1000 testing, Lachman test, pivot shift test, etc.), which are based on knee joint passive response to static and non-weight bearing situations, do not necessarily reflect physiological loading conditions (Brandsson et al., 2002, Papannagari et al., 2006, Pollet et al., 2005, Borjesson et al., 2005). Level walking has been used as the more relevant ambulatory activity for understanding the etiology of OA (Miyazaki et al., 2002, Andriacchi et al., 2009, Andriacchi and Mundermann, 2006, Andriacchi, 2004).

Therefore, a well-designed study of joint kinematics is warranted to characterize the potential benefits of the AMP techniques for improving stability of the knee. In this study, we reported the postsurgical knee joint kinematics for two groups of ACL patients who received single-bundle ACL reconstruction using the TT and AMP technique, respectively. The spatial and temporal parameters of knee joint motion for ACL patients will be compared to those of the healthy controls. The hypothesis was tested that there was no significant difference in six-degree-of-freedom postsurgical knee kinematics between subjects with ACL reconstruction using the AMP technique and the TT technique.

#### 4.1.2. Material and methods

Fourteen patients with unilateral ACL reconstruction were recruited from the same center of OrthoCarolina. All the patients received surgeries from the same orthopedic surgeon between August 2010 and September 2011. The study was conducted following an IRB approved protocol and informed consent was obtained from each subject before testing. Twenty healthy subjects with no history of lower extremity injuries or functional disorders were recruited to test the pre-injury status of knee joint kinematics (TABLE 3.1). Eight subjects underwent ACL reconstruction on their dominant side (Group-d) and six subjects underwent ACL reconstruction on their non-dominant side (Group-n). Patients with chondral lesions, posterior cruciate or collateral ligament tears were excluded from this study. Hamstring tendon grafts were used in both groups according to the surgeon's preference. There was no significant difference in post-surgery time, body weight and height between the two sub-groups (TABLE 4.1). At the time of testing, patients were at least 4 months post-operative from surgery (~8 months in average) and had received permission to perform all daily activities from their treating physician. The involved knees' KT-1000 measurements did not differ significantly ( $p = 0.8$ ) among groups. None of the subjects had diagnosed radiographic or symptomatic OA. No statistically significant differences in post-surgery time ( $p = 0.44$ ), body weight ( $p = 0.61$ ), height ( $p = 0.82$ ), and body mass index (BMI) ( $p = 0.62$ ) were found between these two groups (TABLE 4.1). The lower limb dominance was determined by ball kicking and confirmed with subjects afterwards (Porac and Coren, 1981).

TABLE 4.1 Demographics (mean (SD)) of patients with ACL reconstruction on the dominant side (Group-d) and patients with ACL reconstruction on the non-dominant side (Group-n) and the healthy controls; BMI: body mass index

Variables	Group-d	Group-n	Controls
Gender (m:f)	3:5	4:2	13:7
Age (years)	29.2 (6.2)	31.2 (8.6)	23.4 (3.0)
Weight (kg)	83.1 (10.7)	85.5 (24.5)	70.8 (13.2)
Height (cm)	172 (8)	174 (9)	176 (10)
BMI (kg/m <sup>2</sup> )	27.9 (2.1)	27.9 (5.8)	22.7 (2.6)
Hamstring tendon graft	8	6	N/A
Post Surgery (months)	7.8 (4.0)	9.0 (4.6)	N/A

The motion tests of the AMP patients were following the exact same procedure as the transtibial patients. The knee joint rotations and translations were expressed in the 3 anatomical planes of tibia. A gait cycle was normalized to 0-100% from heel strike to heel strike, and the mean of 3 good trials was used to represent each subject. Inter-segmental external joint moments and resultant forces were calculated using an inverse dynamics approach, and represented in the tibial local coordinate system (Andriacchi et al., 2005). The external knee moment includes the moment about the joint center created by the ground reaction force and inertial forces. It is equal and opposite in direction to the internal joint moment which is created by muscle contraction, ligament pulling and joint contact, etc. Moments and forces were normalized by body mass times height (expressed in (H\*W) %).

Due to the relatively small sample size of AMP subjects, the dominance was not considered this time. Together with the transtibial patients, all knees were categorized into three groups according to their status: ACLR using anteromedial, ACLR using

transtibial and the control group. Comparisons were made between 3 groups by using one way ANOVA (SPSS, IL, USA), and the significance level was set at 0.05. For tests of significant omnibus F result, a pos-hoc analysis test was performed using Tukey's honestly significant difference (HSD) procedure.

#### 4.1.3. Results

##### 1) Rotations

On the sagittal plane, the knees using the AMP technique had more flexion throughout the whole gait cycle, compared to other two groups (FIGURE 4.1 A). The flexion offset was significant at heel strike and flexion valley (FV). The average extension loss at FV was about  $4.5^{\circ}$  ( $5.9^{\circ}$  vs.  $10.2^{\circ}$  of the healthy controls). On the transverse plane, multiple significant differences were observed in axial tibial rotation between the transtibial knees and healthy controls, especially during the weight bearing stance phase (FIGURE 4.1 B). The ACLR knees using the transtibial technique exhibited more internal tibial rotation with an average offset of  $2^{\circ}$  during the stance phase. On the other hand, by using the transportal approach, the axial stability was improved, and significant differences were only observed at the heel strikes. On the frontal plane, transtibial knees had varus offset compared to the healthy controls, although it was not statistically significant during the weight bearing stance phase (FIGURE 4.1 C). For the AMP knees, however, the profile was shifted in valgus direction which yielded a valgus offset compared to the healthy controls. The offset was not statistically significant either. There was significantly less valgus rotation at flexion peak during the swing phase.

## 2) Translations

In anteroposterior direction, the profiles were close to each other during the stance phase. However, the transtibial knees started to exhibit excessive anterior femoral translation after TO. The anterior translation was significantly greater for the transtibial knees than that of healthy controls around FP (FIGURE 4.1 D). For the AMP knees, the normal anteroposterior translation was restored. In the mediolateral direction, the normal translation was mainly restored by using either reconstruction technique, except for a significant difference at HS between AMP knees and healthy controls (FIGURE 4.1E). In the superior-inferior direction, the transtibial knees exhibited greater inferior femur translation than the healthy controls during the stance phase. The inferior offset was largely reduced by using AMP technique during the stance phase.

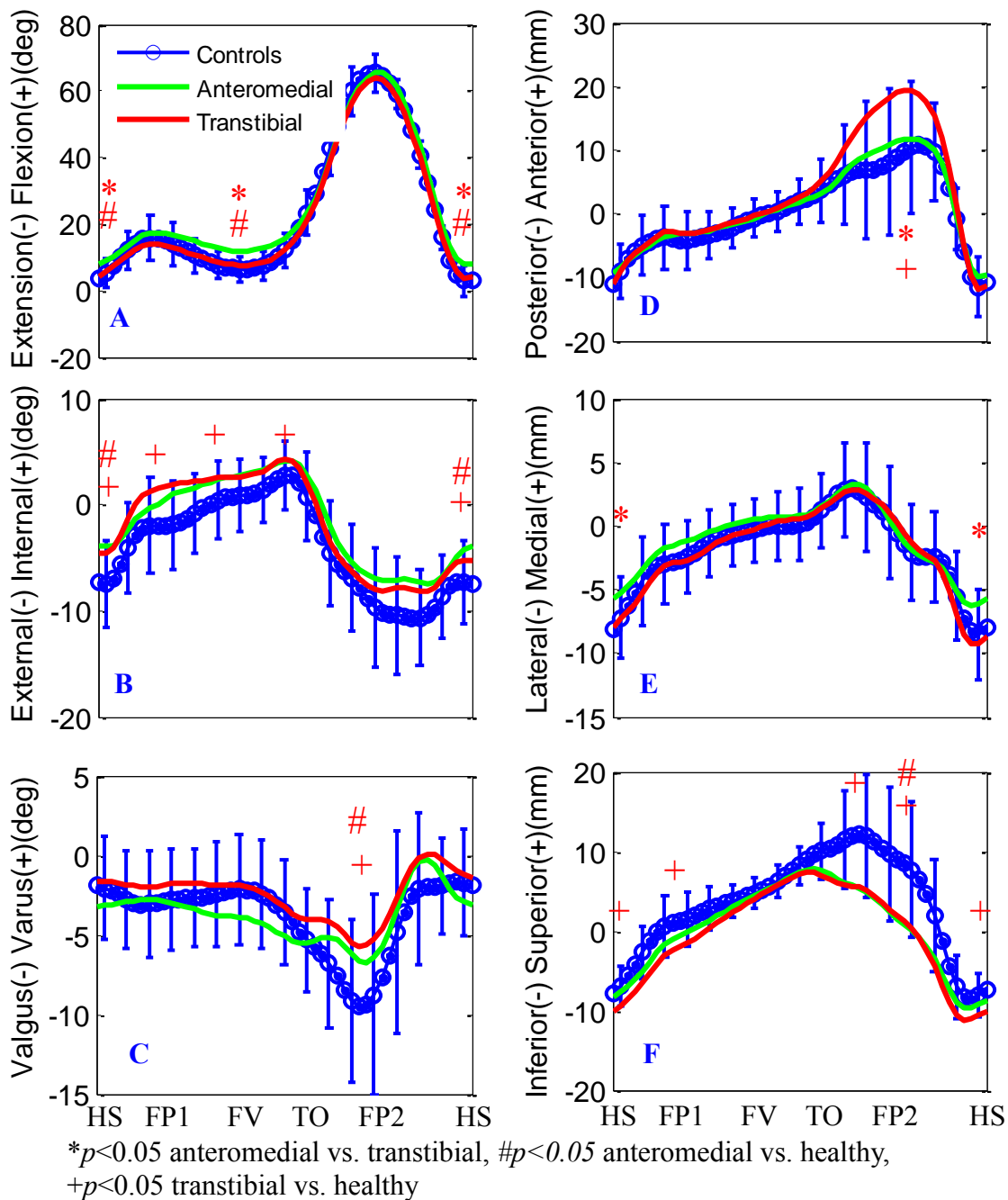


FIGURE 4.1 Knee rotations and translations during a gait cycle. HS-heel strike, FP1-flexion peak during stance phase, FV-flexion valley, TO-toe off, FP2-flexion peak during swing phase. Translations represented the displacement of femoral origin in tibial ACS.

### 3) Timing of key events

The timings of six key events were determined for each group, including CTO-contralateral leg toe-off, FP1-the 1<sup>st</sup> flexion peak during mid-stance, FV-flexion valley, CHS-contralateral heel strike, TO-toe off, FP2-the 2<sup>nd</sup> flexion peak during swing phase (FIGURE 4.2). They were expressed in percentages of gait cycle (from HS-0% to HS-100%). FP1, FV and FP2 were determined by knee joint flexion angle, and TO and CHS were determined by the force plate reaction force. CTO was defined as the instant when the Z-axis coordinate (height) of the contralateral toe marker was minimal following the heel strike. Since the marker placement of toe marker may vary across subjects, the timing may not reflect the truly contralateral toe off instant for everybody.

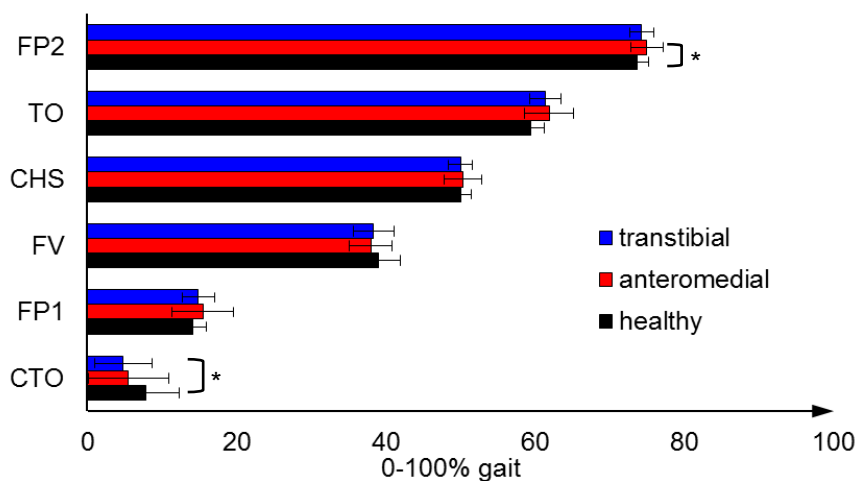


FIGURE 4.2 Timings of key events in the gait cycle for transtibial, AMP and healthy groups. The gait cycle was normalized from one heel strike (0%) to the next heel strike (100%).

One significant difference was found between the transtibial and the control group at CTO, where the contralateral leg of transtibial group was taken off the ground

significantly earlier, following the ACLR hit the ground, than the control group (FIGURE 4.2). The knees of the control group reached to their maximum flexion significantly earlier than the AMP knees.

#### 4) Spatial parameters of gait

The key values of knee joint kinematics were listed in TABLE 4.2. It was found that the AMP knees had significantly greater flexion angle than the other groups at static posture (FIGURE 4.3). The hyper-flexion was maintained during the stance phase of walking. The AMP knees also exhibited external tibial alignment compared to the healthy controls at static posture as well as during stance phase of walking. The AMP group of patients walked slower than the healthy controls while there was no difference in walking speed for the transtibial group. The transtibial knees had significantly greater valgus rotation than the healthy controls around the flexion peak instant during the swing phase.

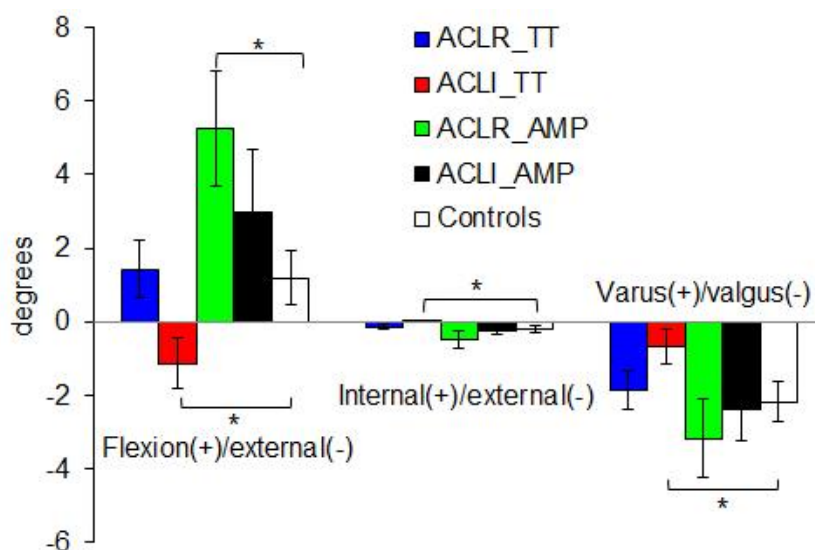


FIGURE 4.3 Knee joint rotation at static posture. TT-transtibial ACL-reconstruction, AMP-anteromedial portal ACL-reconstruction.

TABLE 4.2 Spatial parameters of gait for different groups. Mean (standard deviation).

Kinematic Parameters	Anteromedial	Transtibial	Healthy	p-values <sup>2</sup>
<i>@ static posture ( ° )</i>				
Knee flexion	5.2(5.9)	1.4(4.6)	1.2(4.5)	*,#
Internal tibial rotation	-0.5(0.9)	-0.1(0.2)	-0.2(0.5)	*
Knee varus	-3.2(3.9)	-2.2(3.2)	-2.2(3.4)	
<i>During level walking (mm, °, m/sec)</i>				
Step speed	1.1(0.2)	1.1(0.2)	1.2(0.1)	#
Step length	0.6(0.1)	0.7(0.1)	0.7(0.05)	
Stride speed	1.1(0.1)	1.1(0.2)	1.2(0.1)	#
Stride length	1.3(0.1)	1.3(0.1)	1.3(0.1)	
AP ROM, stance <sup>1</sup>	16.2(6.8)	21.2(7.4)	16.9(5.6)	#
ML ROM, stance	9.5(4.0)	11.0(3.0)	10.9(4.1)	
SI ROM, stance	16.9(5.0)	18.4(6.3)	19.2(4.9)	
Flexion @ toe off	38.8(6.1)	36.8(5.6)	34.0(6.7)	+
Flexion valley, stance	7.6(5.5)	4.0(4.2)	2.9(4.2)	*,#
Internal peak, stance	4.9(2.7)	5.2(2.7)	3.2(3.4)	+
Varus valley, stance	-6.3(4.2)	-4.9(3.7)	-6.4(3.4)	
Varus valley, swing	-8.8(5.2)	-6.7(4.6)	-10.3(5.6)	+

<sup>1</sup>during stance phase, ROM – range of motion; <sup>2</sup>\* $p < 0.05$  AMP vs. transtibial, # $p < 0.05$  AMP vs. healthy, + $p < 0.05$  transtibial vs. healthy

### 5) Torques

In the sagittal plane, during the early stance phase, the quadriceps were active to generate an extensor moment, which acts to balance the external flexion moment and control the amount of knee flexion (FIGURE 4.4 A). The moment direction was reversed at the second half of stance phase. The transtibial knees had significantly smaller external flexion moment than that of the healthy controls at FP1. While the AMP knees has

significantly smaller extensor moment at FV. The profiles of all three groups were replicated well during the swing phase. In the transverse plane, the transtibial knees exhibited significantly greater peak internal moment compared to the healthy controls (FIGURE 4.4 B). The significant difference in peak internal moment was gone in the knees using the AMP technique. In the frontal plane, the profiles of both ACLR groups were shifted in adduction compared to healthy controls throughout the whole stance phase, although it was not statistically significant (FIGURE 4.4 C).

#### 6) Forces

Along the anteroposterior direction, the transtibial knees had smaller posterior force at FP1 (FIGURE 4.4 D). The AP force profile was improved by using the AMP technique. Along the mediolateral direction, the profiles of both ACLR groups have been shifted in the medial direction compared to the healthy controls throughout the stance phase (FIGURE 4.4 E). The medial offset of the force was statistically significant around the FV for both ACLR groups compared to the healthy controls. Along the axial direction (inferior/superior), the external force exerted on the tibia was pointing upward (superior) with the maximum magnitude of about a body weight. To balance the external tibial force, an internal force with equal magnitude and opposite direction needs to be generated, which mainly came from the knee joint surface contact (FIGURE 4.4 F).

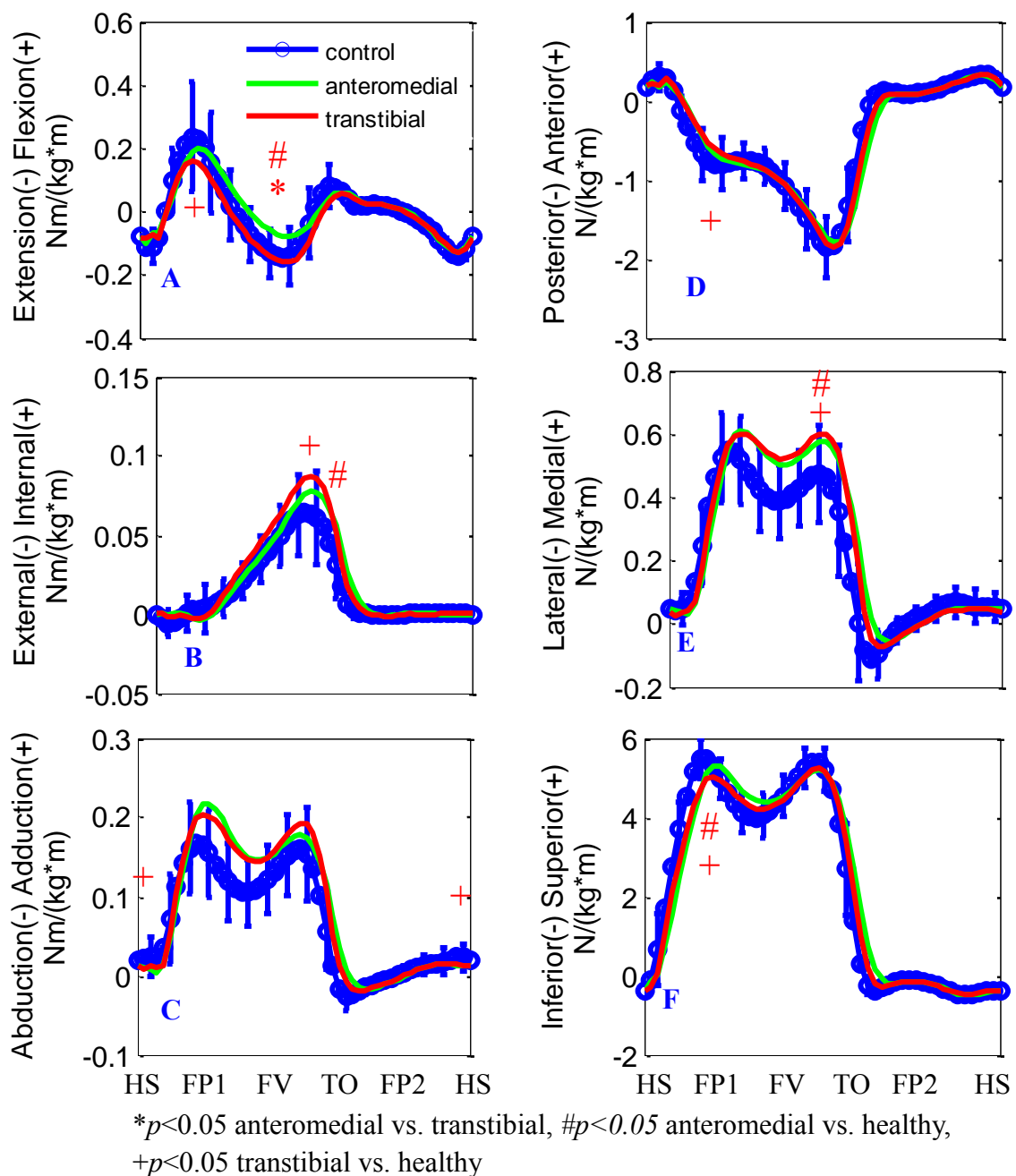


FIGURE 4.4 Normalized external knee joint forces and moments during a gait cycle. HS-heel strike, FP1-flexion peak during stance phase, FV-flexion valley, TO-toe off, FP2-flexion peak during swing phase. The forces and torques are expressed in tibial ACS.

The peak anterior force in AMP knees occurred significantly later than the other groups (TABLE 4.3). The peak medial force was significantly greater in both the

transtibial knees and AMP knees than that in the healthy controls during stance phase. The superior force in the transtibial knees was significantly smaller than the healthy controls during the stance phase. Moreover, the peak external flexion moment during stance phase was also significantly smaller in the transtibial knees than those in the healthy knees. The peak internal moment was significantly greater in the transtibial knees than that in the healthy controls. The internal moment reached its peak value significantly later for both ACLR groups than healthy controls.

TABLE 4.3 Peak values of knee joints loading for different groups. Mean (standard deviation).

Kinematic Parameters	Anteromedial	Transtibial	Healthy	p-values <sup>2</sup>
<i>During level walking</i>				
<i>(N/kg, Nm/kg, %)<sup>1</sup></i>				
AP force valley, stance	-1.92(0.26)	-1.92(0.35)	-1.97(0.39)	
Timing of AP valley	54.6(3.2)	53.6(1.5)	52.2(2.3)	#,+
ML force peak, stance	0.70(0.18)	0.67(0.16)	0.60(0.14)	#,+
Timing of ML peak	31.3(14.4)	29.8(12.4)	26.2(13.8)	
SI force valley, peak	5.70(0.45)	5.47(0.50)	5.80(0.52)	+
Timing of SI peak	28.6(14.9)	36(15.9)	28.8(15.8)	
VV torque peak, stance	0.24(0.09)	0.23(0.06)	0.20(0.06)	
Timing of VV peak	21.7(3.7)	29.7(15.3)	28.9(15.6)	
FE torque peak, stance	0.24(0.12)	0.18(0.09)	0.27(0.15)	+
Timing of FE peak	24.4(14.5)	23.4(17.5)	22.8(16.3)	
IE torque peak, stance	0.08(0.02)	0.09(0.03)	0.07(0.03)	+
Timing of IE peak	50.2(4.6)	49.0(2.3)	45.7(7.0)	#,+

<sup>1</sup>force and torque were normalized by subject's body mass (N/kg, Nm/kg), timing was in percentage of gait cycle; <sup>2</sup> \* $p < 0.05$  AMP vs. transtibial, # $p < 0.05$  AMP vs. healthy, + $p < 0.05$  transtibial vs. healthy

#### 4.1.4. Discussion

By using AMP technique, the more anatomically placed grafts were closer to the native ACL length and orientation (Abebe et al., 2011, Dargel et al., 2009). The AMP graft usually has higher frontal obliquity and sagittal obliquity than the transtibial graft (FIGURE 4.5). As a result, it is more powerful to constrain the anterior and superior tibial translation. In AMP knees, this significantly reduced AP translational during the swing phase will cut down the speed of femur excursion on the tibia plateau which is helpful to protect the graft from excessive elongation as well as to reduce the abrasion between the articular cartilages.

In the sagittal plane, the more oblique ACL graft in AMP knees tends to exert more drag force to the tibial plateau which could stop the knee from full extension. Posteriorly shifted tunnel position may result in excessive tightening of the graft when the knee approaches full extension which could cause extension deficit (Strobel et al., 2001, Loh et al., 2003, Yamamoto et al., 2004). From FIGURE 4.5, it was easy to show that more strain was built up in the AMP graft, which had a posteriorly shifted femoral tunnel entry site, during knee extension. Thus a less vertical graft orientation may contribute to the extension loss in AMP knees during stance phase.

The improved knee axial stability may be contributed by the increased obliquity of ACL graft in the frontal plane (FIGURE 4.5), which is more effective to withstand the internal rotational moment. Unfortunately, the axial stability still has not been fully restored, which may be explained by the material properties of ACL graft which were different from the natural ACL (Handl et al., 2007). In our study, all ACL patients were using single-bundle hamstring tendon (semitendinosus with gracilis enforcement, STG)

grafts. The natural ACL has two bundles; thus the attachment site is much larger than the cross section area of the tunnel (which was taken as the attachment area of the graft). The reduction of ACL attachment area may affect the graft ability to constrain the knee joint axial rotation. In our subjects, the graft was fixed at the bone shaft, instead of at the graft entry point inside the knee joint. Thus the graft would elongate more under the same force, which could increase the laxity of the knee joint. So the graft fixation technique may constitute another explanation to the increased internal tibial rotation. The greater internal tibial rotation may cause more excursion of medial femoral condyle on the tibial plateau, which could cause abnormal cartilage contact and exaggerate the risk for OA in a long term.

The transtibial knees had varus offsets compared to the healthy controls during the stance phase, which tended to create a higher compressive stress on the medial compartment of cartilage and menisci. Previous studies found the occurrence of OA was much higher on the medial side after ACL-reconstruction (Seon et al., 2006), which may be contributed to by the unbalanced compressive stress across the compartments. By using the AMP technique, the knee varus rotation was effectively reduced, and the knee actually exhibited slightly valgus offset. With a more valgus position, the medial compartment tends to be more separated while the lateral compartment tends to be more compressed. This was beneficial to unload the vulnerable medial compartment and evenly distribute the carrying load across the medial and lateral compartments. A decrease in stresses on the medial compartment would be helpful to moderate the high risk of postsurgical OA on the medial compartment. The significantly less valgus rotation and superior translation during the swing phase may indicate that the ACL grafts were

over-tight; it may also be caused by a self-protective strategy that flexor muscles were subconsciously over-activated to constrain the knee motion during the swing phase.

Given the fact that the stride speed was almost equal to the step speed and the stride length was about two times that of the step length, it can be concluded that the contralateral non-involved limb had developed compensatory motion patterns in order to adapt to the involved limb (Gao and Zheng, 2010a). Both transtibial and AMP ACLR limbs had a delayed toe off, which indicated the ACL patients tended to extend the duration of double leg supporting. The prolonged stance phase may be helpful to accomplish a less abrupt weight shift. Since the timing of CTO was determined solely by the position of the marker placed on the toe, there were relatively high errors in the CTO timing compared to the other key events which were determined by the knee joint motion or force plates. The significant difference in the CTO timing may be caused by the systematic errors. Those differences plus the postponed timing of flexion peak during the swing phase indicated that ACLR knees have not been restored to a normal spatiotemporal pattern.

The moment profiles in the sagittal were very close to a previous study (Besier et al., 2009). The peak moments of AMP knees in sagittal and transverse planes were closer to the healthy controls, which indicated the dynamic stability was improved by using the AMP ACL-reconstruction technique. Around the flexion valley during stance phase, the significantly reduced external extension moment indicated that the AMP knee was inefficient in generating enough internal flexor moment. The flexor moment is mainly generated by hamstring muscles. For the subjects in the AMP group, the ACL grafts were cut from the hamstring tendon, and they had a relatively short post surgery time (8

months) at the time of testing compared with the transtibial group (13 months). So they may still have hamstring pain and subconsciously limit the use of hamstring. The increased peak internal rotation moment in transtibial knees indicated the axial instability during stance phase. To balance the increased axial rotation moment, higher strain may be built up in the ACL graft of the transtibial knees.

In the frontal plane, there was no obvious improvement by using the AMP approach. Significant differences were observed in the kinetic key values of the transtibial patients compared to those of healthy controls (TABLE 4.3). The number of significant differences was largely reduced in the AMP groups. The change also indicated that the knee joint stability was improved by using AMP technique.

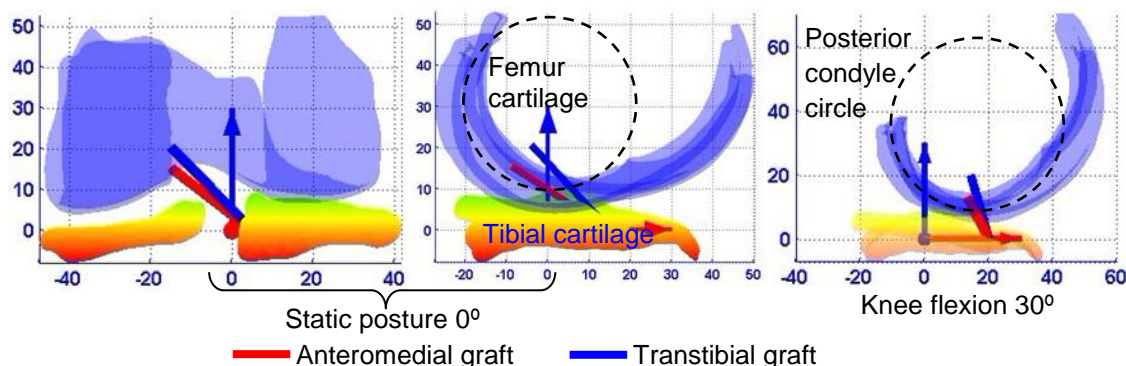


FIGURE 4.5 Diagram of graft orientation in 3d knee joint model (reconstructed from a typical patient's MR images) for different ACL-reconstruction techniques

#### 4.1.5. Conclusion

The hypothesis that the postsurgical knee joint kinematics using the AMP drilling approach is different from that by using the traditional transtibial approach has been proved. In AMP knees, the more anatomically placed grafts restored the normal anteroposterior translation; it also reduced the internal tibial rotation offset and varus

offset. AMP technique also improved the knee joint forces and moments. But the AMP technique may cause knee extension deficit, which needs to be considered when making a decision.

## 4.2. Knee Joint Stability Following ACL-reconstruction Using Anteromedial Portal Technique during Downstairs Pivoting

### 4.2.1. Introduction

The ACL grafts in AMP subjects were more horizontal in the frontal plane and sagittal plane, which may be more effective in resisting the axial rotation and varus rotation of the knee joint during high demand activities. In this section, we aimed to evaluate the knee joint stability during downstairs turning. Since the knee was fully extended during the turning process, only the non-sagittal plane data were presented. The following hypothesis was generated that the knee joint stability was improved by using the AMP tunnel drilling technique compared to the traditional transtibial tunnel drilling technique.

### 4.2.2. Material and methods

For the AMP subjects (TABLE 4.1), the motion data of downstairs pivoting were collected following the exact same procedure as the transtibial subjects (TABLE 3.2). One way ANOVA and Tukey's post hoc tests were used to test the difference of each variable between the dominant knees (dACL: dominant ACL-reconstructed vs. dACLI: dominant ACL-intact vs. dControl: dominant healthy controls) and between the non-dominant knees (nACL vs. nACLI vs. nControl) in SPSS™ (v16, Chicago, IL, USA). Significance level of the statistical analysis was set at 0.05.

### 4.2.3. Results

Transverse plane: There is no significant difference in either the axial tibial rotation or the axial rotational torque between different groups (FIGURE 4.6).

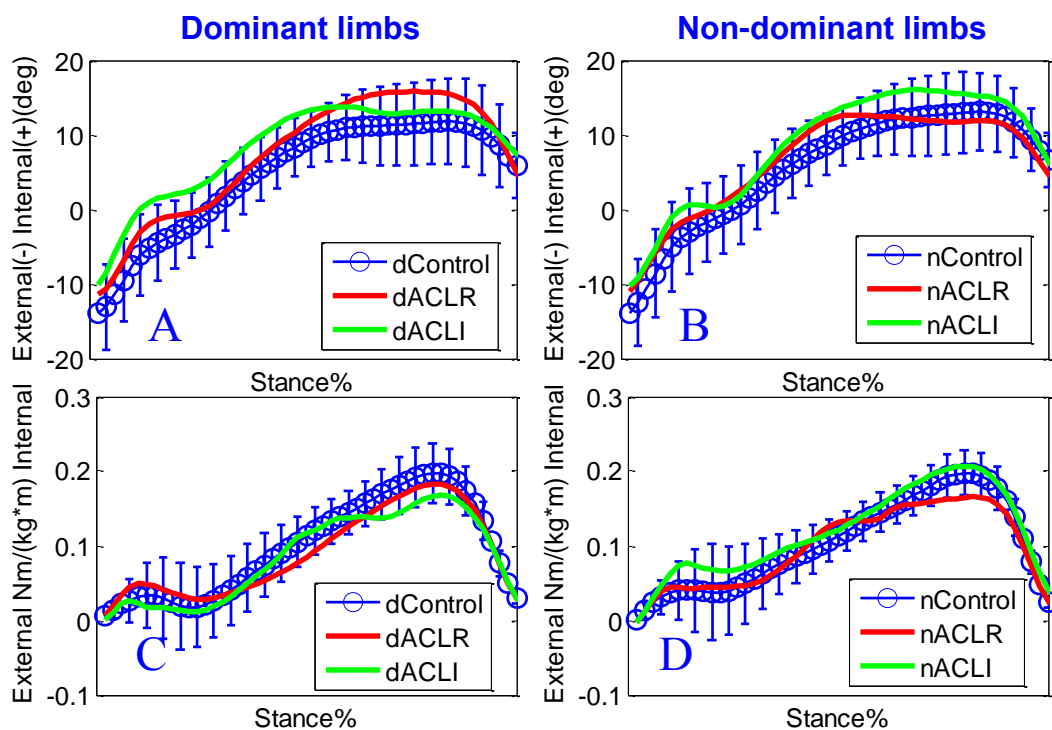


FIGURE 4.6 Knee rotation and external knee axial moment on the transverse plane from the initial contact (IC) to the toe off (TO) during downstairs turning. Dominant and non-dominant knees were plotted separately. Error bar denotes  $\pm 1$  standard deviation of the control group.

Frontal plane: For the dominant limbs, the ACLR knees had significantly less varus rotation at early stance phase compared to the uninvolved knees (FIGURE 4.7 A), whereas, for the non-dominant limbs the ACLR knees had slightly greater varus rotation than the uninvolved knees (FIGURE 4.7 B). The adduction torque was close to each other between the reconstructed and uninvolved knees. No significant differences were found between the patient group and the control group.

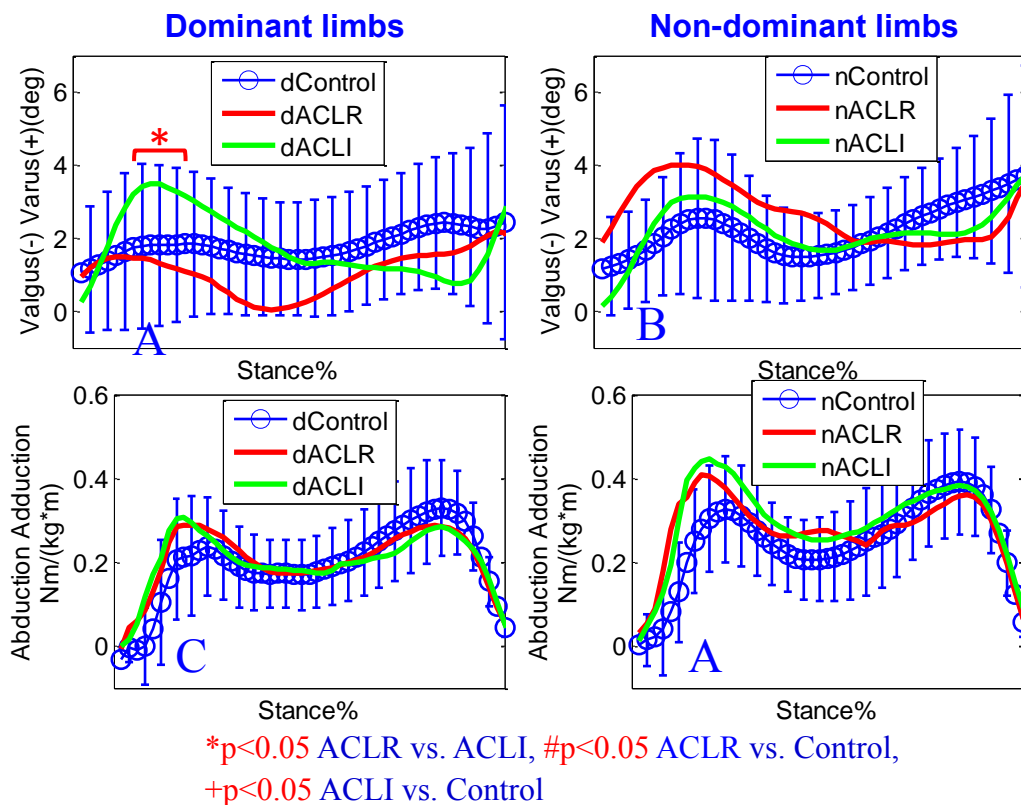


FIGURE 4.7 Knee rotation and external adduction moment on the frontal plane from the initial contact (IC) to the toe off (TO) during downstairs turning. Dominant and non-dominant knees were plotted separately. Error bar denotes  $\pm 1$  standard deviation of the control group. \* $p < 0.05$

#### 4.2.4. Discussion

The knee joint normal rotations and moments had been basically restored on both the transverse and frontal planes, except for a significant malalignment in the frontal plane between the ACL-reconstructed and uninvolved (ACLI) knees on the dominant side during the early turning phase. The findings proved the hypothesis that the knee joint stability had been improved by using the single-bundle AMP surgical technique. The findings also indicated that the dominant knees had developed slightly different motion patterns from the non-dominant knees following ACL-reconstruction.

On the frontal plane, the reconstructed knees had similar adduction moment with the uninvolved knees. Considering that the height, weight and age were close to each other between the group-n and group-d, and all the surgeries were conducted by the same surgeon, the uninvolved limbs could be taken as the pre-injury situation of the reconstructed limbs. Therefore, the results indicated that the AMP surgical technique had restored the normal knee stability in the frontal plane during downstairs turning. The external joint moments in both the reconstructed and uninvolved knees were shifted in adduction. This may be explained by the not fully recovered agility at the time of testing, since all the AMP subjects had relative short post-surgical time.

#### 4.2.5. Conclusion

The knee joint stability during downstairs turning was improved by using the AMP tunnel drilling technique. In AMP knees, the more anatomically placed graft restored the adduction moment to the pre-injury condition; it also restored the knee stability on the transverse plane.

#### 4.3. Summary

This chapter investigated the knee joint kinematics and kinetics for the subjects with ACL reconstruction using the anteromedial portal drilling technique during the high demand downstairs turning activity. This chapter compared the knee joint kinematics and kinetics between transtibial group and anteromedial portal group during level walking and downstairs turning activities. The results showed that the anteromedial portal technique had more advantages than the traditional transtibial technique in stabilizing the knee joint.

## CHAPTER 5: FINITE ELEMENT MODELING TO THE KNEE JOINT

This chapter covers: 1) development of a computational knee joint model with high quality hexahedral finite elements; 2) investigation of the impact of ACL tunnel location on knee joint motion during level walking using the state-of-the-art finite element method.

### 5.1. Introduction

Being the heavily loaded joint in human body, the knee joint is vulnerable to ligament injuries and cartilage degenerative diseases such as osteoarthritis. More than 80% of the human weight is carried by the knee joint, which usually causes compressive loads as large as 3 times of the body weight during a gait cycle (Kutzner et al., 2011b). In the previous chapters, we measured the tibiofemoral motion and calculated the knee joint reaction forces and moments using inverse dynamics. According to the findings, the ACLR knees by using different surgical techniques exhibited significantly different motions and joint reaction moments during level walking. Excessive joint stress is considered to be harmful to the articular tissues in the knee joint. Although the stresses cannot be measured in vivo, they can be predicted by using elegant computational models.

Therefore, in this study we estimated the knee joint contact stresses before and after surgical intervention during a physiological loading situation (level walking) by using a computational knee model. Different graft orientations were modeled to respectively simulate the transtibial and AMP surgical interventions. The results are

helpful to predict the outcome of knee joint performance after ACL-reconstruction and to evaluate the effectiveness of two widely used surgical techniques.

## 5.2. Material and Methods

### 5.2.1. Geometry reconstruction and mesh generation

#### 1) Reconstruction of the knee joint model

High-resolution magnetic resonance (MR) images were acquired in the sagittal plane with the right knee at its natural extension from a healthy subject (male, 23 years old). The images had an interval of 1.00 mm and pixel spacing of 0.35 mm and resolution of  $512 \times 512$  pixels (3D fast spoiled gradient-echo, T1-weighted, fat-saturated, no special preparation). A total of 106 MR images were collected. The medical images produce high quality distinguishable bone surfaces as well as the traceable boundary of soft tissues. A generic knee model including ligament, cartilage, meniscus and bone was created from the MR images (DICOM standard). Medical image segmentation was performed by the author who had extensive hands-on experience and familiarity with knee joint anatomy. Previous studies proved that the inter- and intra- observer reproducibility is very decent (Bae et al., 2009, Shim et al., 2009).

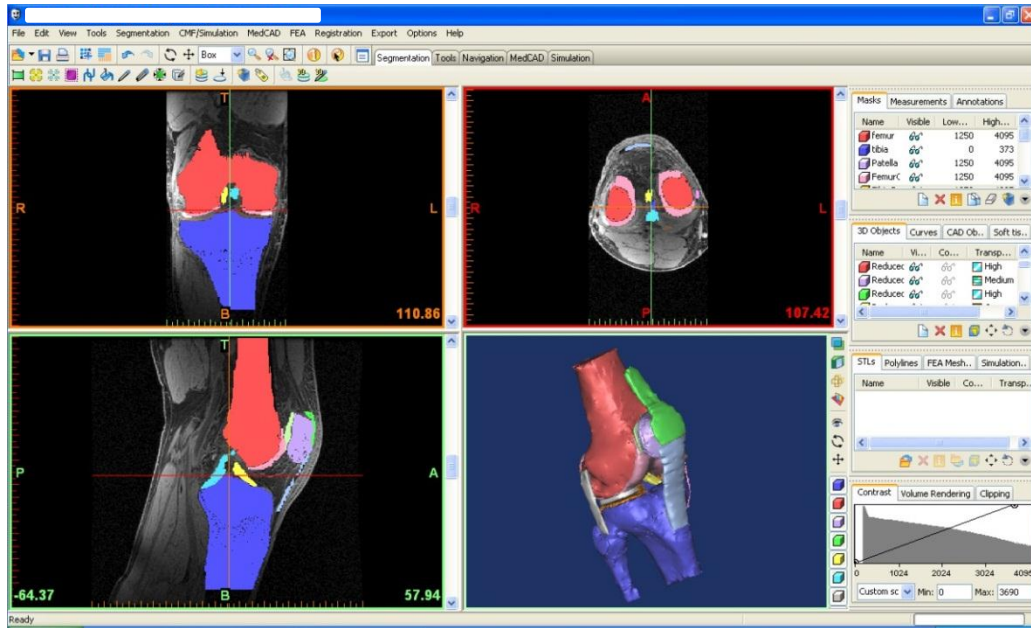


FIGURE 5.1 Medical image segmentation for a typical subject in Mimics.

Image segmentation was performed in the software package Mimics™ (Materialise, Plymouth, MI, USA) (FIGURE 5.1). The boundaries of each part were manually traced on each 2D image by using a tablet computer (Lenovo Thinkpad X60, Morrisville, NC). The tibia and fibula were treated as an entity for simplicity. After finished up masking all the MR image slides, 3D component models were created and exported as triangulated surface files (binary .STL format). The .STL files were then imported into Geomagic Studio™ (Version 12, Geomagic Inc., Research Triangle Park, NC) for further smoothing and creating Non-Uniform Rational B-Spline (NURBS) surfaces. In the software, the “*Mesh Doctor*” function was used to get rid of spikes, fill holes and clean up isolated chips. Then the “*Relax*” function was used to smooth the polygon mesh. This increases smoothness of the surface and makes the model more realistic. The smoothing strength was selected with caution in order to avoid distortion. Some extra parts which were not important in the analysis were removed to reduce the

file size and computational cost. After all holes were filled and the surface was smoothed, the function “*Make Manifold*” was used to create a NURB surface. Then function “*Extract Surfacing*” was used to prepare a polygon object for the process of extracting the surface. After this step, the function “*Detect Contours*” was used to create the contours based on the topological characteristics of the model. At the end, the NURB surfaces were generated by the “*Fit Surfaces*” function. The surfaces were then saved as Initial Graphics Exchange Specification (.IGES) for the further meshing. The process is shown in FIGURE 5.4.

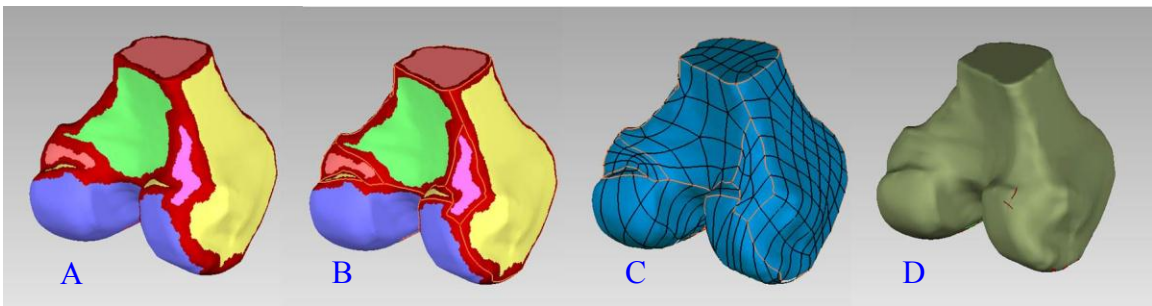


FIGURE 5.2 Process of surface extraction for the femur in Geomagic™. A – auto detect contour, B – create contour lines, C – construct patches, D – fit surfaces.

## 2) Mesh generation and assembling

A Previous study proved that hexahedral elements had superior attributes compared with the tetrahedral elements (Cifuentes and Kalbag, 1992). Generating high quality elements, especially hexahedral elements, for the organic shape parts often proves daunting. There was no doubt that a lot of difficulties were encountered when generating hexahedral meshes for the knee joint parts. In this section, the process for generating 8-noded hexahedral elements is discussed.

Since the bones are more rigid compared to soft tissues, the femur and tibia were meshed by 4-node tetrahedral elements. In this study, the tetrahedral elements for the bones were generated in Altair HyperMesh™ (Altair, Troy, MI, USA). For the soft tissues, hexahedral elements were used to reduce the rigidity of local element as in previous studies (Donahue et al., 2002, Netravali et al., 2011, Pena et al., 2006a, Pena et al., 2006b).

Hexahedral meshes were created by using TrueGrid™ (XYZ Scientific Application, Inc., Livermore, CA). TrueGrid is powerful and generates high quality 8-node hexahedral elements from organic shape geometry by projecting the uniform shape faces of the mesh onto the target surfaces. Moreover, the embedded commands offer users more versatility in terms of mesh density and mesh size. By running a customized code, hexahedral elements were generated. The femoral cartilage and tibial cartilage were meshed as three hexahedral element layers. Menisci were meshed as four hexahedral element layers. An intermediate element size of about 2 mm by 2 mm, which was judged sufficiently fine according to a previous study (Donahue et al., 2002), was used in this study. The element numbers are listed in TABLE 5.1.

The elements of different components were then imported into HyperMesh™ for assembling. The coordinates of each part was inherited from the MR images. In HyperMesh, element penetrations were cleaned up by mildly adjusting the locations of the nodes on interaction surfaces. After clean up all overclosures, the assembly of mesh geometries was then imported into the finite element solver ABAQUS™ (Version 6.10-1, SIMULIA, Providence, RI, USA) for analysis (FIGURE 5.3).

The processes of medical image segmentation, NURB surfaces reconstruction and mesh generation were organized in the following flowchart (FIGURE 5.4).

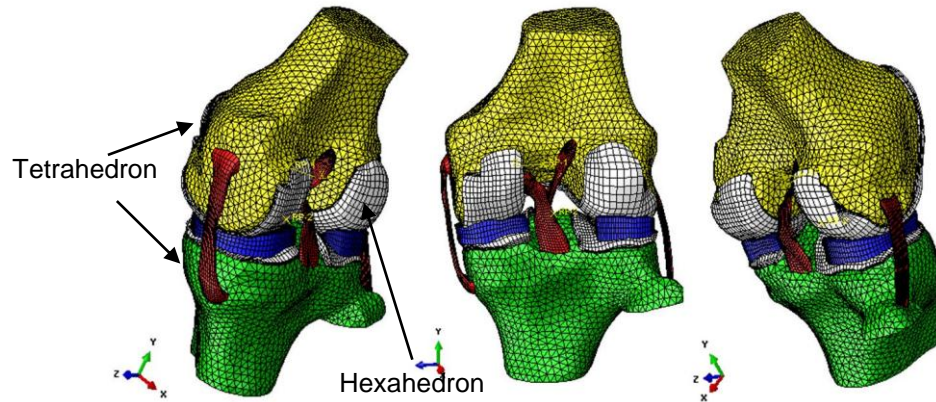


FIGURE 5.3 Assembly of FE knee model in ABAQUS.

TABLE 5.1 Properties of solid elements of each part.

Parts	Element type	Number	Min, max length	Min Jacobian
<sup>1</sup> FCart	C3D8 hex <sup>4</sup>	4275	0.147, 3.92	0.5
<sup>2</sup> Lat. tCart	C3D8 hex	1560	0.186, 2.55	0.48
<sup>3</sup> Med. tCart	C3D8 hex	1191	0.265, 3.15	0.51
Lat. meniscus	C3D8 hex	2640	0.096, 3.17	0.46
Med. meniscus	C3D8 hex	2640	0.197, 2.67	0.42
ACL	C3D8 hex	4096	0.114, 2.46	0.32
PCL	C3D8 hex	5120	0.077, 2.06	0.41
MCL	C3D8 hex	4736	0.113, 3.11	0.35
LCL	C3D8 hex	5824	0.050, 3.73	0.42
Femur	C3D4 tets <sup>5</sup>	67657	0.453, 8.19	1.00
Tibia	C3D4 tets	55193	0.396, 7.87	1.00

<sup>1</sup>F – femoral, Cart – cartilage, <sup>2</sup>Lat – lateral, t – tibial, <sup>3</sup>Med – medial, <sup>4</sup>hex – hexadral, <sup>5</sup>tets – tetrahedral

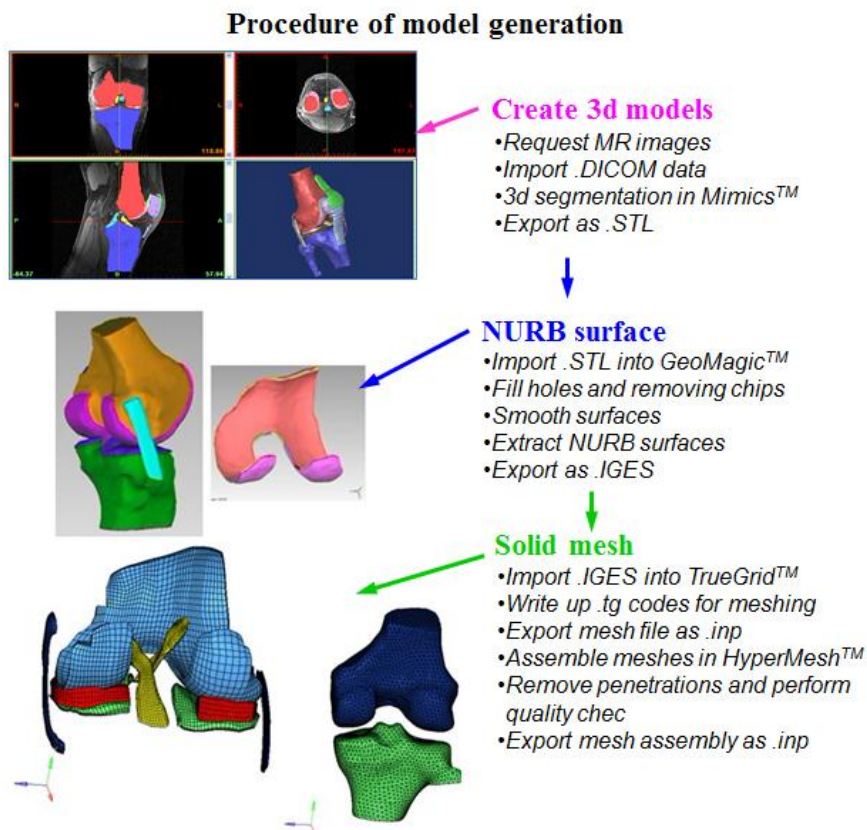


FIGURE 5.4 Medical image segmentation, smoothing and NURB surface creation and mesh generation.

### 5.2.2. Material properties

Material properties were obtained from values identified in the literatures. The bone, whose deformation was neglectable compared to the soft tissues, was assumed to be rigid relative to the soft tissues. Oloyede et al. found that the viscoelastic effects were minimal at short term cartilage response during high strain-rate activities (Oloyede et al., 1992). The viscoelastic time constant was about 1.50 s (Armstrong et al., 1984), which was longer than a gait cycle. Therefore, in this study the articular cartilage was assumed to behave as single-phase linear elastic isotropic material according to the experimental and numerical investigation in the other studies (Blankevoort and Huiskes, 1996,

Blankevoort et al., 1991, Yang et al., 2010) (TABLE 5.2). For the meniscus, due to the Type-1 collagen fibers, it was modeled as transversely isotropic with a higher Young's modulus ( $E_1 = 140$  MPa) in the circumferential direction and relatively low Young's modulus in the axial and radial directions ( $E_2, E_3 = 20$  MPa) (Donahue et al., 2002, Yang et al., 2010). The in-plane Poisson's ratio was 0.2 ( $\nu_{12}, \nu_{13}$ ) and the out-of-plane poisson's ratio was 0.3 ( $\nu_{23}$ ) according to a previous study (Netravali et al., 2011). The elastic moduli and Poisson's ratios are listed in TABLE 5.2.

TABLE 5.2 Material properties used for cartilage, meniscus and bone. <sup>1</sup>fCart – femoral cartilage, <sup>2</sup>tCart – tibial cartilage

Parts	Elastic modulus (MPa)	Poisson's ratio ( $\nu$ )	Density (ton/mm <sup>3</sup> )
<i>Elastic</i>			
<sup>1</sup> fCart	15	0.45	$1 \times 10^{-9}$
<sup>2</sup> tCart	15	0.45	$1 \times 10^{-9}$
meniscus	140, 20, 20	0.3, 0.3, 0.2	$0.8 \times 10^{-9}$
<i>Rigid body</i>			
Femur	infinite	N/A	$2.0 \times 10^{-9}$
Tibia	infinite	N/A	$2.0 \times 10^{-9}$

The ACL has already been stretched at neutral extension posture (Beynon and Fleming, 1998). Since the 3D knee model was inherited from the MR images which were taken at this posture, there was an initial stretch within the ACL. For the same reason, there may be initial stretches in the other ligaments. In a finite element context, modeling the initial stretches in elements corresponding to the already stretched state is a very challenging task. Therefore, for simplicity the ligaments were modeled as nonlinear springs according to their functional bundles based on their anatomic structure. The ACL

was modeled as two bundles: anteromedial bundle and posterolateral bundle. The PCL was represented by anterolateral and posteromedial bundle. The MCL was modeled as a superficial portion and inferior portion, the superficial portion was divided into the anterior bundle and posterior bundle. In a similar way, the LCL was modeled with three bundles. The representation of ligaments using nonlinear springs was similar to that used in the previous studies (Netravali et al., 2011, Yang et al., 2010, Yao et al., 2006, Donahue et al., 2002). Each of the functional ligament bundles was modeled as the following piece-wise force-displacement relationship (Blankevoort et al., 1991).

$$f = \begin{cases} 0 & \varepsilon \leq 0 \\ (1/4)k\varepsilon^2 / \varepsilon_1 & 0 \leq \varepsilon \leq 2\varepsilon_1 \\ k(\varepsilon - \varepsilon_1) & \varepsilon \geq 2\varepsilon_1 \end{cases} \quad (5.1)$$

where  $f$  is the force in each bundle,  $k$  is the axial stiffness which is equivalent to the force per unit strain (structural stiffness times original length),  $\varepsilon$  denotes the strain in the ligament bundle and  $\varepsilon_1$  denotes the strain threshold from nonlinear relationship to a linear relationship.  $\varepsilon_1$  was a constant of 0.03 determined from experiment (Blankevoort et al., 1991).

The initial strains in each ligament bundle at neutral extension posture were listed in TABLE 5.3. Thus the slack length of each ligament can be calculated from  $L_0 = L_r / (1 + \varepsilon_r)$ , where  $L_r$  is the initial length of ligament from MR images. The strain therefore can be calculated from  $\varepsilon = (L - L_0) / L_0$ . The stiffness of ACL was 5 kN which was close to that of 4.9 kN in previous experimental study (Noyes et al., 1984). The initial ACL strain at neutral knee position was 0.12 for the anterior bundle and 0.20 for the posterior bundle according to our preliminary data from cadaver testing.

TABLE 5.3 Material properties used for the ligaments.

Ligament	Bundle	Stiffness parameter <sup>§</sup> , k (N)	$\epsilon_1$	$\epsilon_r$
ACL	Anterior	2500	0.03	0.12
	Posterior	2500	0.03	0.20
PCL	Anterior	9000	0.03	-0.24
	Posterior	9000	0.03	-0.03
LCL	Anterior	2000	0.03	-0.25
	Superior	2000	0.03	-0.05
	Posterior	2000	0.03	0.08
MCL	Anterior	2750	0.03	0.04
	Inferior	2750	0.03	0.04
	Posterior	2750	0.03	0.03

<sup>§</sup>The stiffness of PCL, LCL and MCL are from Butler et al. (Butler et al., 1986), the stiffness of ACL are from Noyes et al. (Noyes et al., 1984). The reference strain values are adapted from Blankevoort et al. (Blankevoort et al., 1991).

To simulate ACL-reconstruction using single-bundle graft (semitendinosus with gracilis enforcement, STG), the graft was modeled as having a single nonlinear spring element. Previous experimental studies reported that the structural stiffness of commonly used four strands STG graft was 954 N/mm (To et al., 1999) and 776 N/mm (Hamner et al., 1999), which is about two times greater than the stiffness of natural ACL (300 N/mm). In this study, we modeled the scenario that the graft was fixed at the half-length of the tunnels, which made the stretchable length approximately twice that of the natural ACL (FIGURE 5.5). That caused a 50% structural stiffness loss of STG graft after installed to the knee joint. Considering the stiffness loss, a spring with stiffness 1.5 times that of ACL bundles (summation of anterior bundle and posterior bundle) was used to model the ACL graft. The initial graft force was set as 500 N at neutral knee position, and the graft length

at the neutral position was adjusted accordingly. The insertion site of ACL tunnels at the femur and tibia were shown in FIGURE 5.5.

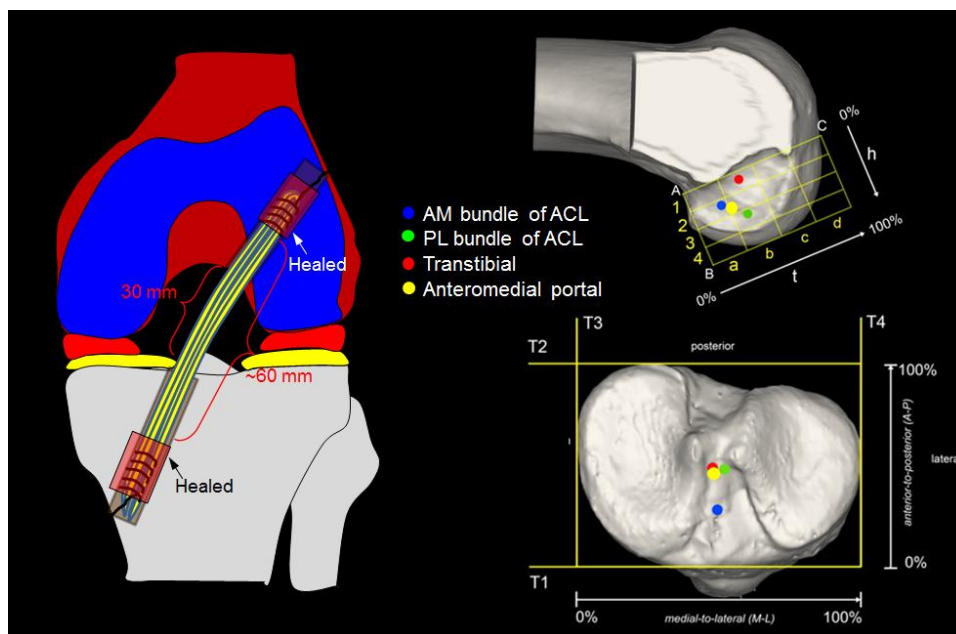


FIGURE 5.5 ACL-reconstruction using single bundle STG graft. The figure of insertion sites were adapted from Kopf et al. (Kopf et al., 2010)

During level walking, the knee joint reaction forces and moments calculated by inverse dynamics must be balanced by a set of internal forces and moments provided by muscle contractions, ligament stretches and articular reaction forces, etc. Muscle force was the major component for balancing the external knee joint moment, at the same time it increased the total contact forces at the joint. Since the number of unknown forces was greater than the number of equations, it was impossible to determine the individual muscle forces without making assumptions. In this study, a muscle force reduction model was used to estimate the forces in major muscles including: hamstring (hams), quadriceps (quads) and gastrocnemius (gast) adapted from a previous study (Yang et al., 2010)

(FIGURE 5.6). For simplicity, it was assumed that there was no muscle co-contraction, which means either the flexor or extensor muscle acts at one time.

For different knee models (healthy, transtibial ACLR and anteromedial portal ACLR), the average flexion/extension moments from the same group of subjects were used. By assuming that the moments provided by ligaments were trivial compared to the moments created by the muscles, the joint reaction moments had to be balanced by muscle contraction. During the stance phase, after heel strike the hamstring contracted to provide the flexion moment to withstand the external extension moment (FIGURE 5.6). After a short period, the moment became an external knee flexion moment which attained the peak at CTO. To balance it, the quadriceps muscles were activated to oppose this external knee flexion moment. At late stance phase, the moment became an external knee extension moment and reached its peak around the CHS. At this moment, the gastrocnemius group was activated to provide a knee flexion moment to stabilize the knee. The gastrocnemius force also created an ankle plantar flexion moment for propulsion. At toe-off, the quadriceps muscle contracted again to balance the external knee flexion moment. The moment arm and line of action for each muscle group vary with knee flexion. The line of action of the hamstring muscle was assumed along the long axis of femur, and the line of action of gastrocnemius muscle was parallel with tibia axis which created no additional shear force to the knee joint. The moment arm of the gastrocnemius muscle was taken as a constant of 25 mm with respect to the knee joint rotation center (Yang et al., 2010). The moment arms and line of action of quadriceps and hamstring muscles were listed in TABLE 5.4.

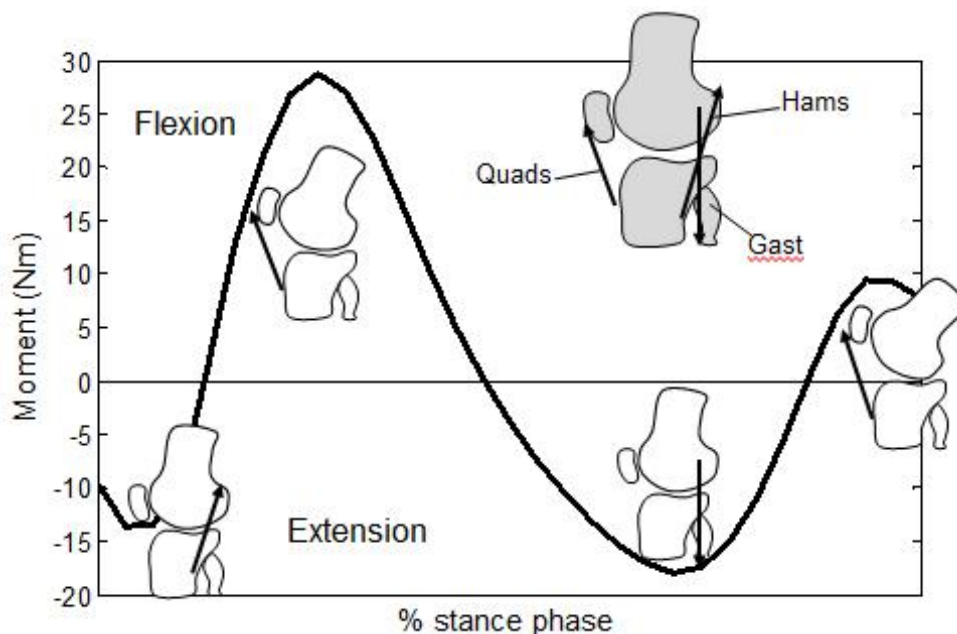


FIGURE 5.6 External flexion/extension moment and the activation muscles during stance phase of level walking. The insets show the knee joint posture and activated muscle respectively at HS, CTO, CHS and TO.

TABLE 5.4 Moment arm and line of action of muscles at different knee flexion adapted from (Yang et al., 2010).

Knee flexion angle (°)	Moment arm of quads (mm)	Line of action of quads (°)	Moment arm of hams (mm)
0-10	36.9	135.7	29.9
11-20	39.3	126.7	25.4
21-30	40.9	118.2	26.6
31-40	42.5	112.8	28.2
41-50	42.6	107.5	27.9
51-60	41.7	101.0	28.3

### 5.2.3. Boundary condition and loading

In this study, the tibia was fixed and the femur was able to move on the tibial plateau. Femoral and tibial elements were constrained to a reference point respectively to form rigid bodies. The femur motions were exerted at the femoral reference point (the

midpoint of the transepicondyle line) which was the location where the joint reaction forces and moments were calculated. Surface-to-surface sliding interaction was defined between femoral cartilage to meniscus and between tibial cartilage to meniscus (FIGURE 5.7). The contact is enforced in an average sense over the slave surface/nodes that the slave nodes cannot penetrate the master surface. The surface with the fine mesh was selected as the master surface. All sliding interaction was simulated with zero friction. “Tie” contacts were defined between the femoral cartilage and femur and between the tibial cartilage and tibia with a position tolerance enforcing the slave nodes within the tolerance to be tied to the master surface. The interactions defined in ABAQUS are listed in TABLE 5.5.

The menisci were attached to tibia plateau using meniscus horn attachments. Horn ligaments and transverse ligament were modeled with linear springs with total stiffness of 2000 N/mm and 900 N/mm respectively (Netravali et al., 2011, Donahue et al., 2002, Yang et al., 2010).

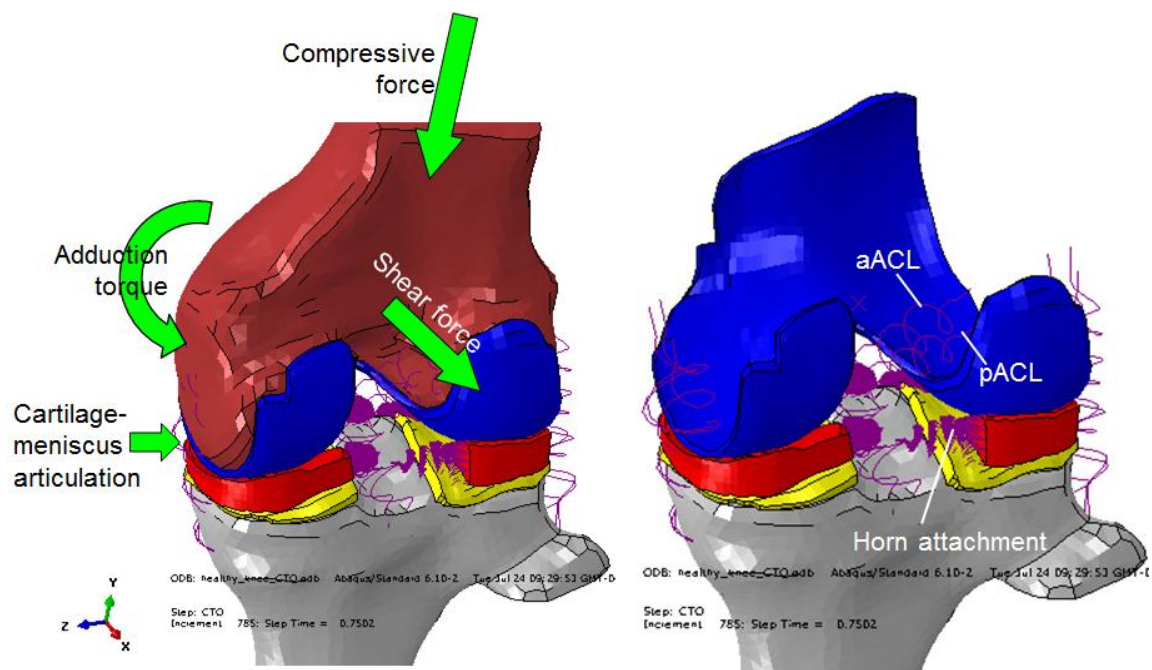


FIGURE 5.7 Boundary conditions and loading in ABAQUS. Ligaments and meniscus horn attachments were modeled as springs. aACL anteromedial bundle, pACL posterolateral bundle.

TABLE 5.5 Interaction and constraint.

Couples	Type	Discretization method	Position tolerance	Interaction properties
F <sub>Cart</sub> to femur	Tie	N2S <sup>1</sup>	0.2 mm	
t <sub>Cart</sub> to tibia	Tie	N2S	0.2 mm	
F <sub>Cart</sub> to med. meniscus	Contact	N2S		Hard, penalty <sup>2</sup>
F <sub>Cart</sub> to lat. meniscus	Contact	N2S		Hard, penalty
Med. T <sub>Cart</sub> to meniscus	Contact	N2S		Hard, penalty
Lat. T <sub>Cart</sub> to meniscus	Contact	N2S		Hard, penalty

<sup>1</sup>N2S – node to surface, <sup>2</sup>Hard – hard contact, penalty – penalty constraint enforcement method, <sup>3</sup>S2S – surface to surface

After determining the muscle forces by using the muscle reduction model, the total knee joint compressive forces and shear forces (anteroposterior) were calculated by deducting the muscle forces from the joint reaction forces (results of the inverse

dynamics, FIGURE 4.4, chapter 4), as shown in FIGURE 5.8. The joint compressive force, shear force and knee adduction moment were used to define the femur loading in FE analysis similar to a previous study (Yang et al., 2010). The resultant adduction moment was also applied to the femur to evaluate the effect of adduction moment on the distribution of contact stresses across the medial and lateral compartment. The average flexion/extension angles were taken as input (results of the chapter 4, FIGURE 4.1); while the other DOFs (2 rotations and 3 translations) of the femur were not controlled. The results of compressive and shear forces in average size people (height 1.75 m, weight 70 kg) for different knee joint physical status are shown in FIGURE 5.9. The adduction moments are shown in FIGURE 5.10.

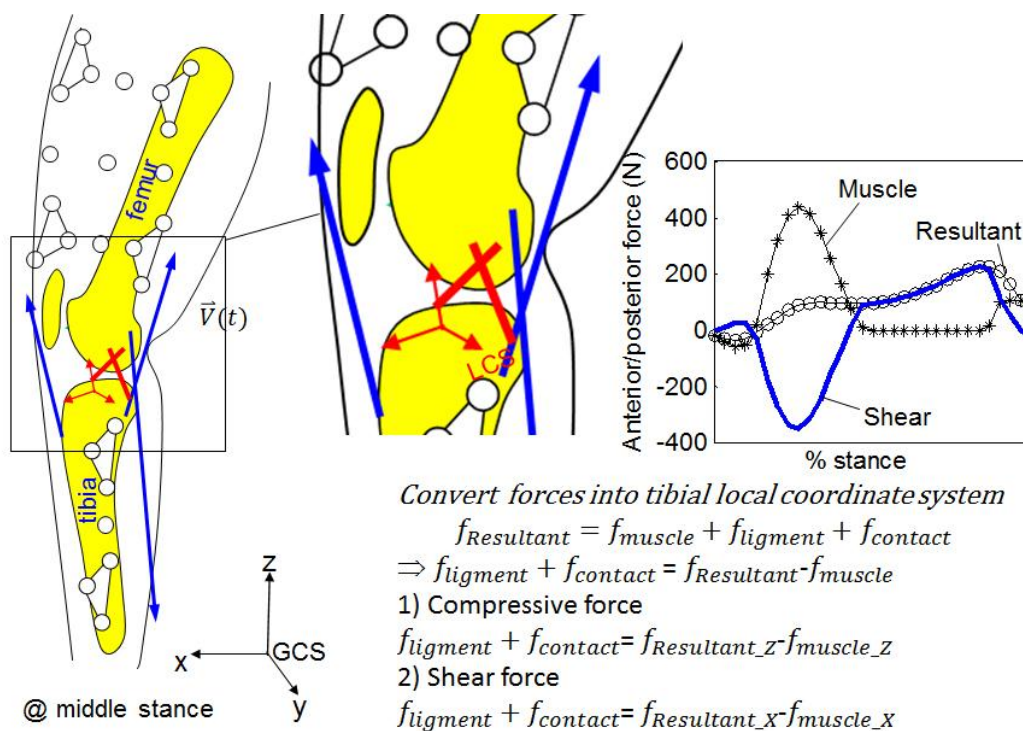


FIGURE 5.8 Calculation of knee joint loading.

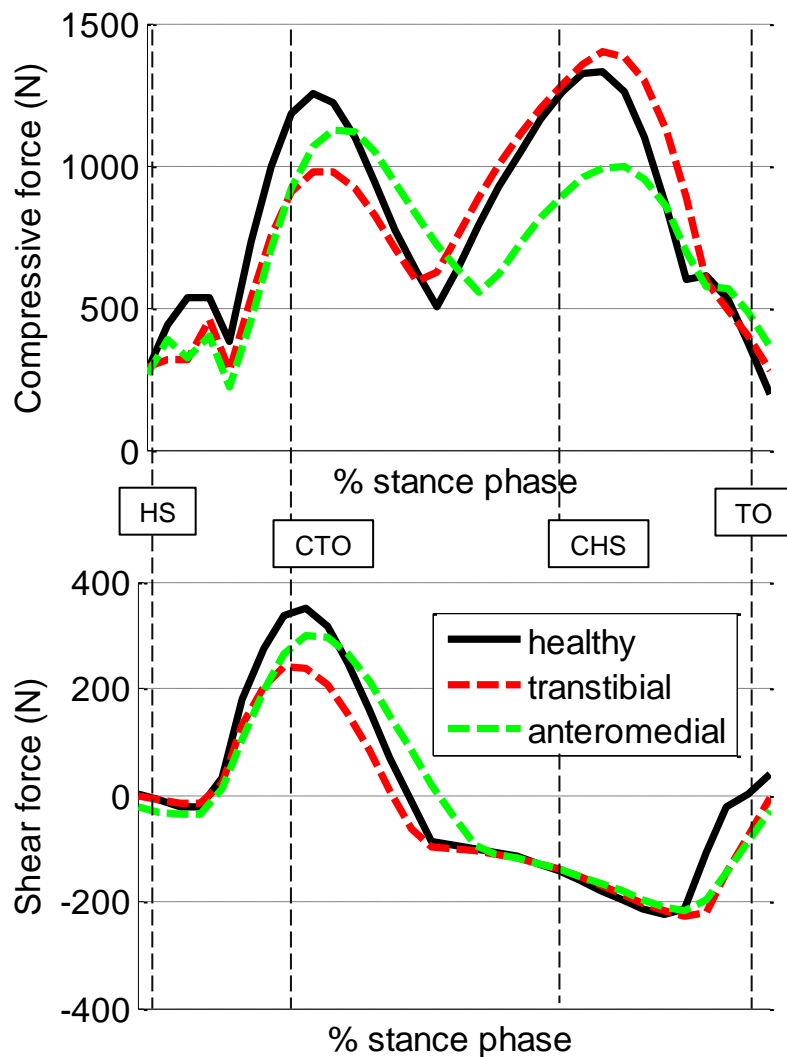


FIGURE 5.9 Total knee force during stance phase for different knees. The compressive force was the axial force and the shear force was the posterior force exerted on the femur in the FE model.

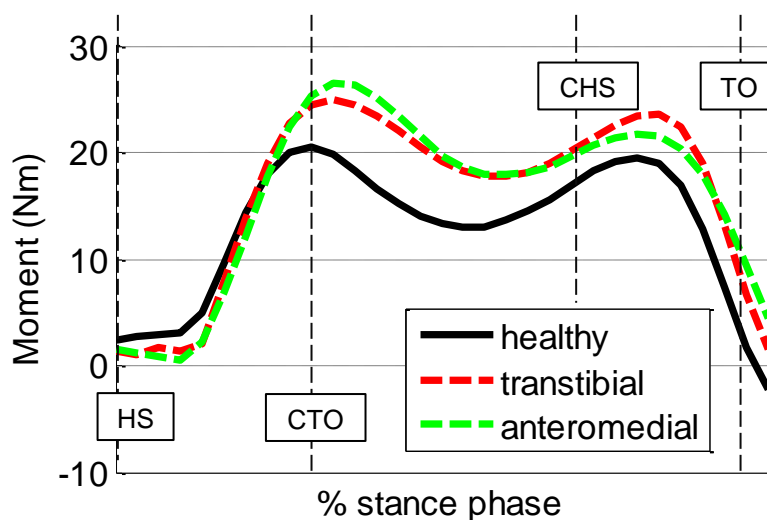


FIGURE 5.10 The adduction moment at knee joint during stance phase.

#### 5.2.4. Finite element solution

There are two approaches in ABAQUS to solve the FE problem, the explicit and the implicit analyses. In explicit analysis the stiffness matrix is updated at the end of each increment based on geometry changes or/and material changes. Then a new force or displacement load is applied to the system after each increment. In this type of analysis, the step size should be small enough (i.e.  $1e-5$  s) to enable accuracy and convergence, since the external forces and internal loads are not enforced to be in equilibrium. Therefore the solution may not be trustable if the time steps are not sufficiently small. On the other hand, in implicit analysis additional Newton-Raphson iterations are performed to enforce equilibrium (tolerances are set by the user, i.e.  $2e-4$ ) of the internal structure forces with the externally applied loads at each increment. Therefore, this type of analysis tends to be more accurate and can take somewhat bigger increment steps (the solver usually adjusts the step size according to the number of iterations needed to enforce equilibrium). Therefore, the explicit method can be recognized as a special case of the

implicit method when the convergence tolerance of equilibrium equation is set as a large number. Explicit analysis is usually used to study the dynamic response of mechanical structures, such as car crash, explosion, etc. Implicit analysis dominates the static or quasi-static problems.

In this study, implicit analysis was used to calculate the cartilage stress variation and ligament force during several key frames of the stance phase. The FE model was solved using ABAQUS/Standard. The input files were submitted to the Viper cluster of the University Research Computing (UNC Charlotte, [urc.uncc.edu](http://urc.uncc.edu)), and the computation was performed by using 32 computing cores (3 GBs/core).

### 5.3. Results

In this study, the knee joint compressive and shear loads were calculated from muscle forces and joint reaction forces. The joint reaction forces were transformed to the tibial local coordinate system (LCS) and all calculations were conducted in the LCS. The maximum compressive forces (1400 N) were about two times the body mass (70kg). The shear force pointed to the posterior, which pulled the tibia backward at the first 40% of the stance and then it became an anterior force during the rest of stance phase (FIGURE 5.9). Compared to the healthy knee, the knee with transtibial ACL-reconstruction had a smaller compressive force and shear force at CTO. On the other hand, the knee with anteromedial portal ACL-reconstruction had a much smaller compressive force at CHS compared to the other two knees. At the TO, Both ACLR knees had anterior shear forces, while the healthy knee had a posterior shear force.

#### 1) FE analysis results – Contact pressure

The contact pressures (MPa) within the femoral cartilage at four key frames during the stance phase of a gait cycle are shown in FIGURE 5.11. For all three knees

(healthy, transtibial and anteromedial portal), the contact pressures were much lower at the beginning (HS) and the end (TO) of stance phase. The pressures reached their peak values at CTO, which was the transient point from double-leg supporting to single-leg supporting. The high pressures were then maintained until the other leg hit the ground at CHS. For the healthy knee, the maximum contact pressures within the femoral cartilage were located on the medial compartment at all of the four key frames. For the ACLR knees, however, the maximum contact pressure within the lateral femoral cartilage was greater than that in the medial at CTO. The contact pressures (MPa) within the tibial cartilage at four different key frames are shown in FIGURE 5.12. The evolution of contact pressures within tibial cartilage during the stance phase exhibited the same tendency as those within femoral cartilage. For the healthy knee, the maximum contact pressures within tibial cartilage were located on the lateral compartment at all key frames. For the ACLR knees, however, the maximum contact pressure translated to the medial tibial cartilage at CTO.

The maximum contact pressures within the tibial cartilage of anteromedial knee were relatively lower than those in the transtibial knee at all key frames (FIGURE 5.12). Similar findings also existed in the femoral cartilage where the maximum contact pressures in the transtibial knee were greater than those in the transportal knee except at the CTO (FIGURE 5.11). The transtibial knee had relatively higher contact pressures in the femoral cartilage compared to the healthy knee at all key frames. The contact pressures within tibial cartilage of the anteromedial knees were lowest in the three groups except at CTO.

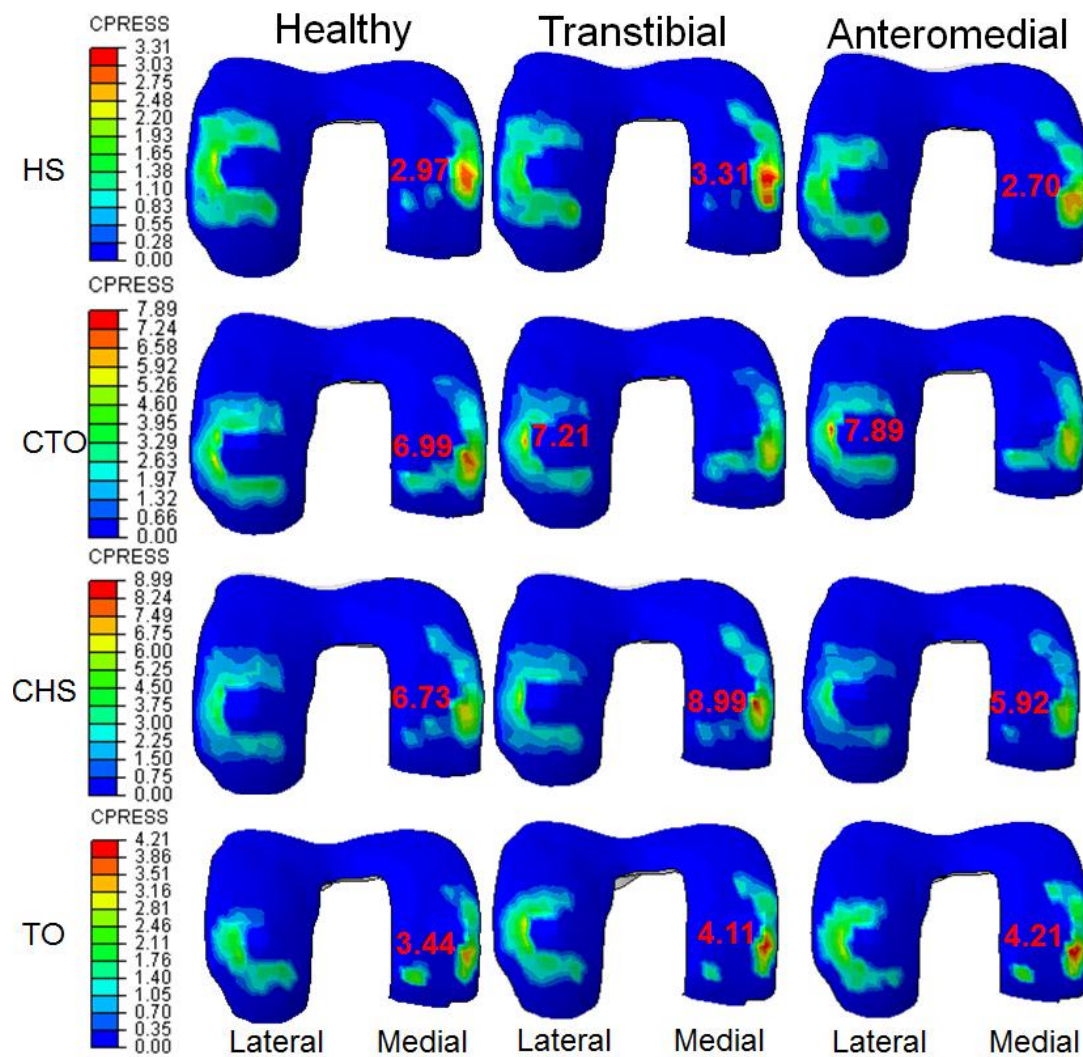


FIGURE 5.11 The contour of pressure on femoral cartilage surface at different key frames during stance phase. The numbers on the contour denote the maximum values of pressure.

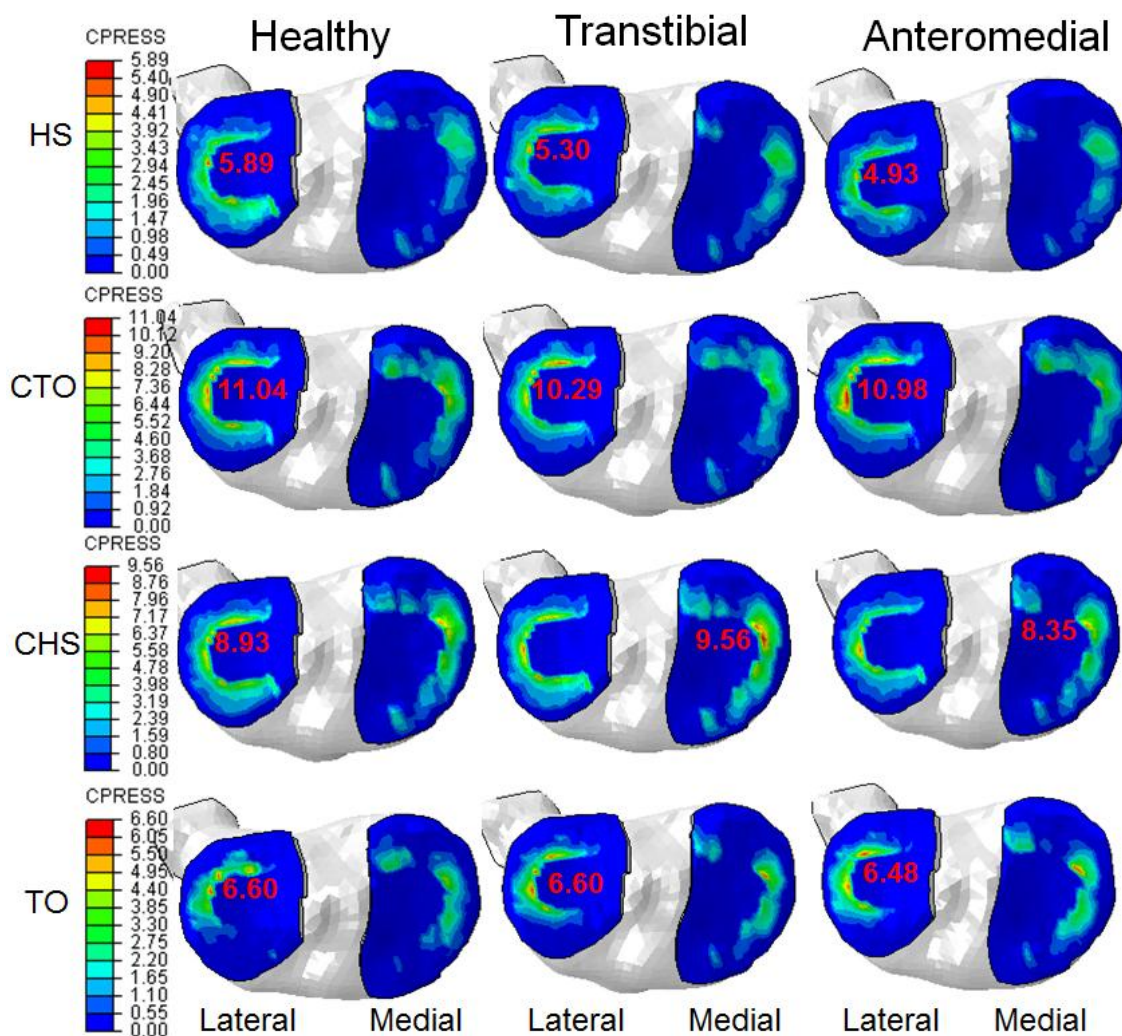


FIGURE 5.12 Stress contour within tibial cartilage at different key frames during stance phase. The numbers on the contour denote the maximum values of pressure.

## 2) FE analysis results – Contact force

The total contact forces on the articular surfaces were exported as History Output in ABAQUS. The contact forces were much greater at CTO and CHS than at the other two key frames (FIGURE 5.13). The load carried by the lateral femoral compartment was greater than that carried by the medial compartment except at CTO. At HS, the load carried by the lateral compartment was much higher in the healthy knee than those in the ACLR knees: 355 N for healthy vs. 270 N for transtibial and 250 N for anteromedial,

while the load on the medial side was close to each other. At CHS, the axial load in the anteromedial knee was much smaller than those in the other two knees.

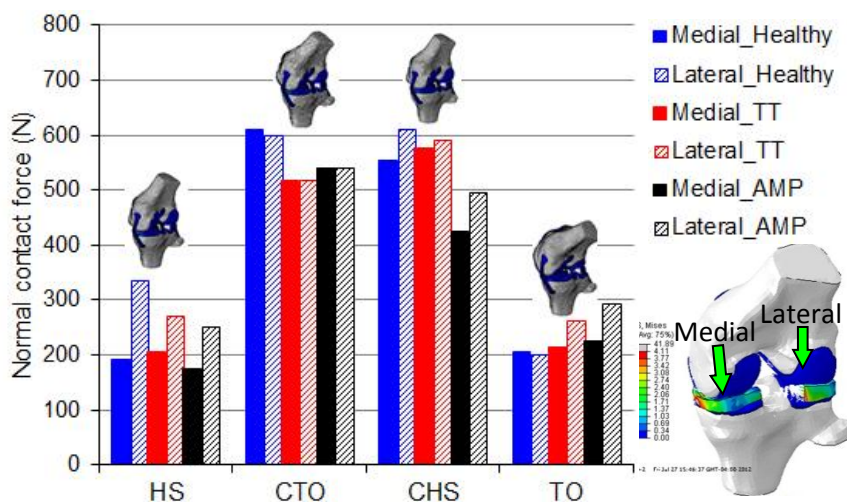


FIGURE 5.13 The normal load carried by the medial and lateral tibial compartments in different knees.

### 3) FE analysis results – Secondary motion

At HS and CHS, all the three knees had posterior tibial translations, and the translation magnitudes in the ACLR knees were greater than that in the healthy knee (FIGURE 5.14). At CTO, the healthy knee had a much smaller anterior tibial translation than the ACLR knees. There were anterior tibial translations at TO for the healthy knee. However, the ACLR knees had posterior tibial translations at TO.

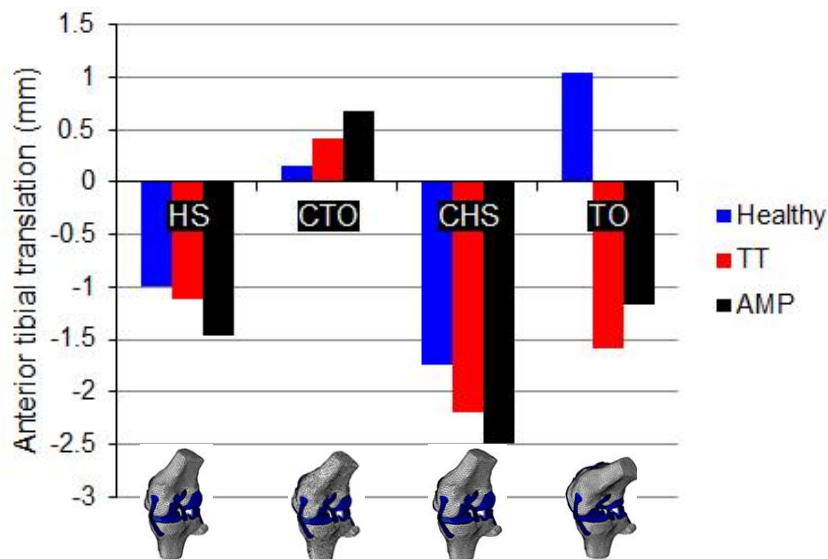


FIGURE 5.14 Anterior/posterior tibial translation. The tibial translation was reported as the opposite value of the femoral translation.

There were concomitant rotations on the non-sagittal planes (FIGURE 5.15). The results showed that the tibia was internally rotated relative to the femur throughout the whole stance phase. The FEA results also showed the healthy knee had relative less axial and varus rotations from HS to CHS compared to the ACLR knees. Compared to the transtibial knee, the anteromedial portal knee had greater varus rotations throughout the whole stance process. The knee joint rotations were much greater at TO than those at the earlier frames. At this time the healthy knee, for the first time, exhibited greater rotations than the ACLR knee.

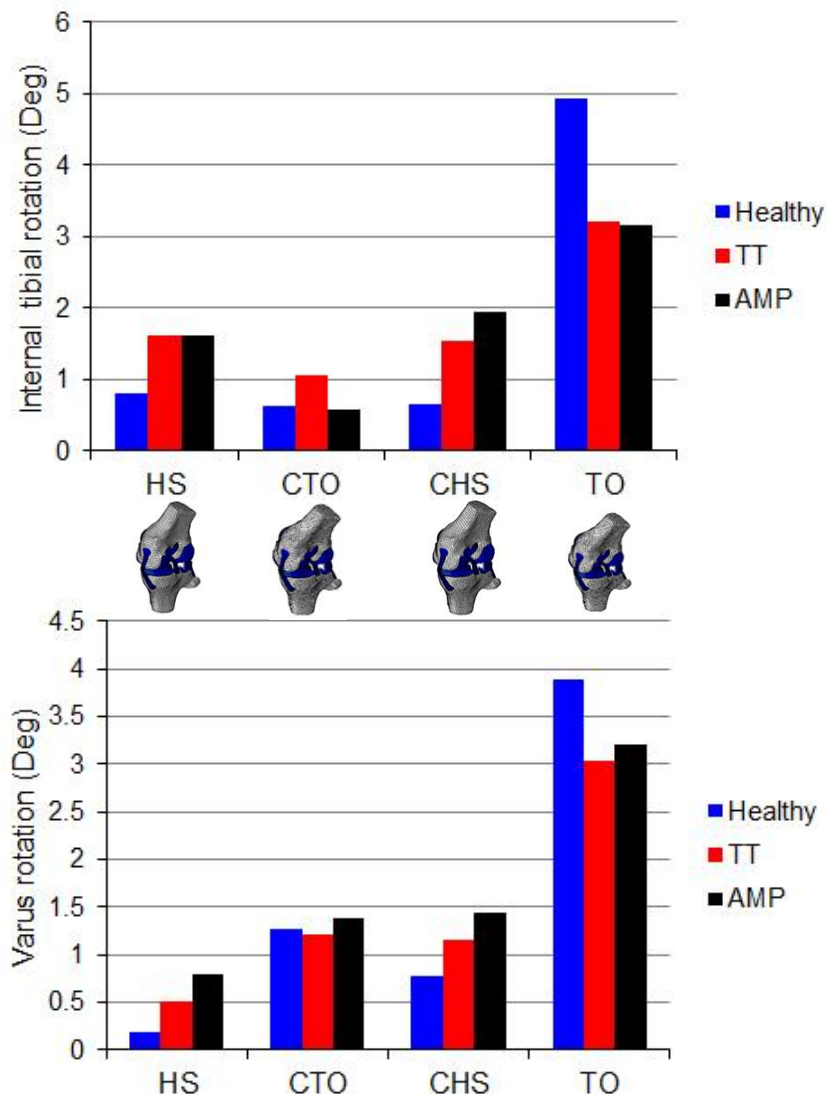


FIGURE 5.15 Internal tibial rotation and varus knee rotation. The internal tibial rotation was reported as the external femoral rotation.

#### 5.4. Discussion

For the first time, the joint contacting mechanics were evaluated under different physical status (healthy vs. ACLR) during the stance phase of walking by using a sophisticated FE model. The inputs and boundary conditions of the FE model were adapted from the results of kinematic and kinetic analysis. The compressive forces estimated by a muscle reduction model in our study was slightly smaller than 200% of

body weight in the previous literature (Kutzner et al., 2011b, Kutzner et al., 2011a). The differences may come from the assumption of no co-contraction of the flexor and extensor muscles. Other than that, the overall profile of the compressive force was in line with the previous studies. In the current study, the joint reaction forces calculated by inverse dynamics were transformed to the tibial local coordinate system to make it consistent with the FE model. The shear force in this study was different from Yang et al.'s study during the second half of the stance phase (Yang et al., 2010). According to our data, the curve of shear force used in Yang et al.'s study was similar to the shear force in the global coordinate system.

More loads were carried by the lateral compartment at the beginning of walking due to the low varus moment. The load was more evenly distributed at CTO when the knee adduction moment reached the first peak. Previous literature has suggested that the external adduction moment was very important in the overall distribution of the contact force across the medial and lateral compartments (Erhart et al., 2010, Zhao et al., 2007). The unbalanced loading across the medial and lateral compartments may be contributed to by the varus knee rotation found in this study (from  $0.2^\circ$  to  $4^\circ$ ) which was similar to another FEA study (Adouni et al., 2012).

The finding of greater maximum contact pressures within the medial femoral cartilage may be explained by the relatively smaller contact area between the medial femoral condyle and meniscus (i.e.  $240 \text{ mm}^2$  on medial,  $355 \text{ mm}^2$  on lateral at CTO). The maximum pressure found on the medial side may explain why it was more common to witness cartilage degenerative diseases on the medial compartment according to clinical data. On the tibial cartilage in the healthy knee, the maximum contact pressures were

found on the lateral compartment, which indicated the importance of the medial meniscus in the distribution of the contact stresses. In the ACLR knees, the maximum contact pressure was retained on the medial tibial cartilage at CHS. This change interrupted the normal knee joint contacting attribute and may increase the risk of developing knee OA on the medial compartment after ACL-reconstruction.

The secondary rotation and anterior/posterior translation of the femur relative to the tibia exhibited an obvious correlation with the knee flexion during the stance phase. According to our finding, the tibial in the healthy knee tends to translate forward (the femur moves posteriorly) when the knee flexion angle was relative high, i.e. at CHS and TO. The result was consistent with the rollback effect reported in a previous cadaver study by Iwaki et al., in which reported that the femur tends to posteriorly translate with respect to the tibia with knee flexion (Iwaki et al., 2000). However, for the ACLR knees, the rollback effect was not found. According to previous studies (Draganich et al., 2002, Draganich et al., 1987), the rollback increases the quadriceps lever arm to enhance quadriceps efficiency especially for high demand activities such as stair climbing, downhill walking and sit-to-stand, because it increases the lever arm of quadriceps. Therefore, the finding changed the rollback pattern after ACL-reconstruction should raise our attention when designing TKA implants. Since the structural stiffness of ACL-graft was 1.5 times of the natural ACL in the FE model, the extra stiffness may cause the tibia to move more posteriorly (femur move more anteriorly) to reduce the graft tension at HS and CHS (FIGURE 5.14) when the knee was close to full extension. The greater posterior tibial translation at these two key frames may contribute to the decrease of graft tension compared to that in the healthy knee (TABLE 5.6). The increased internal tibial rotation

from HS to CHS was consistent with the result of motion analysis. Since one of the ACL functions was to restrain the excessive internal tibial rotation, the diminished graft tension may explain the increased axial laxity in the ACLR knees.

TABLE 5.6 ACL/graft tension at different key frames. (unit: N)

	Healthy	TT	AMP
HS	230	104	37
CTO	50	37	7
CHS	76	0	0
TO	23	0	0

The greater varus rotation in the ACLR knees found in this study may explain why the maximum contact pressure occurred on the medial tibial cartilage at CHS. The varus/valgus rotation is important to maintain the knee joint space; a varus offset tends to decrease the space and increase the contact pressure on the medial compartment which may explain the higher frequency of knee OA on the medial compartment compared to the lateral compartment (Engh, 2003, Sharma et al., 2000).

By studying the simulated cases, we found that the integrity of ACL was very important in maintaining the knee joint motion during physiologic loading. The grafts in ACLR knees had a reduced tension compared to the healthy ACL which may increase knee joint laxity in the transverse and frontal plane during the stance phase of walking. Based on the results, we may conclude that the anteromedial portal technique had more advantages than traditional transtibial technique in protecting the medial compartment from excessive compressive loading especially around the period of CHS.

There were some limitations in this FE model which need to be kept in mind when interpreting the results. First, the stiffness of the ACL graft was assumed to be 1.5 times of the natural ACL according to the literature without considering the inter-subject differences. Second, the initial tension in the ACL and grafts were set as 500 N when the knee was at the neutral extension (the posture for MR imaging). Unfortunately, there were large variances in the pre-strain/tension in ACL/graft across different studies (Beynon and Fleming, 1998). The pre-strain of ACL used in this study was higher than that in other studies (Donahue et al., 2002, Netravali et al., 2011, Yang et al., 2010). Third, the ligaments and ACL graft were simplified as nonlinear springs. However, in reality, there were ligament-to-ligament, ligament-to-meniscus, and ligament-to-bone contact/interaction which were not considered in the model. There were more factors including graft-tunnel contacting, graft-ligament impingement, etc. which could also have significant effects on the outcome of ACL-reconstruction. In a future study, we will develop more complex FE models including the geometrically accurate ligaments and graft for simulating different ACL-reconstruction techniques, and use the powerfulness of computational simulation to addressing the clinical questions concerning the optimal graft orientation, graft pre-tension and fixation technique.

## CHAPTER 6: SUMMARY AND CONCLUSIONS

### 6.1. Summary

The objective of this dissertation was to strengthen the scientific knowledge of post-trauma knee joint motion and loading following reconstruction of anterior cruciate ligament (ACL). Furthermore, the two most currently used ACL reconstruction techniques (transtibial single-bundle and AMP single-bundle) were evaluated and compared in this dissertation.

#### 6.1.1. The novelties and strengths

- A relatively large patient cohort and use of a control group, including 41 ACL patients (30 from OrthoCarolina, Charlotte, NC; 11 from Shands Hospital, Gainesville, FL) who had unilateral ACL reconstruction using transtibial technique, 14 ACL patients using AMP technique and 20 healthy subjects.

- Most of our patients (30 transtibial and 14 AMP) received their surgeries from the same surgeon; hamstring tendon ACL-grafts were used in all our patients, and they went through a similar rehabilitation program after surgery. Thus the number of variations was minimized and the only major factor came to the tunnel location (transtibial vs. AMP).

- ACL patients were grouped according to the dominance of their involved limbs. The effect of lower limb dominance on postsurgical knee joint performance was investigated.

- A redundant marker-set was used in this study. Since the accuracy of skin marker based motion analysis was affected by the soft tissue artifact (STA), it is an effective way to cancel out the STA by putting redundant markers covering a large skin area on each body segment.
- All 6 DOFs of knee joint kinematics and loading were quantified throughout the whole gait cycle. The complete spatiotemporal profiles make it possible for correlation analysis between different variables and between different timings.
- Development of an anatomically correct knee joint FE models. The stress/strain within the knee joint soft tissues was investigated during a simulated dynamic level walking.
- The measured knee contact force and knee flexion angles during the stance phase of level walking was used to drive the FE model via load and boundary conditions. These data maximally mimicked the real physiological loading during the mostly engaged daily activity.

#### 6.1.2. Key points learned from this study

After ACL-reconstruction, the normal knee joint kinematics not restored – Although single bundle ACL-reconstruction technique is effective to restore the knee functions, it does not necessarily restore the normal knee kinematics. The residual change in knee joint motion may increase the risk for knee joint osteoarthritis.

ACL-reconstructed knees exhibited excessive internal tibial rotation during stance phase of level walking – Excessive internal tibial rotation was found in ACL-reconstructed knees from both groups (transtibial and AMP). The abnormal motion will change the contact location on the articular surface of tibial cartilage and meniscus, and it

could also shift the joint loading to the non-weight bearing location. That could accelerate cartilage thinning and cause premature osteoarthritis.

The non-injured contralateral limb has also been affected –Due to the fact that the ACL patients may subconsciously protect their ipsilateral leg by overusing the uninjured contralateral leg, caution should be raised when the contralateral legs, instead of healthy subjects, were used as the controls in musculoskeletal biomechanics studies.

Varus rotation offset was found in ACL-reconstructed knees using transtibial technique –With more varus position, the medial compartment of the knee tends to be more compressed, which could generate greater contacting stresses and accelerate the abrasion within the articular cartilage. This provides a potential explanation to the higher rate of OA on the medial compartment.

Anteromedial portal ACL-reconstruction technique creates significantly different knee joint kinematics compared to the traditional transtibial technique -- The varus offset was gone and the internal offset was reduced by using the anteromedial portal technique. The anteromedial portal technique also restored the anteroposterior femur translation. On the other side, anteromedial portal technique introduced an extension deficit in the knee during stance phase.

Lower limb dominance effect exists in postsurgical knee joint kinematics and kinetics -- Using the same surgical procedure and rehabilitation program, the dominant ACL-reconstructed knees have developed significantly different motion than the non-dominant ACL-reconstructed knees. Thus, in the future, the ACL-reconstruction techniques and rehabilitation programs may be accordingly adjusted for better outcomes.

The characteristics of soft tissue movement could be used as additional constraints for improving the accuracy of motion analysis algorithm –An expedition was made in this study, which included the attributes of soft tissue movements at several bony landmarks as external constraints to tune the results of the optimization process. The results showed improved accuracies on the measurements of internal/external and varus/valgus angles of the knee rotation.

The finite element method (FEM) could be used in studying the physiological loading situation during level walking – Implicit analyses were successfully performed using ABAQUS/Standard. With the relatively accurate boundary conditions and loading conditions, FEM is a useful approach to generate insightful information of soft tissue mechanics.

The graft orientation is important in stabilizing the knee joint especially when the knee is close to full extension – The results of secondary knee joint motion showed that the ACLR knee had greater axial rotation and varus/valgus rotation. The maximum contact pressures on the femoral and tibial cartilage were relatively higher in the transtibial knee and relatively lower in the anteromedial portal knee compared to that in the healthy knee.

## 6.2. Future Directions

A therapeutic method or modality that will produce maximal rehabilitative benefits in a minimal amount of time is the consummate goal of most clinicians. Rehabilitation training that follows surgery plays as an important assisting procedure for regaining the pre-injury activity level. The information to be gained through this dissertation has profound merit for academicians as well as basic and applied science researchers. This knowledge will be useful in identifying the effectiveness of current

treatment strategies, designing innovative motion analysis algorithms, developing novel therapeutic devices or orthoses that assist knee injured individuals in achieving normal knee kinematics and neuromuscular controls. While the current research focuses on discovering the knee kinematic alteration following ACL-reconstruction, further scientific investigation should focus on the specific patterns of the kinematic changes which have the potential to trigger cartilage degeneration and premature osteoarthritis. Knowledge of these specific patterns can lead to direct implementation in the rehabilitation setting and have a profound impact on changing clinical practice.

This dissertation is a starting point, a foundation for future research. The largest limitation of this study was the ACL subjects who had relatively short post-surgery time. According to a previous study, early returning to sports activities may destabilize the ACL-reconstructed knee joint (Fujimoto et al., 2004). About half of our subjects were less than 12 month post-surgery at the time of testing. The knee motion at the early returning may not reflect a long term result of the ACL-reconstructed knees. Moreover, the relatively short postsurgical time may also contribute to the marked motion changes in the contralateral knee. Since osteoarthritis was usually diagnosed between 5-12 years post surgery (Daniel et al., 1994, Lohmander et al., 2004), in future studies, patients with longer postsurgical time should be recruited to investigate the relationship between joint kinematics and degenerative diseases.

Although electromyography (EMG) signals were recorded in a few subjects in this study, they were not included in data analysis. After ACL-rupture, the loss of sensory information about joint position and velocity typically provided by the intact ACL may affect the coordination strategies of the lower extremity (Kurz et al., 2005). As was

discussed in the previous chapters, self-adaptation in a neuromuscular control system might have been developed after ACL-reconstruction. By monitoring the muscle activities using the EMG signals, deeper discussions and persuasive conclusions may be generated. Furthermore, with the EMG signal, the muscle force could be estimated which can be used in the FE analysis to increase the modeling accuracy.

The FE results presented in this dissertation were based on a linear isotropic material model for cartilage, even though the cartilage has different stiffness along the depth. Thus in future studies, a new material model should be derived from more advanced material testing techniques. For the cartilage, different layers should be assigned with different material properties. Cadaver experiments with implant pressure sensors and strain gages should be done to validate the accuracy of FE modeling.

## REFERENCES

- Abebe, E.S., Kim, J.P., Utturkar, G.M., Taylor, D.C., Spritzer, C.E., Moorman, C.T., 3rd, Garrett, W.E. & Defrate, L.E. (2011) The effect of femoral tunnel placement on ACL graft orientation and length during in vivo knee flexion. *J Biomech*, 44, 1914-20.
- Adili, A., Bhandari, M., Giffin, R., Whately, C. & Kwok, D.C. (2002) Valgus high tibial osteotomy. Comparison between an Ilizarov and a Coventry wedge technique for the treatment of medial compartment osteoarthritis of the knee. *Knee Surg Sports Traumatol Arthrosc*, 10, 169-76.
- Adouni, M., Shirazi-Adl, A. & Shirazi, R. (2012) Computational biodynamics of human knee joint in gait cycle: from muscle forces to cartilage stresses. *ORS*. San Francisco.
- Akbarshahi, M., Schache, A.G., Fernandez, J.W., Baker, R., Banks, S. & Pandy, M.G. (2010a) Non-invasive assessment of soft-tissue artifact and its effect on knee joint kinematics during functional activity. *J Biomech*, 43, 1292-301.
- Akbarshahi, M., Schache, A.G., Fernandez, J.W., Baker, R., Banks, S. & Pandy, M.G. (2010b) Non-invasive assessment of soft-tissue artifact and its effect on knee joint kinematics during functional activity. *J Biomech*, 43, 1292-1301.
- Alentorn-Geli, E., Lajara, F., Samitier, G. & Cugat, R. (2010a) The transtibial versus the anteromedial portal technique in the arthroscopic bone-patellar tendon-bone anterior cruciate ligament reconstruction. *Knee Surg Sports Traumatol Arthrosc*, 18, 1013-37.
- Alentorn-Geli, E., Myer, G.D., Silvers, H.J., Samitier, G., Romero, D., Lazaro-Haro, C. & Cugat, R. (2009) Prevention of non-contact anterior cruciate ligament injuries in soccer players. Part 1: Mechanisms of injury and underlying risk factors. *Knee Surg Sports Traumatol Arthrosc*, 17, 705-29.
- Alentorn-Geli, E., Samitier, G., Alvarez, P., Steinbacher, G. & Cugat, R. (2010b) Anteromedial portal versus transtibial drilling techniques in ACL reconstruction: a blinded cross-sectional study at two- to five-year follow-up. *Int Orthop*, 34, 747-54.
- Andriacchi, T.P. & Alexander, E.J. (2000) Studies of human locomotion: past, present and future. *J Biomech*, 33, 1217-24.
- Andriacchi, T.P., Alexander, E.J., Toney, M.K., Dyrby, C. & Sum, J. (1998) A point cluster method for in vivo motion analysis: applied to a study of knee kinematics. *J Biomech Eng*, 120, 743-9.

- Andriacchi, T.P. & Dyrby, C.O. (2005) Interactions between kinematics and loading during walking for the normal and ACL deficient knee. *J Biomech*, 38, 293-8.
- Andriacchi, T.P., Johnson, T.S., Hurwitz, D.E. & Natarajan, R.N. (2005) Musculoskeletal dynamics, locomotion, and clinical applications. IN MOW, V. C. & HUISKES, R. (Eds.) *Basic Orthopaedic Biomechanics & Mechano-Biology*. 3rd ed. Philadelphia, PA, Lippincott Williams&Wilkins.
- Andriacchi, T.P., Koo, S. & Scanlan, S.F. (2009) Gait mechanics influence healthy cartilage morphology and osteoarthritis of the knee. *J Bone Joint Surg Am*, 91 Suppl 1, 95-101.
- Andriacchi, T.P. & Mundermann, A. (2006) The role of ambulatory mechanics in the initiation and progression of knee osteoarthritis. *Curr Opin Rheumatol*, 18, 514-8.
- Andriacchi, T.P., Mundermann a, Smith RI, Et Al (2004) A framework for the in vivo pathomechanics of osteoarthritis at the knee. *Ann Biomed Eng*, 293-298.
- Appleyard, R.C., Ghosh, P. & Swain, M.V. (1999) Biomechanical, histological and immunohistological studies of patellar cartilage in an ovine model of osteoarthritis induced by lateral meniscectomy. *Osteoarthritis Cartilage*, 7, 281-94.
- Armstrong, C.G., Lai, W.M. & Mow, V.C. (1984) An analysis of the unconfined compression of articular cartilage. *J Biomech Eng*, 106, 165-73.
- Arnold, M.P., Kooloos, J. & Van Kampen, A. (2001) Single-incision technique misses the anatomical femoral anterior cruciate ligament insertion: a cadaver study. *Knee Surg Sports Traumatol Arthrosc*, 9, 194-9.
- Arun, K.S., Huang, T.S. & Blostein, S.D. (1987) Least-squares fitting of two 3-D point sets. *IEEE Trans on Pattern Analysis and Machine Intelligence*, 9, 698-700.
- Bae, K.T., Shim, H., Tao, C., Chang, S., Wang, J.H., Boudreau, R. & Kwoh, C.K. (2009) Intra- and inter-observer reproducibility of volume measurement of knee cartilage segmented from the OAI MR image set using a novel semi-automated segmentation method. *Osteoarthritis Cartilage*, 17, 1589-97.
- Baltzopoulos, V. (1995) A videofluoroscopy method for optical distortion correction and measurement of knee-joint kinematics. *Clin Biomech (Bristol, Avon)*, 10, 85-92.
- Barrance, P.J., Williams, G.N., Novotny, J.E. & Buchanan, T.S. (2005) A method for measurement of joint kinematics in vivo by registration of 3-D geometric models with cine phase contrast magnetic resonance imaging data. *J Biomech Eng*, 127, 829-37.

- Barrance, P.J., Williams, G.N., Snyder-Mackler, L. & Buchanan, T.S. (2006) Altered knee kinematics in ACL-deficient non-copers: a comparison using dynamic MRI. *J Orthop Res*, 24, 132-40.
- Begon, M., Monnet, T. & Lacouture, P. (2007) Effects of movement for estimating the hip joint centre. *Gait Posture*, 25, 353-9.
- Bell, A.L., Pedersen, D.R. & Brand, R.A. (1990) A comparison of the accuracy of several hip center location prediction methods. *J Biomech*, 23, 617-21.
- Besier, T.F., Fredericson, M., Gold, G.E., Beaupre, G.S. & Delp, S.L. (2009) Knee muscle forces during walking and running in patellofemoral pain patients and pain-free controls. *J Biomech*, 42, 898-905.
- Beynon, B.D. & Fleming, B.C. (1998) Anterior cruciate ligament strain in-vivo: a review of previous work. *J Biomech*, 31, 519-25.
- Blankevoort, L. & Huiskes, R. (1996) Validation of a three-dimensional model of the knee. *J Biomech*, 29, 955-61.
- Blankevoort, L., Kuiper, J.H., Huiskes, R. & Grootenboer, H.J. (1991) Articular contact in a three-dimensional model of the knee. *J Biomech*, 24, 1019-31.
- Borjesson, M., Weidenhielm, L., Mattsson, E. & Olsson, E. (2005) Gait and clinical measurements in patients with knee osteoarthritis after surgery: a prospective 5-year follow-up study. *Knee*, 12, 121-7.
- Brady, M.F., Bradley, M.P., Fleming, B.C., Fadale, P.D., Hulstyn, M.J. & Banerjee, R. (2007) Effects of initial graft tension on the tibiofemoral compressive forces and joint position after anterior cruciate ligament reconstruction. *Am J Sports Med*, 35, 395-403.
- Brandsson, S., Karlsson, J., Sward, L., Kartus, J., Eriksson, B.I. & Karrholm, J. (2002) Kinematics and laxity of the knee joint after anterior cruciate ligament reconstruction: pre- and postoperative radiostereometric studies. *Am J Sports Med*, 30, 361-7.
- Brophy, R., Silvers, H.J., Gonzales, T. & Mandelbaum, B.R. (2010) Gender influences: the role of leg dominance in ACL injury among soccer players. *Br J Sports Med*, 40, 694-697.
- Brophy, R.H., Wright, R.W. & Matava, M.J. (2009) Cost analysis of converting from single-bundle to double-bundle anterior cruciate ligament reconstruction. *Am J Sports Med*, 37, 683-7.
- Buss, D.D., Min, R., Skyhar, M., Galinat, B., Warren, R.F. & Wickiewicz, T.L. (1995) Nonoperative treatment of acute anterior cruciate ligament injuries in a selected group of patients. *Am J Sports Med*, 23, 160-5.

- Butler, D.L., Kay, M.D. & Stouffer, D.C. (1986) Comparison of material properties in fascicle-bone units from human patellar tendon and knee ligaments. *J Biomech*, 19, 425-32.
- Cappozzo, A., Catani, F., Leardini, A., Benedetti, M.G. & Croce, U.D. (1996) Position and orientation in space of bones during movement: experimental artefacts. *Clin Biomech (Bristol, Avon)*, 11, 90-100.
- Cereatti, A., Della Croce, U. & Cappozzo, A. (2006) Reconstruction of skeletal movement using skin markers: comparative assessment of bone pose estimators. *J Neuroeng Rehabil*, 3, 7.
- Chaudhari, A.M., Briant, P.L., Bevill, S.L., Koo, S. & Andriacchi, T.P. (2008) Knee kinematics, cartilage morphology, and osteoarthritis after ACL injury. *Med Sci Sports Exerc*, 40, 215-22.
- Cheze, L., Fregly, B.J. & Dimnet, J. (1995) A solidification procedure to facilitate kinematic analyses based on video system data. *J Biomech*, 28, 879-84.
- Chhabra, A., Kline, A.J., Nilles, K.M. & Harner, C.D. (2006) Tunnel expansion after anterior cruciate ligament reconstruction with autogenous hamstrings: a comparison of the medial portal and transtibial techniques. *Arthroscopy*, 22, 1107-12.
- Chouliaras, V., Ristanis, S., Moraiti, C., Stergiou, N. & Georgoulis, A.D. (2007) Effectiveness of reconstruction of the anterior cruciate ligament with quadrupled hamstrings and bone-patellar tendon-bone autografts: an in vivo study comparing tibial internal-external rotation. *Am J Sports Med*, 35, 189-96.
- Cifuentes, A.O. & Kalbag, A. (1992) A performance study of tetrahedral and hexahedral elements in 3-D finite element structural analysis. *Finite Elements in Analysis and Design*, 12, 313-318.
- Crenshaw, S.J., Pollo, F.E. & Calton, E.F. (2000) Effects of lateral-wedged insoles on kinetics at the knee. *Clin Orthop Relat Res*, 185-92.
- Daniel, D.M., Stone, M.L., Dobson, B.E., Fithian, D.C., Rossman, D.J. & Kaufman, K.R. (1994) Fate of the ACL-injured patient. A prospective outcome study. *Am J Sports Med*, 22, 632-44.
- Dargel, J., Schmidt-Wiethoff, R., Fischer, S., Mader, K., Koebke, J. & Schneider, T. (2009) Femoral bone tunnel placement using the transtibial tunnel or the anteromedial portal in ACL reconstruction: a radiographic evaluation. *Knee Surg Sports Traumatol Arthrosc*, 17, 220-7.
- Defrate, L.E., Papannagari, R., Gill, T.J., Moses, J.M., Pathare, N.P. & Li, G. (2006) The 6 degrees of freedom kinematics of the knee after anterior cruciate ligament deficiency: an in vivo imaging analysis. *Am J Sports Med*, 34, 1240-6.

- Dennis, D.A., Mahfouz, M.R., Komistek, R.D. & Hoff, W. (2005) In vivo determination of normal and anterior cruciate ligament-deficient knee kinematics. *J Biomech*, 38, 241-53.
- Dingwell, J.B. & Cusumano, J.P. (2000) Nonlinear time series analysis of normal and pathological human walking. *Chaos*, 10, 848-863.
- Donahue, T.L., Hull, M.L., Rashid, M.M. & Jacobs, C.R. (2002) A finite element model of the human knee joint for the study of tibio-femoral contact. *J Biomech Eng*, 124, 273-80.
- Draganich, L.F., Andriacchi, T.P. & Andersson, G.B. (1987) Interaction between intrinsic knee mechanics and the knee extensor mechanism. *J Orthop Res*, 5, 539-47.
- Draganich, L.F., Piotrowski, G.A., Martell, J. & Pottenger, L.A. (2002) The effects of early rollback in total knee arthroplasty on stair stepping. *J Arthroplasty*, 17, 723-30.
- Dumas, R. & Cheze, L. (2009) Soft tissue artifact compensation by linear 3D interpolation and approximation methods. *J Biomech*, 42, 2214-7.
- Duquin, T.R., Wind, W.M., Fineberg, M.S., Smolinski, R.J. & Buyea, C.M. (2009) Current trends in anterior cruciate ligament reconstruction. *J Knee Surg*, 22, 7-12.
- Dyrby, C.O. & Andriacchi, T.P. (2004) Secondary motions of the knee during weight bearing and non-weight bearing activities. *J Orthop Res*, 22, 794-800.
- Eckstein, F., Muller, S., Faber, S.C., Englmeier, K.H., Reiser, M. & Putz, R. (2002) Side differences of knee joint cartilage volume, thickness, and surface area, and correlation with lower limb dominance--an MRI-based study. *Osteoarthritis Cartilage*, 10, 914-21.
- Engh, G.A. (2003) The difficult knee: severe varus and valgus. *Clin Orthop Relat Res*, 58-63.
- Erhart, J.C., Dyrby, C.O., D'lima, D.D., Colwell, C.W. & Andriacchi, T.P. (2010) Changes in in vivo knee loading with a variable-stiffness intervention shoe correlate with changes in the knee adduction moment. *J Orthop Res*, 28, 1548-53.
- Fletcher, R. (1971) A modified Marquardt subroutine for nonlinear least squares. *Atomic Energy Research Establishment report R6799, Harwell, England*.
- Fu, F.H. (2011) Double-bundle ACL reconstruction. *Orthopedics*, 34, 281-3.
- Fu, F.H. & Cohen, S.B. (2008) *Current concepts in ACL reconstruction*, SLACK Inc. NJ.
- Fujimoto, E., Sumen, Y., Urabe, Y., Deie, M., Murakami, Y., Adachi, N. & Ochi, M. (2004) An early return to vigorous activity may destabilize anterior cruciate

ligaments reconstructed with hamstring grafts. *Arch Phys Med Rehabil*, 85, 298-302.

- Fukuda, Y., Woo, S.L., Loh, J.C., Tsuda, E., Tang, P., McMahon, P.J. & Debski, R.E. (2003) A quantitative analysis of valgus torque on the ACL: a human cadaveric study. *J Orthop Res*, 21, 1107-12.
- Fuller, J., Liu, L.J., Murphy, M.C. & Mann, R.W. (1997) A comparison of lower-extremity skeletal kinematics measured using skin- and pin-mounted markers. *Human Movement Science*, 16, 219-242.
- Gabriel, M.T., Wong, E.K., Woo, S.L., Yagi, M. & Debski, R.E. (2004) Distribution of in situ forces in the anterior cruciate ligament in response to rotatory loads. *J Orthop Res*, 22, 85-9.
- Gabriel, S.E., Crowson, C.S., Champion, M.E. & O'fallon, W.M. (1997) Direct medical costs unique to people with arthritis. *J Rheumatol*, 24, 719-25.
- Gammons, M. (2011) Anterior Cruciate Ligament Injury. *Medscape Reference*.
- Gao, B. (2009) A new soft tissue artifact compensation technique in human motion analysis and clinical applications. Gainesville, University of Florida.
- Gao, B., Conrad, B. & Zheng, N. (2007) Comparison of skin error reduction techniques for skeletal motion analysis. *J Biomech*, 40, 551.
- Gao, B., Cordova, M.L. & Zheng, N.N. (2012) Three-dimensional joint kinematics of ACL-deficient and ACL-reconstructed knees during stair ascent and descent. *Hum Mov Sci*, 31, 222-35.
- Gao, B. & Zheng, N. (2010a) Alterations in three-dimensional joint kinematics of anterior cruciate ligament-deficient and -reconstructed knees during walking. *Clin Biomech (Bristol, Avon)*, 25, 222-229.
- Gao, B. & Zheng, N.N. (2008) Investigation of soft tissue movement during level walking: translations and rotations of skin markers. *J Biomech*, 41, 3189-95.
- Gao, B. & Zheng, N.N. (2010b) Alterations in three-dimensional joint kinematics of anterior cruciate ligament-deficient and -reconstructed knees during walking. *Clin Biomech (Bristol, Avon)*, 25, 222-9.
- Garling, E.H., Kaptein, B.L., Mertens, B., Barendregt, W., Veeger, H.E., Nelissen, R.G. & Valstar, E.R. (2007) Soft-tissue artefact assessment during step-up using fluoroscopy and skin-mounted markers. *J Biomech*, 40 Suppl 1, S18-24.
- Gavriilidis, I., Mosis, E.K., Pakos, E.E., Georgoulis, A.D., Mitsionis, G. & Xenakis, T.A. (2008) Transtibial versus anteromedial portal of the femoral tunnel in ACL reconstruction: a cadaveric study. *Knee*, 15, 364-7.

- Georgoulis, A.D., Papadonikolakis, A., Papageorgiou, C.D., Mitsou, A. & Stergiou, N. (2003) Three-dimensional tibiofemoral kinematics of the anterior cruciate ligament-deficient and reconstructed knee during walking. *Am J Sports Med*, 31, 75-9.
- Georgoulis, A.D., Ristanis, S., Chouliaras, V., Moraiti, C. & Stergiou, N. (2007) Tibial rotation is not restored after ACL reconstruction with a hamstring graft. *Clin Orthop Relat Res*, 454, 89-94.
- Gokeler, A., Schmalz, T., Knopf, E., Freiwald, J. & Blumentritt, S. (2003) The relationship between isokinetic quadriceps strength and laxity on gait analysis parameters in anterior cruciate ligament reconstructed knees. *Knee Surg Sports Traumatol Arthrosc*, 11, 372-8.
- Hamilton, W.R. (1866) *Elements of Quaternions*, London, U.K., Longman.
- Hamner, D.L., Brown, C.H., Jr., Steiner, M.E., Hecker, A.T. & Hayes, W.C. (1999) Hamstring tendon grafts for reconstruction of the anterior cruciate ligament: biomechanical evaluation of the use of multiple strands and tensioning techniques. *J Bone Joint Surg Am*, 81, 549-57.
- Handl, M., Drzik, M., Cerulli, G., Povysil, C., Chlpik, J., Varga, F., Amler, E. & Trc, T. (2007) Reconstruction of the anterior cruciate ligament: dynamic strain evaluation of the graft. *Knee Surg Sports Traumatol Arthrosc*, 15, 233-41.
- Helwig, N.E., Hong, S., Hsiao-Wecksler, E.T. & Polk, J.D. (2011) Methods to temporally align gait cycle data. *J Biomech*, 44, 561-6.
- Heming, J.F., Rand, J. & Steiner, M.E. (2007) Anatomical limitations of transtibial drilling in anterior cruciate ligament reconstruction. *Am J Sports Med*, 35, 1708-15.
- Holden, M. (2008) A review of geometric transformations for nonrigid body registration. *IEEE Trans Med Imaging*, 27, 111-28.
- Holm, I., Oiestad, B.E., Risberg, M.A. & Aune, A.K. (2010) No difference in knee function or prevalence of osteoarthritis after reconstruction of the anterior cruciate ligament with 4-strand hamstring autograft versus patellar tendon-bone autograft: a randomized study with 10-year follow-up. *Am J Sports Med*, 38, 448-54.
- Houck, J., Yack, H.J. & Cuddeford, T. (2004) Validity and comparisons of tibiofemoral orientations and displacement using a femoral tracking device during early to mid stance of walking. *Gait Posture*, 19, 76-84.
- Hreljac, A. & Marshall, R.N. (2000) Algorithms to determine event timing during normal walking using kinematic data. *J Biomech*, 33, 783-6.

- Hurd, W.J. & Snyder-Mackler, L. (2007) Knee instability after acute ACL rupture affects movement patterns during the mid-stance phase of gait. *J Orthop Res*, 25, 1369-77.
- Inoue, M., Mcgurk-Burleson, E., Hollis, J.M. & Woo, S.L. (1987) Treatment of the medial collateral ligament injury. I: The importance of anterior cruciate ligament on the varus-valgus knee laxity. *Am J Sports Med*, 15, 15-21.
- Ishii, Y., Terajima, K., Terashima, S. & Koga, Y. (1997) Three-dimensional kinematics of the human knee with intracortical pin fixation. *Clin Orthop Relat Res*, 144-50.
- Iwaki, H., Pinskerova, V. & Freeman, M.A. (2000) Tibiofemoral movement 1: the shapes and relative movements of the femur and tibia in the unloaded cadaver knee. *J Bone Joint Surg Br*, 82, 1189-95.
- Johansson, H., Sjolander, P. & Sojka, P. (1990) Activity in receptor afferents from the anterior cruciate ligament evokes reflex effects on fusimotor neurones. *Neurosci Res*, 8, 54-9.
- Johnson, D.L., Swenson, T.M., Irrgang, J.J., Fu, F.H. & Harner, C.D. (1996) Revision anterior cruciate ligament surgery: experience from Pittsburgh. *Clin Orthop Relat Res*, 100-9.
- Kim, S. & Pandy, M.G. (1993) A two-dimensional dynamic model of the human knee joint. *Biomed Sci Instrum*, 29, 33-46.
- Klous, M. & Klous, S. (2010) Marker-based reconstruction of the kinematics of a chain of segments: a new method that incorporates joint kinematic constraints. *J Biomech Eng*, 132, 074501.
- Kohn, D., Busche, T. & Carls, J. (1998) Drill hole position in endoscopic anterior cruciate ligament reconstruction. Results of an advanced arthroscopy course. *Knee Surg Sports Traumatol Arthrosc*, 6 Suppl 1, S13-5.
- Konishi, Y., Ikeda, K., Nishino, A., Sunaga, M., Aihara, Y. & Fukubayashi, T. (2007) Relationship between quadriceps femoris muscle volume and muscle torque after anterior cruciate ligament repair. *Scand J Med Sci Sports*, 17, 656-61.
- Kopf, S., Forsythe, B., Wong, A.K., Tashman, S., Anderst, W., Irrgang, J.J. & Fu, F.H. (2010) Nonanatomic tunnel position in traditional transtibial single-bundle anterior cruciate ligament reconstruction evaluated by three-dimensional computed tomography. *J Bone Joint Surg Am*, 92, 1427-31.
- Kozanek, M., Van De Velde, S.K., Gill, T.J. & Li, G. (2008) The contralateral knee joint in cruciate ligament deficiency. *Am J Sports Med*, 36, 2151-7.
- Kreyszig, E. (2005) *Advanced Engineering Mathematics*, John Wiley & Sons.

- Kuipers, J. (2002) *Quaternions and Rotation Sequences: A Primer With Applications to Orbits, Aerospace, and Virtual Reality*, Princeton University Press.
- Kurz, M.J., Stergiou, N., Buzzi, U.H. & Georgoulis, A.D. (2005) The effect of anterior cruciate ligament reconstruction on lower extremity relative phase dynamics during walking and running. *Knee Surg Sports Traumatol Arthrosc*, 13, 107-15.
- Kutzner, I., Damm, P., Heinlein, B., Dymke, J., Graichen, F. & Bergmann, G. (2011a) The effect of laterally wedged shoes on the loading of the medial knee compartment-in vivo measurements with instrumented knee implants. *J Orthop Res*, 29, 1910-5.
- Kutzner, I., Kuther, S., Heinlein, B., Dymke, J., Bender, A., Halder, A.M. & Bergmann, G. (2011b) The effect of valgus braces on medial compartment load of the knee joint - in vivo load measurements in three subjects. *J Biomech*, 44, 1354-60.
- Lafortune, M.A., Cavanagh, P.R., Sommer, H.J., 3rd & Kalenak, A. (1992) Three-dimensional kinematics of the human knee during walking. *J Biomech*, 25, 347-57.
- Lam, M.H., Fong, D.T., Yung, P.S., Ho, E.P., Fung, K.Y. & Chan, K.M. (2011) Knee rotational stability during pivoting movement is restored after anatomic double-bundle anterior cruciate ligament reconstruction. *Am J Sports Med*, 39, 1032-8.
- Lawrence, R.C., Felson, D.T., Helmick, C.G., Arnold, L.M., Choi, H., Deyo, R.A., Gabriel, S., Hirsch, R., Hochberg, M.C., Hunder, G.G., Jordan, J.M., Katz, J.N., Kremers, H.M. & Wolfe, F. (2008) Estimates of the prevalence of arthritis and other rheumatic conditions in the United States. Part II. *Arthritis Rheum*, 58, 26-35.
- Leardini, A., Chiari, L., Della Croce, U. & Cappozzo, A. (2005) Human movement analysis using stereophotogrammetry. Part 3. Soft tissue artifact assessment and compensation. *Gait Posture*, 21, 212-25.
- Lethbridge-Cejku, M., Helmick, C.G. & Popovic, J.R. (2003) Hospitalizations for arthritis and other rheumatic conditions: data from the 1997 National Hospital Discharge Survey. *Med Care*, 41, 1367-73.
- Levenberg, K. (1944) A Method for the Solution of Certain Non-linear Problems in Least Square. *The Quarterly of Applied Mathematics* 2, 164-168.
- Li, G., Lopez, O. & Rubash, H. (2001) Variability of a three-dimensional finite element model constructed using magnetic resonance images of a knee for joint contact stress analysis. *J Biomech Eng*, 123, 341-6.
- Li, G., Moses, J.M., Papannagari, R., Pathare, N.P., Defrate, L.E. & Gill, T.J. (2006) Anterior cruciate ligament deficiency alters the in vivo motion of the tibiofemoral

cartilage contact points in both the anteroposterior and mediolateral directions. *J Bone Joint Surg Am*, 88, 1826-34.

- Li, G., Van De Velde, S.K. & Bingham, J.T. (2008) Validation of a non-invasive fluoroscopic imaging technique for the measurement of dynamic knee joint motion. *J Biomech*, 41, 1616-22.
- Loh, J.C., Fukuda, Y., Tsuda, E., Steadman, R.J., Fu, F.H. & Woo, S.L. (2003) Knee stability and graft function following anterior cruciate ligament reconstruction: Comparison between 11 o'clock and 10 o'clock femoral tunnel placement. 2002 Richard O'Connor Award paper. *Arthroscopy*, 19, 297-304.
- Lohmander, L.S., Englund, P.M., Dahl, L.L. & Roos, E.M. (2007) The long-term consequence of anterior cruciate ligament and meniscus injuries: osteoarthritis. *Am J Sports Med*, 35, 1756-69.
- Lohmander, L.S., Ostenberg, A., Englund, M. & Roos, H. (2004) High prevalence of knee osteoarthritis, pain, and functional limitations in female soccer players twelve years after anterior cruciate ligament injury. *Arthritis Rheum*, 50, 3145-52.
- Lorentzon, R., Elmqvist, L.G., Sjostrom, M., Fagerlund, M. & Fuglmeier, A.R. (1989) Thigh musculature in relation to chronic anterior cruciate ligament tear: muscle size, morphology, and mechanical output before reconstruction. *Am J Sports Med*, 17, 423-9.
- Lu, T.W. & O'connor, J.J. (1999) Bone position estimation from skin marker co-ordinates using global optimisation with joint constraints. *J Biomech*, 32, 129-34.
- Lucchetti, L., Cappozzo, A., Cappello, A. & Della Croce, U. (1998) Skin movement artefact assessment and compensation in the estimation of knee-joint kinematics. *J Biomech*, 31, 977-84.
- Lundberg, A. (1989) Kinematics of the ankle and foot. In vivo roentgen stereophotogrammetry. *Acta Orthop Scand Suppl*, 233, 1-24.
- Markolf, K.L., Burchfield, D.M., Shapiro, M.M., Shepard, M.F., Finerman, G.A. & Slauterbeck, J.L. (1995) Combined knee loading states that generate high anterior cruciate ligament forces. *J Orthop Res*, 13, 930-5.
- Marquardt, D. (1963) An Algorithm for Least-Squares Estimation of Nonlinear Parameters. *SIAM Journal on Applied Mathematics* 11, 431-441.
- McLean, S.G., Walker, K.B. & Van Den Bogert, A.J. (2005) Effect of gender on lower extremity kinematics during rapid direction changes: an integrated analysis of three sports movements. *J Sci Med Sport*, 8, 411-22.
- Meier, B. (December 27, 2011) The high cost of failing artificial hips. *The New York Times*.

- Meredick, R.B., Vance, K.J., Appleby, D. & Lubowitz, J.H. (2008) Outcome of single-bundle versus double-bundle reconstruction of the anterior cruciate ligament: a meta-analysis. *Am J Sports Med*, 36, 1414-21.
- Misonoo, G., Kanamori, A., Ida, H., Miyakawa, S. & Ochiai, N. (2012) Evaluation of tibial rotational stability of single-bundle vs. anatomical double-bundle anterior cruciate ligament reconstruction during a high-demand activity - A quasi-randomized trial. *Knee*, 19, 87-93.
- Miyazaki, T., Wada, M., Kawahara, H., Sato, M., Baba, H. & Shimada, S. (2002) Dynamic load at baseline can predict radiographic disease progression in medial compartment knee osteoarthritis. *Ann Rheum Dis*, 61, 617-22.
- Moeinzadeh, M.H. & Engin, A.E. (1983) Response of a two-dimensional dynamic model of the human knee to the externally applied forces and moments. *J Biomed Eng*, 5, 281-91.
- Moraiti, C.O., Stergiou, N., Ristanis, S., Vasiliadis, H.S., Patras, K., Lee, C. & Georgoulis, A.D. (2009) The effect of anterior cruciate ligament reconstruction on stride-to-stride variability. *Arthroscopy*, 25, 742-9.
- Moraiti, C.O., Stergiou, N., Vasiliadis, H.S., Motsis, E. & Georgoulis, A. (2010) Anterior cruciate ligament reconstruction results in alterations in gait variability. *Gait Posture*, 32, 169-75.
- Mow, V.C., Gu, W.Y. & Chen, F.H. (2005) Structure and Function of Articular Cartilage and Meniscus. IN MOW, V. C. & HUISKES, R. (Eds.) *Basic Orthopaedic Biomechanics & Mechano-Biology*. Philadelphia, PA, LIPPINCOTT WILLIAMS & WILKINS.
- Muneta, T., Sekiya, I., Yagishita, K., Ogiuchi, T., Yamamoto, H. & Shinomiya, K. (1999) Two-bundle reconstruction of the anterior cruciate ligament using semitendinosus tendon with endobuttons: operative technique and preliminary results. *Arthroscopy*, 15, 618-24.
- Nebelung, W. & Wuschech, H. (2005) Thirty-five years of follow-up of anterior cruciate ligament-deficient knees in high-level athletes. *Arthroscopy*, 21, 696-702.
- Negrete, R.J., Schick, E.A. & Cooper, J.P. (2007) Lower-limb dominance as a possible etiologic factor in noncontact anterior cruciate ligament tears. *J Strength Cond Res*, 21, 270-3.
- Netravali, N.A., Koo, S., Giori, N.J. & Andriacchi, T.P. (2011) The effect of kinematic and kinetic changes on meniscal strains during gait. *J Biomech Eng*, 133, 011006.
- Noyes, F.R., Butler, D.L., Grood, E.S., Zernicke, R.F. & Hefzy, M.S. (1984) Biomechanical analysis of human ligament grafts used in knee-ligament repairs and reconstructions. *J Bone Joint Surg Am*, 66, 344-52.

- Noyes, F.R., Mooar, P.A., Matthews, D.S. & Butler, D.L. (1983) The symptomatic anterior cruciate-deficient knee. Part I: the long-term functional disability in athletically active individuals. *J Bone Joint Surg Am*, 65, 154-62.
- Oloyede, A., Flachsmann, R. & Broom, N.D. (1992) The dramatic influence of loading velocity on the compressive response of articular cartilage. *Connect Tissue Res*, 27, 211-24.
- Pandy, M.G. & Sasaki, K. (1998) A Three-Dimensional Musculoskeletal Model of the Human Knee Joint. Part 2: Analysis of Ligament Function. *Comput Methods Biomech Biomed Engin*, 1, 265-283.
- Pandy, M.G., Sasaki, K. & Kim, S. (1998) A Three-Dimensional Musculoskeletal Model of the Human Knee Joint. Part 1: Theoretical Construct. *Comput Methods Biomech Biomed Engin*, 1, 87-108.
- Papannagari, R., Gill, T.J., Defrate, L.E., Moses, J.M., Petruska, A.J. & Li, G. (2006) In vivo kinematics of the knee after anterior cruciate ligament reconstruction: a clinical and functional evaluation. *Am J Sports Med*, 34, 2006-12.
- Pena, E., Calvo, B., Martinez, M.A. & Doblare, M. (2006a) A three-dimensional finite element analysis of the combined behavior of ligaments and menisci in the healthy human knee joint. *J Biomech*, 39, 1686-701.
- Pena, E., Calvo, B., Martinez, M.A., Palanca, D. & Doblare, M. (2005) Finite element analysis of the effect of meniscal tears and meniscectomies on human knee biomechanics. *Clin Biomech (Bristol, Avon)*, 20, 498-507.
- Pena, E., Calvo, B., Martinez, M.A., Palanca, D. & Doblare, M. (2006b) Influence of the tunnel angle in ACL reconstructions on the biomechanics of the knee joint. *Clin Biomech (Bristol, Avon)*, 21, 508-16.
- Pereira, H.M., Nowotny, A.H., Santos, A.B. & Cardoso, J.R. (2009) Electromyographic activity of knee stabilizer muscles during six different balance board stimuli after anterior cruciate ligament surgery. *Electromyogr Clin Neurophysiol*, 49, 117-24.
- Peters, A., Galna, B., Sangeux, M., Morris, M. & Baker, R. (2010) Quantification of soft tissue artifact in lower limb human motion analysis: a systematic review. *Gait Posture*, 31, 1-8.
- Petschnig, R., Baron, R. & Albrecht, M. (1998) The relationship between isokinetic quadriceps strength test and hop tests for distance and one-legged vertical jump test following anterior cruciate ligament reconstruction. *J Orthop Sports Phys Ther*, 28, 23-31.
- Piasecki, D.P., Bach, B.R., Jr., Espinoza Orias, A.A. & Verma, N.N. (2011) Anterior cruciate ligament reconstruction: can anatomic femoral placement be achieved with a transtibial technique? *Am J Sports Med*, 39, 1306-15.

- Pollet, V., Barrat, D., Meirhaeghe, E., Vaes, P. & Handelberg, F. (2005) The role of the Rolimeter in quantifying knee instability compared to the functional outcome of ACL-reconstructed versus conservatively-treated knees. *Knee Surg Sports Traumatol Arthrosc*, 13, 12-8.
- Porac, C. & Coren, S. (1981) *Lateral Preferences and Human Behaviour*, New York, Springer.
- Quinn, T.M., Hunziker, E.B. & Hauselmann, H.J. (2005) Variation of cell and matrix morphologies in articular cartilage among locations in the adult human knee. *Osteoarthritis Cartilage*, 13, 672-8.
- Reinschmidt, C., Van Den Bogert, A.J., Murphy, N., Lundberg, A. & Nigg, B.M. (1997a) Tibiocalcaneal motion during running, measured with external and bone markers. *Clin Biomech (Bristol, Avon)*, 12, 8-16.
- Reinschmidt, C., Van Den Bogert, A.J., Nigg, B.M., Lundberg, A. & Murphy, N. (1997b) Effect of skin movement on the analysis of skeletal knee joint motion during running. *J Biomech*, 30, 729-32.
- Ristanis, S., Giakas, G., Papageorgiou, C.D., Moraiti, T., Stergiou, N. & Georgoulis, A.D. (2003) The effects of anterior cruciate ligament reconstruction on tibial rotation during pivoting after descending stairs. *Knee Surg Sports Traumatol Arthrosc*, 11, 360-5.
- Ristanis, S., Stergiou, N., Patras, K., Tsepis, E., Moraiti, C. & Georgoulis, A.D. (2006) Follow-up evaluation 2 years after ACL reconstruction with bone-patellar tendon-bone graft shows that excessive tibial rotation persists. *Clin J Sport Med*, 16, 111-6.
- Ristanis, S., Stergiou, N., Patras, K., Vasiliadis, H.S., Giakas, G. & Georgoulis, A.D. (2005) Excessive tibial rotation during high-demand activities is not restored by anterior cruciate ligament reconstruction. *Arthroscopy*, 21, 1323-9.
- Sadoghi, P., Kropfl, A., Jansson, V., Muller, P.E., Pietschmann, M.F. & Fischmeister, M.F. (2011) Impact of tibial and femoral tunnel position on clinical results after anterior cruciate ligament reconstruction. *Arthroscopy*, 27, 355-64.
- Scanlan, S.F., Chaudhari, A.M., Dyrby, C.O. & Andriacchi, T.P. (2010) Differences in tibial rotation during walking in ACL reconstructed and healthy contralateral knees. *J Biomech*, 43, 1817-22.
- Schmidt, J. & Niemann, H. (2001) Using Quaternions for Parametrizing 3-D Rotations in Unconstrained Nonlinear Optimization. *Vision, Modeling, and Visualization, Stuttgart, Germany*, pp. 399-406.

- Scopp, J.M., Jasper, L.E., Belkoff, S.M. & Moorman, C.T., 3rd (2004) The effect of oblique femoral tunnel placement on rotational constraint of the knee reconstructed using patellar tendon autografts. *Arthroscopy*, 20, 294-9.
- Sedgman, R., Goldie, P., & Ianssek, R. (1994) Development of a measure of turning during walking. Advancing Rehabilitation. *In Proceedings inaugural conference of the faculty of health sciences*. La Trobe University, Melbourne, Australia.
- Seon, J.K., Song, E.K. & Park, S.J. (2006) Osteoarthritis after anterior cruciate ligament reconstruction using a patellar tendon autograft. *Int Orthop*, 30, 94-8.
- Sharma, L., Hurwitz, D.E., Thonar, E.J., Sum, J.A., Lenz, M.E., Dunlop, D.D., Schnitzer, T.J., Kirwan-Mellis, G. & Andriacchi, T.P. (1998) Knee adduction moment, serum hyaluronan level, and disease severity in medial tibiofemoral osteoarthritis. *Arthritis Rheum*, 41, 1233-40.
- Sharma, L., Lou, C., Cahue, S. & Dunlop, D.D. (2000) The mechanism of the effect of obesity in knee osteoarthritis: the mediating role of malalignment. *Arthritis Rheum*, 43, 568-75.
- Sheehan, F.T. & Drace, J.E. (1999) Quantitative MR measures of three-dimensional patellar kinematics as a research and diagnostic tool. *Med Sci Sports Exerc*, 31, 1399-405.
- Sheehan, F.T., Zajac, F.E. & Drace, J.E. (1999) In vivo tracking of the human patella using cine phase contrast magnetic resonance imaging. *J Biomech Eng*, 121, 650-6.
- Shim, H., Chang, S., Tao, C., Wang, J.H., Kwoh, C.K. & Bae, K.T. (2009) Knee cartilage: efficient and reproducible segmentation on high-spatial-resolution MR images with the semiautomated graph-cut algorithm method. *Radiology*, 251, 548-56.
- Shimokochi, Y. & Shultz, S.J. (2008) Mechanisms of noncontact anterior cruciate ligament injury. *J Athl Train*, 43, 396-408.
- Souryal, T.O. (2012) Rehabilitation for Anterior Cruciate Ligament Injury. *Medscape Reference*.
- Spindler, K.P., Kuhn, J.E., Freedman, K.B., Matthews, C.E., Dittus, R.S. & Harrell, F.E., Jr. (2004) Anterior cruciate ligament reconstruction autograft choice: bone-tendon-bone versus hamstring: does it really matter? A systematic review. *Am J Sports Med*, 32, 1986-95.
- Spoor, C.W. & Veldpaus, F.E. (1980) Rigid body motion calculated from spatial coordinates of markers. *J Biomech*, 13, 391-3.

- Stagni, R., Fantozzi, S., Cappello, A. & Leardini, A. (2005) Quantification of soft tissue artefact in motion analysis by combining 3D fluoroscopy and stereophotogrammetry: a study on two subjects. *Clin Biomech (Bristol, Avon)*, 20, 320-9.
- Steiner, M.E. (2009) Independent drilling of tibial and femoral tunnels in anterior cruciate ligament reconstruction. *J Knee Surg*, 22, 171-6.
- Stergiou, N., Ristanis, S., Moraiti, C. & Georgoulis, A.D. (2007) Tibial rotation in anterior cruciate ligament (ACL)-deficient and ACL-reconstructed knees: a theoretical proposition for the development of osteoarthritis. *Sports Med*, 37, 601-13.
- Strobel, M.J., Castillo, R.J. & Weiler, A. (2001) Reflex extension loss after anterior cruciate ligament reconstruction due to femoral "high noon" graft placement. *Arthroscopy*, 17, 408-11.
- Tashman, S. & Anderst, W. (2003) In-vivo measurement of dynamic joint motion using high speed biplane radiography and CT: application to canine ACL deficiency. *J Biomech Eng*, 125, 238-45.
- Tashman, S., Kolowich, P., Collon, D., Anderson, K. & Anderst, W. (2007) Dynamic function of the ACL-reconstructed knee during running. *Clin Orthop Relat Res*, 454, 66-73.
- Thambyah, A., Nather, A. & Goh, J. (2006) Mechanical properties of articular cartilage covered by the meniscus. *Osteoarthritis Cartilage*, 14, 580-8.
- To, J.T., Howell, S.M. & Hull, M.L. (1999) Contributions of femoral fixation methods to the stiffness of anterior cruciate ligament replacements at implantation. *Arthroscopy*, 15, 379-87.
- Trikha, P. (2012) Double bundle, traditional single bundle or 'more anatomic' single bundle ACL reconstruction? , <http://www.kneeguru.co.uk/KNEENotes/node/2447>.
- Tsarouhas, A., Iosifidis, M., Kotzamitelos, D., Spyropoulos, G., Tsatalas, T. & Giakas, G. (2010) Three-dimensional kinematic and kinetic analysis of knee rotational stability after single- and double-bundle anterior cruciate ligament reconstruction. *Arthroscopy*, 26, 885-93.
- Tsarouhas, A., Iosifidis, M., Spyropoulos, G., Kotzamitelos, D., Tsatalas, T. & Giakas, G. (2011) Tibial rotation under combined in vivo loading after single- and double-bundle anterior cruciate ligament reconstruction. *Arthroscopy*, 27, 1654-62.
- Tudisco, C. & Bisicchia, S. (2012) Drilling the Femoral Tunnel During ACL Reconstruction: Transtibial Versus Anteromedial Portal Techniques. *Orthopedics*, 35, e1166-72.

- Valeriani, M., Restuccia, D., Di Lazzaro, V., Franceschi, F., Fabbriani, C. & Tonali, P. (1999) Clinical and neurophysiological abnormalities before and after reconstruction of the anterior cruciate ligament of the knee. *Acta Neurol Scand*, 99, 303-7.
- Van De Velde, S.K., Gill, T.J. & Li, G. (2009) Evaluation of kinematics of anterior cruciate ligament-deficient knees with use of advanced imaging techniques, three-dimensional modeling techniques, and robotics. *J Bone Joint Surg Am*, 91 Suppl 1, 108-14.
- Van Der Harst, J.J., Gokeler, A. & Hof, A.L. (2007) Leg kinematics and kinetics in landing from a single-leg hop for distance. A comparison between dominant and non-dominant leg. *Clin Biomech (Bristol, Avon)*, 22, 674-80.
- Veldpaus, F.E., Woltring, H.J. & Dortmans, L.J. (1988) A least-squares algorithm for the equiform transformation from spatial marker co-ordinates. *J Biomech*, 21, 45-54.
- Wang, H., Fleischli, J.E. & Nigel Zheng, N. (2012) Effect of lower limb dominance on knee joint kinematics after anterior cruciate ligament reconstruction. *Clin Biomech (Bristol, Avon)*, 27, 170-5.
- Wang, H. & Zheng, N. (2010a) Knee rotation and loading during spin and step turn. *Int J Sports Med*, 31, 742-6.
- Wang, H. & Zheng, N.N. (2010b) Knee joint secondary motion accuracy improved by quaternion-based optimizer with bony landmark constraints. *J Biomech Eng*, 132, 124502.
- Wang, W., Wang, K., Dang, X., Bai, C., Wang, C., Shi, Z. & Ma, S. (2007) Influencing factors analysis of spontaneous knee joint osteoarthritis among middle aged and old aged people in Xi'an. *Journal of Medical Colleges of PLA*, 22, 179-184.
- Webster, K.E. & Feller, J.A. (2011) Alterations in joint kinematics during walking following hamstring and patellar tendon anterior cruciate ligament reconstruction surgery. *Clin Biomech (Bristol, Avon)*, 26, 175-80.
- Webster, K.E., Palazzolo, S.E., Mcclelland, J.A. & Feller, J.A. (2012) Tibial rotation during pivoting in anterior cruciate ligament reconstructed knees using a single bundle technique. *Clin Biomech (Bristol, Avon)*, 27, 480-484.
- Weiss, J.A., Maker, B. & Govindjee, S. (1996) Finite element implementation of incompressible, transversely isotropic hyperelasticity. *Comput. Meth. Appl. Mech. Eng.*, 135, 107-128.
- Winter, A.D. (1991) *The biomechanics and motor control of human gait: normal, elderly and pathological*, Waterloo, Ontario, University of Waterloo Press.

- Winter, D.A. (1990) *The Biomechanics and Motor Control of Human Movement* Waterloo, Ontario, Canada A Wiley-Interscience Publication.
- Woo, S.L.-Y., Lee, T.Q., Abramowitch, S.D. & Gilbert, T.W. (2005) Structure and Function of Ligaments and Tendons. IN MOW, V. C. & HUISKES, R. (Eds.) *Basic Orthopaedic Biomechanics and Mechano-Biology*. 3rd Edition ed. Philadelphia, PA, LIPPINCOTT WILLIAMS & WILKINS.
- Woo, S.L., Kanamori, A., Zeminski, J., Yagi, M., Papageorgiou, C. & Fu, F.H. (2002) The effectiveness of reconstruction of the anterior cruciate ligament with hamstrings and patellar tendon . A cadaveric study comparing anterior tibial and rotational loads. *J Bone Joint Surg Am*, 84-A, 907-14.
- Yamamoto, Y., Hsu, W.H., Woo, S.L., Van Scyoc, A.H., Takakura, Y. & Debski, R.E. (2004) Knee stability and graft function after anterior cruciate ligament reconstruction: a comparison of a lateral and an anatomical femoral tunnel placement. *Am J Sports Med*, 32, 1825-32.
- Yang, N.H., Canavan, P.K., Nayeb-Hashemi, H., Najafi, B. & Vaziri, A. (2010) Protocol for constructing subject-specific biomechanical models of knee joint. *Comput Methods Biomech Biomed Engin*, 13, 589-603.
- Yao, J., Snibbe, J., Maloney, M. & Lerner, A.L. (2006) Stresses and strains in the medial meniscus of an ACL deficient knee under anterior loading: a finite element analysis with image-based experimental validation. *J Biomech Eng*, 128, 135-41.
- Zhao, D., Banks, S.A., Mitchell, K.H., D'lima, D.D., Colwell, C.W., Jr. & Fregly, B.J. (2007) Correlation between the knee adduction torque and medial contact force for a variety of gait patterns. *J Orthop Res*, 25, 789-97.
- Zheng, N., Fleisig, G.S., Escamilla, R.F. & Barrentine, S.W. (1998) An analytical model of the knee for estimation of internal forces during exercise. *J Biomech*, 31, 963-7.